Department of Physics and Astronomy
University of Heidelberg

Master Thesis in Physics
submitted by

Jan Philipp Bartels

born in Kiel (Germany)

2025

Free Thermal Bosonic Quasiparticles and the Emergence of Riemann's Zeta Function in the Pressure of SU(2) Quantum Yang–Mills Theory

This Bachelor Thesis has been carried out by Jan Philipp Bartels at the
Institute for Theoretical Physics, Heidelberg
under the supervision of
PD Dr. Ralf Hofmann

Zusammenfassung. Diese Arbeit untersucht eine mögliche Verbindung zwischen dem Auftreten thermischer Quasiteilchenmassen in der dekonfinierten Phase der SU(2) Yang–Mills Theorie und den analytischen Eigenschaften der Riemannschen Zetafunktion. Ausgehend vom thermischen Druck zur führenden Ordnung wird eine logarithmische Reihenentwicklung in der Quasiteilchenmasse hergeleitet, deren Koeffizienten zwei äquivalente Darstellungen besitzen: eine Doppelsummenformulierung mit modifizierten Besselfunktionen und Stirling-Zahlen zweiter Art sowie eine Mellin-Barnes-Darstellung, die die Zetafunktion im kritischen Streifen testet. Letztere enthält eine kompakt getragene Gewichtsfunktion, deren Freiheit allein durch die Polstruktur begrenzt ist. Mittels der Sattelpunktmethode wird eine einheitliche asymptotische Entwicklung der Koeffizienten für große Ordnungen gewonnen. Der Vergleich dieser Entwicklung mit der Mellin-Barnes-Darstellung–unter Annahmen über die Lage der nichttrivialen Nullstellen der Zetafunktion–könnte nichttriviale Konsistenzbedingungen für diese Annahmen erzeugen. Die Ergebnisse deuten darauf hin, dass analytische Strukturen der Yang–Mills Thermodynamik zur Untersuchung von Eigenschaften der Zetafunktion genutzt werden können und damit eine neue Verbindung zwischen Quantenfeldtheorie und Zahlentheorie eröffnen.

Abstract. This thesis investigates a possible connection between the emergence of thermal quasiparticle masses in the deconfined phase of SU(2) Yang–Mills theory and the analytic properties of the Riemann zeta function. Starting from the thermal one-loop pressure, we derive a logarithmic series expansion in the quasiparticle mass whose coefficients admit two complementary representations: a double-sum form involving modified Bessel functions and Stirling numbers of the second kind, and a Mellin-Barnes form probing the zeta function inside the critical strip. The Mellin-Barnes representation uses a compactly supported weight function, constrained only by its pole structure, enabling analytic access to different regions. A uniform asymptotic expansion of the coefficients for large order is obtained using the method of steepest descent. Comparison of this expansion with the Mellin-Barnes representation–under assumptions about the distribution of the nontrivial zeros of the zeta function– may provide nontrivial statements concerning the validity of these assumptions. The results suggest that analytic structures arising in finite-temperature Yang–Mills theory may serve as probes of the zeta function, indicating towards a hidden interplay between quantum field theory and number theory.

Acknowledgements

I would like to express my sincere gratitude to PD Dr. Ralf Hofmann for giving me the opportunity to work on such a fascinating topic and for his guidance, constructive criticism, and continuous support throughout the development of this thesis.

I am also grateful to the Institute for Theoretical Physics at the University of Heidelberg for enabling my participation in the Clay Mathematics Institute workshop *Zeta and L-Functions*, held on the occasion of the twenty-fifth anniversary of the Millennium Prize Problems. This workshop provided an excellent overview of contemporary research on the Riemann zeta function, and the discussions with other participants were highly stimulating and encouraged me to pursue several of the ideas explored in this work.

Finally, I would like to thank Janning Meinert for carefully proof-reading this thesis and for many helpful comments that improved its readability and precision.

Erklärung

Ich versichere, dass ich diese Arbeit selbstständig verfasst und keine anderen als die angegebenen Quellen und Hilfsmittel benutzt habe.

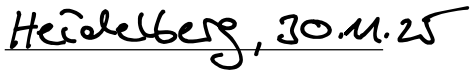

Ort, Datum

Unterschrift

Contents

List of Figures

Chapter 1

Introduction

This thesis explores a possible connection between the emergence of thermal bosonic quasiparticle masses in the deconfined phase of SU(2) Yang–Mills theory, purely a quantum phenomenon, and analytic properties of the Riemann zeta function $\zeta(s)$, a central object in number theory and particularly in the study of the prime distribution. The central insight is that analytically continuing, in the quasiparticle mass, the remainder term of the small-mass expansion of the thermal bosonic one-loop pressure may reveal properties of the Riemann zeta function.

Over the past few decades, surprising links between number theory and theoretical physics have emerged, particularly in the context of the Riemann zeta function and random matrix theory (RMT). Building on Montgomery's work on the pair correlation of consecutive zeros of $\zeta(s)$ [1], Dyson [2] conjectured that the two-point correlation function of the non-trivial zeros on the critical line matches the spacing statistics of eigenvalues of large random Hermitian matrices drawn from the Gaussian Unitary Ensemble (GUE). This conjecture was strongly supported by the numerical investigations of Odlyzko [3], based on the algorithm developed by Odlyzko and Schönhage [4], showing remarkable agreement between high-lying zeros of $\zeta(s)$ and GUE statistics. Berry's work [5] further established how the zeros reflect the transition to the random-matrix regime at increasing heights in the critical strip. Beyond two-point correlations, higher-order statistics have been studied by Bogomolny and Keating and collaborators [6, 7]. Keating and Snaith [8] later generalised this correspondence by modelling the moments of the Riemann zeta function over intervals $[0, T]$ using those of characteristic polynomials of unitary matrices of size $N \sim \log T$. Extensions to families of L-functions were developed by Katz and Sarnak [9], with broader discussions provided in [10, 11]. Despite these striking statistical parallels, they have not yet led to progress on the Riemann Hypothesis.

Whereas these developments connect quantum mechanics and number theory at the level of statistical behaviour, a different class of connections may exist at the level of analytic structure. In this work, we explore such a relationship within the context of finite-temperature SU(2) Yang–Mills theory, whose thermodynamics involves non-perturbative effects associated with

topologically non-trivial field configurations.

In finite-temperature quantum field theory (QFT), the thermodynamics of pure Yang–Mills theory presents significant challenges that cannot be resolved by perturbative methods alone. Perturbative expansions fail to account for topologically non-trivial field configurations whose contributions vanish in the weak-coupling limit while they dominate in the infrared regime (see also Example A.2.1). As first emphasised by Polyakov [12], infrared divergences in non-Abelian gauge theories indicate the necessity of dynamically generated finite correlation lengths induced by such topological fluctuations.

To address this, a non-perturbative estimate of the thermal ground state in the deconfined phase of SU(2) and SU(3) Yang–Mills theory has been constructed. This estimate is obtained by spatial coarse-graining over a densely packed ensemble of Bogomolny-Prasad-Sommerfield (BPS) saturated Harrington-Shepard (anti)calorons with topological charge $k = \pm 1$ and trivial holonomy [13, 14, 15]. BPS saturation renders these configurations (anti)selfdual, ensuring vanishing energy-momentum density, while moduli-space arguments exclude contributions from calorons with $|k| > 1$. Together, these properties guarantee the uniqueness of the resulting ground-state estimate up to global gauge rotations.

The coarse-graining procedure begins by determining the kernel of a linear, second-order differential operator $\mathcal{D}$ acting on adjoint-valued phases $\{\hat{\phi}\}$. Imposing BPS conditions transforms the implicit temperature dependence of $\mathcal{D}$ into a first-order differential equation for a scalar potential $V(\phi^2)$ of the scalar field $\phi = \hat{\phi}|\phi|$. Its solution introduces an integration constant identified as the Yang–Mills scale Λ. The resulting non-propagating adjoint scalar field ϕ has constant modulus, which sets the maximal spatial resolution of the effective theory and imposes constraints on the allowed momentum transfers at four-vertices. This non-perturbative effect dynamically regulates ultraviolet divergences by preventing resolution of the underlying Harrington-Shepard calorons, thereby removing the need for conventional renormalisation.

This procedure contrasts with Wilsonian renormalisation, which proceeds by integrating out high-energy modes. Here, instead, the trivial-topology sector emerges from coarse-graining over topologically non-trivial configurations [16]. Spatial correlations within the caloron ensemble are encoded in the inert adjoint scalar field ϕ. This field breaks gauge symmetry dynamically in directions orthogonal to the Cartan subalgebra, namely U(1) for SU(2) and $\mathrm{U}(1) \times \mathrm{U}(1)$ for SU(3), and gives rise to a thermal, temperature-dependent mass for the off-Cartan gauge bosons via the adjoint Higgs mechanism [16, 17]. Because ϕ is statistically inert, the associated massive thermal quasiparticles remain on-shell throughout the deconfined regime, supporting their interpretation as genuine thermal excitations. Since the emergence of a temperature-dependent quasiparticle mass follows directly from the adjoint Higgs mechanism, the effective coupling $e(T)$ between the gauge fields and the background field ϕ determines the magnitude of this mass.

Interactions between calorons, mediated through overlapping peripheral regions and centres, further enrich the ground-state structure. These interactions generate topologically trivial pure-gauge configurations that seed the dynamics of coarse-grained, propagating quantum fluctuations, leading to a deformation of trivial holonomy [16]. The nature of these interactions depends critically on the holonomy structure. Small-holonomy calorons generate an attractive interaction between their constituent monopoles, leading to a negative pressure contribution by the thermal ground state. Large-holonomy calorons, conversely, dissociate into stable monopole-antimonopole pairs that are screened either by unstable magnetic charges originating from small-holonomy calorons or by other stable magnetic charges present in the thermal medium [18, 19].

The resulting effective action in the deconfined (electric) phase, valid for both SU(2) and SU(3), contains interaction vertices tightly constrained by BPS saturation and by the maximal resolution scale $|\phi|$, which restricts momentum transfer at each vertex. Although the functional form of this action is identical for SU(2) and SU(3), the structure of the adjoint scalar field differs in each case and reflects the distinct gauge groups.

The mechanism of deconfinement is reflected in the degeneracy of the thermal ground state: a $\mathbb{Z}_2$ symmetry for SU(2) and $\mathbb{Z}_3$ for SU(3), indicating multiple physically equivalent vacua. Thermodynamic quantities within this setting are derived using an effective loop expansion, where the aforementioned vertex constraints strongly restrict the support of higher-loop integrals and lead to the conjecture that only a finite number of n-particle-irreducible (nPI) bubble diagrams, up to possible resummations, contribute [20].

A key thermodynamic parameter is the effective gauge coupling $e(T)$, which governs the screening of magnetic (test) charges. In the deconfined phase, screening originates from the interaction of a test charge with transient monopole-antimonopole pairs generated by small holonomy shifts of calorons, while the dissociation channel of large-holonomy configurations remains virtual in the thermal medium [19]. Across most of the deconfined phase the coupling is approximately constant, taking the value $e = \sqrt{8}\,\pi$ [19]. However, as the temperature approaches its critical value from above, $e(T)$ develops a logarithmic divergence. In this regime, the dissociation of calorons into monopole-antimonopole pairs becomes increasingly likely, since screening effects drive both the mass and the effective magnetic charge of isolated monopoles towards zero, triggering monopole condensation and signalling the onset of the preconfined phase.

Thermodynamic self-consistency in the presence of implicit temperature dependences of parameters in the effective action requires that Legendre transformations remain invariant under such dependences [19, 21]. Applied to the Legendre transformation relating the energy density to the pressure P, this requirement leads to the condition $\partial_m P = 0$. Solving this constraint yields a first-order differential equation that relates the quasiparticle mass m (or, equivalently,

the effective gauge coupling) to the temperature [19].

In the high-temperature limit, the temperature-dependent evolution of $e(T)$ involves a term whose expansion in powers of the small mass parameter is accompanied by a remainder R that is analytic within a finite radius of convergence [22]. Importantly, we show that this remainder evaluates the Riemann zeta function at infinitely many odd integer arguments. This motivates us to seek an analytic continuation of the remainder term beyond its range of convergence, using Mellin-Barnes (MB) integral techniques, with the aim of uncovering a potential connection between the analytic structure of $\zeta(s)$ and the mechanism of thermal mass generation in Yang–Mills theory.

This thesis is organised as follows. Chapter 2 introduces the special functions employed throughout this work, in particular the gamma function, the Riemann zeta function, and the modified Bessel function, together with some historical remarks concerning the zeta function.

Chapter 3 reviews finite-temperature aspects of SU(2) Yang–Mills theory and re-derives the thermal one-loop pressure when massive quasiparticles contribute to the excitation spectrum. Here we obtain asymptotic expansions in both the small- and large-mass limits, compute the temperature-dependent running of the quasiparticle mass and effective gauge coupling, and semi-analytically determine the leading-order critical temperature of the deconfined phase.

In Chapter 4, the one-loop pressure is expanded into powers of the logarithm of the quasiparticle mass. The resulting coefficients admit two complementary representations: a double-sum expression involving modified Bessel functions and Stirling numbers of the second kind, and a MB representation that probes the zeta function within the critical strip. A uniform large-order asymptotic expansion is then derived using the method of steepest descent.

The final chapter discusses how comparing this steepest-descent asymptotic expansion with the MB representation–under assumptions about the distribution of the non-trivial zeros of the zeta function–may yield non-trivial information concerning the validity of these assumptions. This provides the motivation for inferring properties of the zeta function within the critical strip at large imaginary part from those properties that are well controlled at large real and imaginary parts. We conclude that the analytic structures arising in finite-temperature Yang–Mills theory may serve as potentially useful probes of the zeta function.

Appendix A collects mathematical tools used throughout the text, with proofs and examples relevant to the analysis. Appendix B presents alternative derivations of the one-loop asymptotic expansions of the pressure, following Dolan and Jackiw, included primarily for historical context, as these calculations formed the starting point of the present research.

Chapter 2

Special Functions

Throughout this work, various special functions arise naturally in the context of MB integral representations and asymptotic expansions. In particular, the *gamma function* $\Gamma(x)$, the *Riemann zeta function* $\zeta(x)$ and the *modified Bessel function of the second kind* $K_\nu(x)$ play a central rôle in the methods and results that follow. For this reason, we begin by assembling the most relevant definitions and fundamental properties required in later chapters.

Some of these properties will be derived explicitly in Section A.2, while the classical references [23, 24, 25] provide a comprehensive treatment.

2.1 The Gamma Function

The gamma function analytically extends the factorial function $n!$ to the complex domain $\mathbb{C} \setminus \mathbb{Z}_{\leq 0}$. Its defining properties are uniquely characterised by *Wielandt's theorem* [26]. According to this result, the function $\Gamma(z)$ is holomorphic on $\mathbb{C}\setminus\mathbb{Z}_{\leq 0}$, satisfies the normalisation $\Gamma(1) = 1$, and obeys the *fundamental recurrence relation*

$$\Gamma(z+1) = z\,\Gamma(z) \qquad (z \neq 0), \tag{2.1.1}$$

while being bounded on the vertical strip $1 \leq \Re(z) \leq 2$.

The gamma function is central to MB integral methods, where it frequently appears in the integrands of MB representations as well as in identities describing how transformations act under the Mellin transform. For instance, differentiation, scaling and logarithmic factors translate into multiplicative expressions involving ratios of gamma functions, as captured by the identities listed in Sect. A.3.

The first generalisation of the factorial was introduced by Euler in [27], leading to what is now

known as *Euler's integral of the second kind*:

$$\Gamma(z) = \int_0^\infty \mathrm{e}^{-t} t^{z-1}\,\mathrm{d}t \qquad (\Re(z) > 0), \tag{2.1.2}$$

where the integration path follows the positive real axis and t^{z-1} takes its principal value. *Euler's integral of the first kind* defines the *beta function*, introduced later in Eq. (2.1.24).

Eq. (2.1.2) reveals that $\Gamma(z)$ is the Mellin transform of e^{-t}. By Mellin inversion, one obtains the *Cahen-Mellin integral*

$$\mathrm{e}^{-z} = \frac{1}{2\pi i}\int_{\sigma-i\infty}^{\sigma+i\infty} \Gamma(s) z^{-s}\,\mathrm{d}s \qquad (\sigma > 0), \tag{2.1.3}$$

valid for $(|\arg(z)| < \frac{\pi}{2})$ and $z \neq 0$, or for $(|\arg(z)| = \frac{\pi}{2},\ 0 < \sigma \leq \frac{1}{2})$.

Differentiation of Eq. (2.1.2) yields

$$\frac{\mathrm{d}^n}{\mathrm{d}z^n}\Gamma(z) = \int_0^\infty t^{z-1}(\log t)^n\,\mathrm{e}^{-t}\,\mathrm{d}t \qquad (\Re(z) > 0). \tag{2.1.4}$$

Moreover, the restriction to $\Re(z) > 0$ can be removed by analytic continuation. A particularly elegant continuation is given by the *Hadamard-Weierstrass product representation* [28] as

$$\frac{1}{\Gamma(z)} = z\,\mathrm{e}^{\gamma z}\prod_{n=1}^{\infty}\left(1+\frac{z}{n}\right)\mathrm{e}^{-z/n}, \tag{2.1.5}$$

where γ denotes the *Euler-Mascheroni constant*

$$\gamma = \lim_{N\to\infty}\left(\sum_{n=1}^{N}\frac{1}{n} - \log N\right). \tag{2.1.6}$$

This formula is valid for all $z \in \mathbb{C}$ and explicitly exhibits the simple poles of $\Gamma(z)$ at the non-positive integers. (The historical attribution of this product formula remains debated; see [29] for a detailed discussion.)

From Eq. (2.1.5), the local expansion near $z = 0$ follows immediately

$$\Gamma(z) = \frac{1}{z} - \gamma + O(z). \tag{2.1.7}$$

An equivalent representation, also due to Weierstrass, expresses $\Gamma(z)$ as a limit through

$$\Gamma(z) = \lim_{N\to\infty}\frac{N!\,N^z}{z(z+1)\cdots(z+N-1)} \qquad (z \in \mathbb{C}\setminus\mathbb{Z}_{\leq 0}). \tag{2.1.8}$$

The denominator here is the rising factorial, or *Pochhammer symbol*, $(z)_N$.

From the limit representation (2.1.8), the Laurent expansion around the simple poles at $z = -n$ ($n \in \mathbb{N}_0$) is obtained as

$$\Gamma(\epsilon - n) = \frac{(-1)^n}{n!}\left(\frac{1}{\epsilon} - \gamma + H_n\right) + O(\epsilon) \qquad (n \in \mathbb{N}_0), \tag{2.1.9}$$

where H_n denotes the *n-th harmonic number* $H_n = \sum_{k=1}^{n} \frac{1}{k}$.

Induced by its recurrence relation, the gamma function satisfies several classical functional identities of central importance. *Euler's reflection formula* reads

$$\Gamma(z)\,\Gamma(1-z) = \frac{\pi}{\sin(\pi z)} \qquad (z \notin \mathbb{Z}), \tag{2.1.10}$$

while *Legendre's duplication formula* takes the form

$$\Gamma(z)\,\Gamma\left(z + \frac{1}{2}\right) = 2^{(1-2z)}\sqrt{\pi}\,\Gamma(2z). \tag{2.1.11}$$

From Eq. (2.1.10), one derives the more general shift identity

$$\Gamma(z - n) = (-1)^{n-1}\frac{\Gamma(-z)\,\Gamma(1+z)}{\Gamma(n+1-z)} \qquad (n \in \mathbb{N}). \tag{2.1.12}$$

Because the gamma function is the Mellin transform of the exponential, it appears commonly in the kernels of asymptotic expansions obtained via *h-transform* methods. Consequently, explicit knowledge of its asymptotic behaviour in the complex plane is essential for deriving precise error estimates. Using Euler-Maclaurin summation techniques, we show in Example A.4.5 that the logarithm of the gamma function admits the *Stirling series*

$$\log\Gamma(z) = \left(z - \frac{1}{2}\right)\log z - z + \frac{1}{2}\log 2\pi + \Omega(z), \tag{2.1.13}$$

where the remainder term $\Omega(z)$ is given explicitly by the Euler-Maclaurin remainder form

$$\Omega(z) = \int_0^\infty \frac{\Delta_2(t)}{2\,(t+z)^2}\,\mathrm{d}t \qquad (|\arg(z)| < \pi), \tag{2.1.14}$$

with $\Delta_2(t) = B_{2r} - B_{2r}(t - \lfloor t \rfloor)$ defined in terms of *Bernoulli numbers* and *periodic Bernoulli polynomials* (see Def. A.4.2). Repeated integration by parts of Eq. (2.1.14) yields the asymptotic expansion

$$\Omega(z) \sim \sum_{r=1}^{\infty} \frac{B_{2r}}{2r(2r-1)z^{2r-1}} \qquad (|z| \to \infty,\ |\arg(z)| < \pi), \tag{2.1.15}$$

which demonstrates in particular that $\Omega(z) = O(|z|^{-1})$, thereby yielding Stirling's approximation

$$|\Gamma(z+\alpha)| \sim \sqrt{2\pi}\, \mathrm{e}^{-\Re(z)} |z|^{\Re(z+\alpha)-\frac{1}{2}} \mathrm{e}^{-\Im(z+\alpha)\arg(z)}. \tag{2.1.16}$$

For asymptotic estimates along complex contours, one may employ the representation [30]

$$\begin{aligned} \log|\Gamma(\alpha+s\beta)| &\sim \beta R\cos\theta\log(\beta R) - \beta R\big(\theta\sin\theta+\cos\theta\big) + \left(\Re\alpha-\tfrac{1}{2}\right)\log(\beta R), \\ \log|\Gamma(\alpha-s\beta)| &\sim -\beta R\cos\theta\log(\beta R) + \beta R\big(\theta\sin\theta+\cos\theta\big) + \left(\Re\alpha-\tfrac{1}{2}\right)\log(\beta R) \\ &\quad - \log\big|\sin\big(\pi(\alpha-\beta s)\big)\big|, \end{aligned} \tag{2.1.17}$$

where $s = R\mathrm{e}^{\mathrm{i}\theta}$ and $\beta > 0$. For $\theta \to 0$, these reduce to

$$\log|\Gamma(\alpha \pm \beta s)| = \pm\beta R\log(\beta R) + O(R), \tag{2.1.18}$$

while for $\theta \to \pm\pi/2$ one obtains

$$\log|\Gamma(\alpha \pm \beta s)| = -\frac{\pi}{2}\beta R + \left(\Re\alpha - \frac{1}{2}\right)\log(\beta R). \tag{2.1.19}$$

These estimates determine the decay behaviour of MB integrands along limiting contours. The restriction ($|\arg(z)| < \frac{\pi}{2}$) in Eq. (2.1.3) arises solely from the chosen contour; it may be lifted by deformation of the contour into the left half-plane $\frac{\pi}{2} < |\arg(s)| < \pi$, enclosing the negative real axis. Thus, such angular limitations are not intrinsic to the MB representation itself but rather to the contour of integration.

For later reference, we also collect several explicit values of the gamma function and its derivatives, as these frequently appear in residue evaluations.

Legendre's duplication formula (2.1.11) gives the half-integer values as

$$\Gamma\left(\frac{2n+1}{2}\right) = \frac{\sqrt{\pi}\,\Gamma(2n+1)}{2^n\,\Gamma(n+1)} \qquad (n \in \mathbb{N}_0). \tag{2.1.20}$$

From which follow $\Gamma\left(\frac{1}{2}\right) = \sqrt{\pi}$, $\Gamma\left(\frac{3}{2}\right) = \frac{\sqrt{\pi}}{2}$, $\Gamma\left(\frac{5}{2}\right) = \frac{3\sqrt{\pi}}{4}$.

Using Eq. (2.1.8), we have

$$\begin{aligned} \log\Gamma(z) &= \lim_{N\to\infty}\left[z\log N + \log(N!) - \sum_{n=0}^{N}\log(z+n)\right], \\ \frac{\mathrm{d}}{\mathrm{d}z}\log\Gamma(z) &= -\gamma + \sum_{n=0}^{\infty}\left(\frac{1}{n+1} - \frac{1}{z+n}\right), \end{aligned} \tag{2.1.21}$$

where γ denotes the Euler-Mascheroni constant (2.1.6). Evaluating at $z = \frac{1}{2}$ gives

$$\begin{aligned} &\frac{\mathrm{d}}{\mathrm{d}z}\log\Gamma(z)\Big|_{z=\frac{1}{2}} = -\gamma - 2\log 2, \\ \Rightarrow \quad &\frac{\mathrm{d}}{\mathrm{d}z}\Gamma(z)\Big|_{z=\frac{1}{2}} = -\sqrt{\pi}\left(\log 4 + \gamma\right). \end{aligned} \tag{2.1.22}$$

Similarly, for $z = 3$ one finds

$$\begin{aligned} &\frac{\mathrm{d}}{\mathrm{d}z}\log\Gamma(z)\Big|_{z=3} = -\gamma + \frac{3}{2}, \\ \Rightarrow \quad &\frac{\mathrm{d}}{\mathrm{d}z}\Gamma(z)\Big|_{z=3} = 2\left(\frac{3}{2} - \gamma\right). \end{aligned} \tag{2.1.23}$$

Lastly, the beta function, or Euler's integral of the first kind, is defined in terms of Γ by

$$B(z_1, z_2) = \frac{\Gamma(z_1)\Gamma(z_2)}{\Gamma(z_1+z_2)}. \tag{2.1.24}$$

Inserting the integral definition (2.1.2) and substituting $u = st$, $v = s - u$, one obtains

$$\Gamma(z_1)\Gamma(z_2) = \int_0^\infty s^{z_1+z_2-1}\mathrm{e}^{-s}\,\mathrm{d}s\int_0^1 t^{z_1-1}(1-t)^{z_2-1}\,\mathrm{d}t \qquad (\Re(z_1) > 0,\ \Re(z_2) > 0). \tag{2.1.25}$$

An additional integral representation is given by

$$\int_0^{\pi/2}\cos^{x-1}\theta\,\cos(y\theta)\,\mathrm{d}\theta = \frac{\pi}{2^x x\,B\left(\frac{x+y+1}{2},\,\frac{x-y+1}{2}\right)}. \tag{2.1.26}$$

2.2 The Riemann Zeta Function

The Riemann zeta function originates from the Dirichlet series

$$\zeta(s) = \sum_{n=1}^{\infty}\frac{1}{n^s} \qquad (\Re(s) > 1), \tag{2.2.1}$$

which, by Cauchy's integral test, converges absolutely and uniformly on any half-plane $\Re(s) = \sigma > 1 + \varepsilon$, for arbitrary $\varepsilon > 0$. It generalises to the *Hurwitz zeta function*

$$\zeta(s, a) = \sum_{n=0}^{\infty} \frac{1}{(n+a)^s} \qquad (\Re(s) > 1,\ a \in \mathbb{R} \setminus \mathbb{Z}_{\leq 0}), \tag{2.2.2}$$

which coincides with $\zeta(s)$ at $a = 1$.

The study of series of reciprocal powers traces back to Pietro Mengoli and, in particular, the celebrated Basel problem

$$\sum_{n=1}^{\infty} \frac{1}{n^2} = 1 + \frac{1}{2^2} + \frac{1}{3^2} + \dots .$$

Euler resolved this problem by establishing the identity $\zeta(2) = \pi^2/6$ [31] and subsequently obtained the general formula for $\zeta(2n)$ in terms of Bernoulli numbers (see Eq. (2.2.6)), giving explicit evaluations up to $\zeta(12)$.

A fundamental property of $\zeta(s)$ is its connection to the prime numbers, expressed through *Euler's product formula* [32]

$$\zeta(s) = \prod_{p \in \mathbb{P}} \frac{1}{1 - p^{-s}} \qquad (\Re(s) > 1), \tag{2.2.3}$$

where the product is taken over all primes. Euler deduced from this identity that the divergence of $\zeta(1)$ implies the divergence of the series $\sum_p 1/p$, proving that the primes are dense. More generally, Euler products arise for Dirichlet series with multiplicative coefficients, reflecting the unique prime factorisation of integers.

A major breakthrough in the understanding of $\zeta(s)$ was achieved by Riemann in his 1859 memoir [33]. He extended $\zeta(s)$ to a meromorphic function on the entire complex plane, analytic except for a simple pole at $s = 1$, and obtained the contour integral representation

$$\zeta(s) = \frac{\Gamma(1-s)}{2\pi i} \int_{\mathcal{H}} \frac{(-x)^{s-1}}{e^x - 1}\, \mathrm{d}x \qquad (s \in \mathbb{C} \setminus \{1\}), \tag{2.2.4}$$

where $\mathcal{H}$ denotes a *Hankel contour* encircling the positive real axis (see Example A.3.2).

Expanding (2.2.4) about the pole at $s = 1$ yields the Laurent expansion

$$\begin{aligned} \zeta(s) &= \frac{1}{s-1} + \gamma + \gamma_1 (s-1) + \gamma_2 (s-1)^2 + \cdots , \\ \gamma_k &= \lim_{n \to \infty} \left[\sum_{\nu=1}^{n} \frac{(\log \nu)^k}{\nu} - \frac{(\log n)^{k+1}}{k+1} \right], \end{aligned} \tag{2.2.5}$$

where $\gamma = \gamma_0$ is the Euler-Mascheroni constant.

Furthermore, expanding the integrand in (2.2.4) using the geometric series and evaluating the resulting Mellin transforms gives the values of the zeta function at even positive integers as

$$\zeta(2n) = \frac{(-1)^{n+1} B_{2n} (2\pi)^{2n}}{2(2n)!} \qquad (n \in \mathbb{N}), \tag{2.2.6}$$

expressing $\zeta(2n)$ in terms of Bernoulli numbers B_{2n} and thereby recovering Euler's results. A detailed derivation is given in Example A.3.2 together with Definition A.4.2.

A central feature of $\zeta(s)$ is its *functional equation*, established in [33] (and derived in Example A.3.2),

$$\pi^{-s/2}\Gamma\left(\frac{s}{2}\right)\zeta(s) = \pi^{-(1-s)/2}\Gamma\left(\frac{1-s}{2}\right)\zeta(1-s), \tag{2.2.7}$$

which is symmetric under $s \mapsto 1-s$. It shows that $\zeta(s)$ has *trivial zeros* at negative even integers $s = -2n$ due to the poles of $\Gamma(s/2)$. Using the Euler product together with (2.2.7), one finds that all remaining, or *non-trivial*, zeros must lie in the strip $0 \le \Re(s) \le 1$. Hadamard [34] and La Vallée Poussin [35] sharpened this to show that $\zeta(s) \neq 0$ on the boundary lines $\Re(s) = 0$ and $\Re(s) = 1$; hence all non-trivial zeros lie in the *critical strip* $0 < \Re(s) < 1$.

The symmetry of the functional equation motivated Riemann's celebrated conjecture that all non-trivial zeros lie on the *critical line* $\Re(s) = \frac{1}{2}$, now known as the *Riemann Hypothesis* (RH). This conjecture remains open and is one of the Clay Mathematics Institute's Millennium Prize Problems [36].

Riemann introduced the *xi function*

$$\xi(s) = \frac{1}{2}s(s-1)\pi^{-s/2}\Gamma\left(\frac{s}{2}\right)\zeta(s), \tag{2.2.8}$$

which satisfies the functional identity

$$\xi(s) = \xi(1-s). \tag{2.2.9}$$

He anticipated the factorisation

$$\xi(s) = \xi(0)\prod_{\rho}\left(1 - \frac{s}{\rho}\right), \tag{2.2.10}$$

where the product runs over non-trivial zeros ρ of $\zeta(s)$. Using Stirling's estimate (2.1.16), one sees that $\xi(s)$ is an entire function of order 1, implying that the sum of reciprocals of $|\rho|$ diverges and therefore that infinitely many non-trivial zeros exist. Hardy [37] later proved that infinitely many lie on the critical line.

The factorisation (2.2.10) was rigorously established by Hadamard [38], who obtained the

product representation

$$\zeta(s) = \frac{\mathrm{e}^{(\log(2\pi)-1-\gamma/2)\,s}}{2(s-1)\Gamma(1+s/2)} \prod_{\rho} \left(1 - \frac{s}{\rho}\right) \mathrm{e}^{s/\rho}. \tag{2.2.11}$$

Regarding the asymptotic behaviour of the zeta function, note that for $\Re(s) = \sigma > 1$ the Dirichlet series representation implies the uniform bound

$$|\zeta(s)| \leq \zeta(\sigma). \tag{2.2.12}$$

Combined with the functional equation, this yields the asymptotic estimate

$$\zeta(s) = O\left(t^{\frac{1}{2}-\sigma}\right) \qquad (\sigma < 0,\ t \to \infty). \tag{2.2.13}$$

Inside the critical strip $0 < \sigma < 1$, general Dirichlet series theory provides

$$\zeta(s) = O\left(t^{\frac{1}{2}(1-\sigma)+\varepsilon}\right) \qquad (0 < \sigma < 1), \tag{2.2.14}$$

leading to Lindelöf's estimate [39],

$$\zeta(s) = O\left(t^{\mu(\sigma)} \log^{A} t\right), \tag{2.2.15}$$

where

$$\mu(\sigma) = \begin{cases} 0 & \sigma > 1, \\ \frac{1}{2}(1-\sigma) & 0 \leq \sigma \leq 1, \\ \frac{1}{2} - \sigma & \sigma < 0, \end{cases}$$

and $A > 0$ in the critical strip. The *Lindelöf hypothesis* (implied by RH [40]) sharpens this to

$$\mu(\sigma) = \begin{cases} 0 & \sigma \geq \frac{1}{2}, \\ \frac{1}{2} - \sigma & \sigma \leq \frac{1}{2}. \end{cases} \tag{2.2.16}$$

Such bounds directly influence the size of possible zero-free regions and thus the accuracy of error terms in the prime number theorem [41, 42].

Concerning the number of roots in the critical strip, let $N(T)$ denote the number of non-trivial zeros $\rho = \sigma + it$ with $0 < \sigma < 1$ and $0 \leq t < T$. Riemann conjectured, and Mangoldt proved [44], that

$$N(T) = \frac{T}{2\pi} \log \frac{T}{2\pi} - \frac{T}{2\pi} + O(\log T). \tag{2.2.17}$$

Consequently, to identify the zeros, one counts the sign changes of the ξ-function along the critical line, since $\xi\left(\frac{1}{2}+it\right)$ is real for real t by the functional equation (2.2.9), and compares this with the asymptotic formula for $N(T)$. In this way one verifies that all zeros found indeed lie on the critical line, thereby providing strong numerical evidence in favour of the RH . Using approximate functional equations, the RH has been tested numerically up to $T \approx 10^{13}$ [3, 45, 46].

The connection between primes and zeros is made precise through Riemann's explicit formula. Mangoldt [43] established, for the *second Chebyshev function*

$$\psi(x) = \sum_{p^n<x} \log p = x - \sum_{\rho} \frac{x^\rho}{\rho} - \frac{\zeta'(0)}{\zeta(0)} - \frac{1}{2}\log(1-x^{-2}), \tag{2.2.18}$$

where the sum is over non-trivial zeros ρ. Gauss [47] and Legendre [48] conjectured that the *prime-counting function* $\pi(x)$ satisfies the *prime number theorem* (PNT)

$$\pi(x) \sim \frac{x}{\log x} \qquad (x \to \infty).$$

Chebyshev [49] showed that this is equivalent to $\psi(x) \sim x$. From (2.2.18), the PNT follows once one proves that

$$\lim_{x\to\infty} \sum_{\rho} \frac{x^{\rho-1}}{\rho} = 0,$$

which holds if and only if every non-trivial zero satisfies $\Re(\rho) < 1$. Drawing on the result of Mangoldt, who confirmed that the limit can be taken termwise, Hadamard [34] and La Vallée Poussin [35] independently established precisely this zero-free region, thereby completing the first proof of the PNT .

Finally, Eq. (2.2.18) shows that sharper error terms in the PNT correspond directly to enlarging the zero-free region of $\zeta(s)$ within the critical strip. In particular, the RH is equivalent to the optimal bound

$$\psi(x) = x + o\left(\sqrt{x}\,\log x\right) \qquad (x \to \infty).$$

2.3 The Modified Bessel Function of the Second Kind

Modified Bessel functions arise as solutions of the *modified Bessel differential equation*

$$z^2\frac{\mathrm{d}^2 w}{\mathrm{d}z^2} + z\frac{\mathrm{d}w}{\mathrm{d}z} - (z^2+\nu^2)\,w = 0 \qquad (\nu \in \mathbb{C}). \tag{2.3.1}$$

This equation admits solutions representable via MB integrals. A general contour representa-

tion is

$$w(z) = \frac{C}{2\pi i} \int_{\sigma-i\infty}^{\sigma+i\infty} \Gamma\left(s + \tfrac{\nu}{2}\right) \Gamma\left(s - \tfrac{\nu}{2}\right) p(s) \left(\tfrac{1}{2}z\right)^{-2s} \mathrm{d}s, \tag{2.3.2}$$

where $p(s)$ denotes a periodic function of unit period and σ lies within the strip of analyticity of the integrand. Here $(\frac{z}{2})^{\nu}$ is taken in its principal branch, inducing a cut along $\arg(z) = \pm\pi$. A full derivation of Eq. (2.3.2) is deferred to Example A.3.4.

The simplest choice $p(s) = 1$ with $(2\sigma > |\Re\nu|)$ leads, using the gamma asymptotics (2.1.19), to a convergent representation whenever $(|\arg(z)| < \frac{\pi}{2})$. By displacing the contour and evaluating residues at $s = \pm\frac{\nu}{2} - k$ $(k \in \mathbb{N}_0)$, one recovers the series expansions

$$I_\nu(z) = \left(\tfrac{1}{2}z\right)^{\nu} \sum_{k=0}^{\infty} \frac{\left(\frac{1}{4}z^2\right)^k}{k!\,\Gamma(\nu + k + 1)}, \tag{2.3.3}$$

$$K_\nu(z) = \frac{\pi}{2} \frac{I_{-\nu}(z) - I_\nu(z)}{\sin(\pi\nu)}, \tag{2.3.4}$$

which define the *modified Bessel function of the first kind* $I_\nu(z)$ and the modified Bessel function of the second kind $K_\nu(z)$. Both functions are real for real ν and positive real z.

For large $|z|$, the modified Bessel function of the second kind decays exponentially [50]:

$$K_\nu(z) \sim \sqrt{\frac{\pi}{2z}}\, \mathrm{e}^{-z} \left(1 + O\left(\tfrac{1}{z}\right)\right) \qquad \left(|\arg(z)| < \tfrac{3\pi}{2}\right). \tag{2.3.5}$$

In contrast, near the origin its leading behaviour is given by [23]

$$K_\nu(z) \sim \frac{\Gamma(\nu)}{2}\left(\frac{2}{z}\right)^{\nu} \qquad (\Re\nu > 0,\ z \to 0), \tag{2.3.6}$$

$$K_0(z) \sim -\log z \qquad (z \to 0). \tag{2.3.7}$$

For later purposes, we insert $p(s) = 1$ into (2.3.2) to express $K_\nu(z)$ [51] as:

$$K_\nu(z) = \frac{\left(\frac{1}{2}z\right)^{\nu}}{4\pi i} \int_{c-i\infty}^{c+i\infty} \Gamma(t)\, \Gamma(t - \nu) \left(\tfrac{1}{2}z\right)^{-2t} \mathrm{d}t, \tag{2.3.8}$$

valid for

$$c > \max\{0, \Re\nu\} \qquad |\arg(z)| < \tfrac{\pi}{2}.$$

The first condition ensures that the contour lies to the right of the poles of the integrand, while the second condition guarantees convergence via the gamma asymptotics (2.1.19).

Chapter 3

One-Loop Thermal Quasiparticle Pressure

Performing the spatial coarse-graining procedure mentioned in Sect. 1, and incorporating fluctuations of the trivial-topology sector through an effective gauge field a_μ, the scalar field ϕ couples minimally via

$$D_\mu \phi = \partial_\mu \phi + ie \left[\phi, a_\mu\right] . \tag{3.0.1}$$

The resulting effective Yang–Mills action in the deconfined phase takes the form [19]

$$S = \mathrm{tr} \int_0^\beta \mathrm{d}\tau \int \mathrm{d}^3 x \left(\frac{1}{2} G_{\mu\nu} G_{\mu\nu} + (D_\mu \phi)^2 + \frac{\Lambda^6}{\phi^2} \right), \tag{3.0.2}$$

where the field-strength tensor

$$G_{\mu\nu} = \partial_\mu a_\nu - \partial_\nu a_\mu - ie[a_\mu, a_\nu] \tag{3.0.3}$$

encodes fluctuations of the effective gauge field a_μ. Here, Λ denotes the Yang–Mills scale, and e represents the effective gauge coupling [21].

The existence of the scalar field ϕ is attributed to non-interacting, unit-topological-charge (anti)calorons whose size is comparable to the maximal resolution set by $|\phi|$. Reinstating explicit powers of $\hbar$, one observes by dimensional power counting of the kinetic term that the gauge field a_μ scales as $\sqrt{\hbar}$. Consequently, inspection of the self-interaction term reveals that the effective coupling e scales as $1/\sqrt{\hbar}$, reflecting its emergent quantum character [52].

3.1 Quasiparticle Spectrum and Effective Thermodynamics

The covariant derivative induces quasiparticle masses through the adjoint Higgs mechanism associated with each broken generator t^a. Specialising to SU(2) and working in unitary gauge yields the symmetry-breaking pattern

$$\mathrm{SU}(2) \to \mathrm{U}(1), \tag{3.1.1}$$

such that the spectrum consists of two tree-level heavy (TLH) and one tree-level massless (TLM) gauge mode:

$$m_a^2 = -2\mathrm{e}^2 \,\mathrm{tr}[\phi, t^a][\phi, t^a], \tag{3.1.2}$$

$$m_1^2 = m_2^2 = 4\mathrm{e}^2 \frac{\Lambda^3}{2\pi T}, \qquad m_3 = 0. \tag{3.1.3}$$

The above has been evaluated in unitary gauge $\phi = 2|\phi|t^3$, with $|\phi|^2 = \Lambda^3/(2\pi T)$ setting the effective mass scale. Mass generation is therefore a quantum effect originating from the non-trivial background configuration ϕ. Owing to the inertness of this background field, the TLH modes remain on their mass shell and contribute only through thermal propagation.

Expanding the action (3.0.2) to quadratic order in the fluctuations δa_μ about the background configuration $a_\mu = a_\mu^{\mathrm{gs}} + \delta a_\mu$, and subsequently integrating out the Gaussian fluctuations, yields the one-loop effective potential. This expression is obtained after performing a Wick rotation to Euclidean time and subtracting the zero-temperature contribution. The latter is negligible because the inert background field ϕ imposes a maximal resolution scale $|\phi|$ on all interaction vertices, thereby suppressing hard vacuum fluctuations [19].

The resulting one-loop pressure and energy density read [19, 21, 22, 53]

$$P(\lambda) = -\Lambda^4 \left\{ \frac{2\lambda^4}{(2\pi)^6} \left[2\overline{P}(0) + 6\overline{P}(a) \right] + 2\lambda \right\}, \tag{3.1.4}$$

$$\rho(\lambda) = \Lambda^4 \left\{ \frac{2\lambda^4}{(2\pi)^6} \left[2\overline{\rho}(0) + 6\overline{\rho}(a) \right] + 2\lambda \right\}, \tag{3.1.5}$$

where the dimensionless integrals

$$\overline{P}(y) = \int_0^\infty \mathrm{d}x\, x^2 \log\left[1 - \exp\left(-\sqrt{x^2 + y^2} \right) \right], \tag{3.1.6}$$

$$\overline{\rho}(y) = \int_0^\infty \mathrm{d}x\, x^2 \frac{\sqrt{x^2 + y^2}}{\exp\left(\sqrt{x^2 + y^2} \right) - 1}, \tag{3.1.7}$$

encode the thermal quasiparticle contributions, and we have introduced the abbreviations

$$a = \frac{m}{T}, \qquad \lambda = \frac{2\pi T}{\Lambda}. \tag{3.1.8}$$

The prefactors in (3.1.4)-(3.1.5) account for the two polarisations of the TLM mode, the three of each TLH mode (counted twice), and the thermal ground state contribution represented by the term 2λ.

Proceeding beyond one-loop order differs substantially from conventional Yang–Mills computations. The momentum transfers at each vertex are restricted so as to not resolve the constituent calorons that emerged in the coarse-graining procedure. In unitary Coulomb gauge, this restriction manifests itself as hard cutoffs in the momentum integrals, thereby avoiding the ultraviolet divergences that would otherwise necessitate renormalisation. Infrared divergences are absent as well, due to the presence of a mass gap in two of the gauge-field directions of SU(2). Furthermore, each additional vertex insertion in higher-loop diagrams further constrains the allowed momentum transfers and off-shell deviations. It is conjectured that, by virtue of these constraints, the loop expansion of the deconfining pressure terminates at finite order, up to possible resummations of certain n-PI diagrams [19]. Numerical Monte Carlo simulations show that, up to the three-loop level, the one-loop approximation already attains an accuracy better than one percent [20].

3.2 Mass Parameter Evolution

Thermodynamic consistency requires that $\partial_m P = 0$, ensuring that no implicit temperature dependence of the mass $m(T)$ contaminates the derivative $\mathrm{d}P/\mathrm{d}T$ entering the identity $\rho = T\,\mathrm{d}P/\mathrm{d}T - P$. Together with this identity, the condition $\partial_m P = 0$ yields a first-order differential equation for the dimensionless mass parameter $a(\lambda)$

$$\partial_a \lambda = -\frac{6\lambda^4}{(2\pi)^6}\,\frac{a\,\overline{D}(a)}{1+\frac{6\lambda^3 a^2}{(2\pi)^6}\overline{D}(a)}, \tag{3.2.1}$$

where

$$\overline{D}(a) = \int_0^\infty \mathrm{d}x\,\frac{x^2}{\sqrt{x^2+a^2}}\,\frac{1}{\exp\left(\sqrt{x^2+a^2}\right)-1}. \tag{3.2.2}$$

The auxiliary function $\overline{D}(a)$ is related to $\overline{P}(a)$ by

$$\overline{D}(a) = 2\,\partial_{a^2}\overline{P}(a), \tag{3.2.3}$$

and satisfies the identity

$$\overline{\rho}(a) + 3\,\overline{P}(a) = a^2\overline{D}(a), \tag{3.2.4}$$

which follows from integration by parts.

3.3 Dimensional Formulation and Asymptotic Expansions

To analyse the fixed points of Eq. (3.2.1) and to access the limiting behaviour of the mass parameter at high and low temperatures, one requires asymptotic representations of the integral functions $\overline{P}(a)$ and $\overline{D}(a)$. In particular, the regimes $a \to 0$ and $a \to \infty$ correspond to the relativistic (high-temperature) and Boltzmann-suppressed (low-temperature) limits, respectively. Before deriving these asymptotic series explicitly, it is instructive to generalise the formulation of the pressure to $d + 1$ spacetime dimensions.

This is motivated by the fact that dimensional extensions often reveal structural connections between thermodynamic quantities and analytic properties of the Riemann zeta function. For example, the total number of particles N in a non-relativistic, non-interacting, spin-zero Bose gas can be shown to be directly proportional to $\zeta\left(\frac{d}{2}\right)$. Here, the pole of the Riemann zeta function at $s = 1$, corresponds to $d = 2$, where infrared divergences prevent the existence of a finite critical temperature for Bose–Einstein condensation, reflecting the Mermin–Wagner–Hohenberg theorem [54, 55].

Additionally, apart from its interpretation as a spatial dimension, it turns out that the additional parameter d simplifies derivative expansions. In this extended sense, the differential relation

$$2\,\partial_{a^2}\overline{P}_d(a) = (2-d)\,\overline{P}_{(d-2)}(a) \tag{3.3.1}$$

establishes a recursion identity connecting the pressure in d and $(d-2)$ dimensions. This relation renders subsequent derivations almost trivial.

3.3.1 Dimensional Generalisation of the Pressure

Starting from the three-dimensional representation (3.1.6), the generalisation to d spatial dimensions is achieved by exploiting the homogeneity of the dispersion relation. The corre-

sponding dimensionless pressure is

$$\begin{aligned}\overline{P}_d(a) &= \int_0^\infty x^{d-1} \log\left(1 - \mathrm{e}^{-\sqrt{x^2+a^2}}\right) \mathrm{d}x \\ &= -\sum_{n=1}^{\infty} \frac{1}{n} \int_0^\infty x^{d-1} \mathrm{e}^{-n\sqrt{x^2+a^2}} \,\mathrm{d}x \\ &= -\sum_{n=1}^{\infty} \frac{1}{n} \int_a^\infty t\,(t^2-a^2)^{\frac{d}{2}-1} \mathrm{e}^{-nt} \,\mathrm{d}t.\end{aligned} \tag{3.3.2}$$

In the second line, the logarithm is expanded as the exponent within is smaller than one and the order of summation and integration is interchanged. This is justified because for all $n \geq 1$ and $x \geq 0$,

$$0 \leq x^{d-1}\mathrm{e}^{-n\sqrt{x^2+a^2}} \leq x^{d-1}\mathrm{e}^{-nx},$$

and the latter integrates to $\Gamma(d)/n^d$, giving a uniform integrable bound. Thus the dominated convergence theorem ensures that the exchange of sum and integral is valid. Finally, the substitution $t = \sqrt{x^2 + a^2}$ with $t\,\mathrm{d}t = x\,\mathrm{d}x$ yields the last line of (3.3.2).

To evaluate this expression systematically, we employ the MB technique A.3. Identifying $h(t) = \mathrm{e}^{-t}$, whose Mellin transform is $\mathcal{M}[h; s] = \Gamma(s)$, and defining the auxiliary function

$$f(t) = \begin{cases} 0, & (0 \leq t < a)\,, \\ t\,(t^2-a^2)^{\frac{d}{2}-1}, & (t \geq a)\,, \end{cases} \tag{3.3.3}$$

Parseval's identity for Mellin transforms (cf. Theorem A.3.1) can be applied in the form

$$\int_0^\infty f(t)\, h(xt)\,\mathrm{d}t = \frac{1}{2\pi i} \int_{c-i\infty}^{c+i\infty} x^{-s}\, \mathcal{M}[f; 1-s]\, \mathcal{M}[h; s]\,\mathrm{d}s, \tag{3.3.4}$$

interpreted in a generalised sense: although individual Mellin transforms may diverge, their analytic continuations yield meaningful asymptotic results when the contour is deformed across the poles of the integrand.

The Mellin transform of f is computed in Example A.3.1, and reads

$$\mathcal{M}[f; s] = \tfrac{1}{2}a^{s+d-1}\, B\left(\tfrac{d}{2}, -\tfrac{s+d-1}{2}\right) = \tfrac{1}{2}a^{s+d-1} \frac{\Gamma\left(\frac{d}{2}\right)\Gamma\left(-\frac{s+d-1}{2}\right)}{\Gamma\left(\frac{1-d-s}{2} + \frac{d}{2}\right)}. \tag{3.3.5}$$

Note, that the Mellin transform of (3.3.3) is initially defined only for $\Re(s) < 1 - d$. The analytic continuation of the gamma functions, however, extends its validity to all complex s.

Substitution into Eq. (3.3.4) gives

$$\overline{P}_d(a) = -\sum_{n=1}^{\infty} \frac{1}{n} \left[\frac{1}{4\pi i} \int_{\sigma-i\infty}^{\sigma+i\infty} n^{-s} a^{d-s} \frac{\Gamma\left(\frac{d}{2}\right) \Gamma\left(\frac{s-d}{2}\right)}{\Gamma\left(\frac{s}{2}\right)} \Gamma(s)\, \mathrm{d}s \right], \tag{3.3.6}$$

where $\sigma > d$ ensures convergence of the integral.

Applying Legendre's duplication formula (2.1.11), interchanging the order of summation and integration, and simplifying by scaling and shifting the contour, we obtain

$$\overline{P}_d(a) = -\frac{a^{2\kappa}\Gamma\left(\frac{d}{2}\right)}{4\sqrt{\pi}} \left[\frac{1}{2\pi i} \int_{\sigma-i\infty}^{\sigma+i\infty} \left(\frac{a}{2}\right)^{-2s} \zeta(2s)\Gamma(s)\Gamma(s-\kappa)\, \mathrm{d}s \right], \tag{3.3.7}$$

where $\kappa = \frac{d+1}{2}$ and $\sigma > \max\left(\frac{1}{2}, \kappa\right)$.

Introducing the surface area of the unit d-sphere,

$$\Omega_d = \frac{2\pi^{d/2}}{\Gamma(d/2)}, \tag{3.3.8}$$

and writing $a = 2\pi z$, the dimensionally generalised pressure becomes

$$P_d(a) = -\pi^{\kappa} \left(\frac{z}{\beta}\right)^{2\kappa} \left[\frac{1}{2\pi i} \int_{\sigma-i\infty}^{\sigma+i\infty} \zeta(2s)\, \Gamma(s)\, \Gamma(s-\kappa)\, (\pi z)^{-2s}\, \mathrm{d}s \right]. \tag{3.3.9}$$

The contour integral converges absolutely for $|\arg z| < \frac{\pi}{2}$ (cf. (2.1.19)). Analytic continuation beyond this sector can be achieved by deforming the contour to the left, which crosses the poles of the integrand and thereby generates the asymptotic expansion. The contour passes through the singular structures of $\Gamma(s)$, $\Gamma(s-\kappa)$, and $\zeta(2s)$, each contributing distinct residue series.

Expressing the zeta function through its Dirichlet series and employing the standard integral representation of the modified Bessel function, we arrive at the equivalent series form

$$\overline{P}_d(a) = -(2a)^{\kappa} \frac{\Gamma\left(\kappa - \frac{1}{2}\right)}{2\sqrt{\pi}} \sum_{n=1}^{\infty} n^{-\kappa} K_{\kappa}(na) \tag{3.3.10}$$

$$P_d(a) = -2\left(\frac{a}{2\pi\beta^2}\right)^{\kappa} \sum_{n=1}^{\infty} n^{-\kappa} K_{\kappa}(na). \tag{3.3.11}$$

Inspection of Eq. (3.3.9) reveals that the integrand possesses poles at $s = 0$ and $s = \frac{1}{2}$, as well as at $s = \kappa - n$ with $n \in \mathbb{N}$. For even d, the poles of the Riemann zeta function coincide with those of the gamma function, whereas for odd d their product yields a double pole. In both

cases, a logarithmic singularity in $\log z$ remains, signalling the characteristic non-analytic term in the asymptotic expansion.

Crucially, by $\overline{D}_d(a) = 2\partial_{a^2}\overline{P}_d(a)$ and gamma's recurrence relation

$$\begin{aligned}\overline{D}_d(a) &= \frac{a^{2(\kappa-1)}\Gamma\left(\frac{d}{2}\right)}{2\sqrt{\pi}}\left[\frac{1}{2\pi i}\int_{\sigma-i\infty}^{\sigma+i\infty}\left(\frac{a}{2}\right)^{-2s}\zeta(2s)\,\Gamma(s)\,\Gamma(s+1-\kappa)\;\mathrm{d}s\right] \\ &= (2-d)\overline{P}_{(d-2)}(a),\end{aligned} \tag{3.3.12}$$

which proves Eq. (3.3.1).

3.3.2 Asymptotic Power Series Expansion

We now derive the convergent expansion of the integral in Eq. (3.3.9) for small z,

$$I = \frac{1}{2\pi i}\int_{\sigma-i\infty}^{\sigma+i\infty}\zeta(2s)\Gamma(s)\Gamma(s-\kappa)(\pi z)^{-2s}\,\mathrm{d}s \qquad \left(\sigma > \max\left(\tfrac{1}{2}, \Re\kappa\right)\right). \tag{3.3.13}$$

For convenience, we temporarily treat κ as a complex parameter, $\kappa \in \mathbb{C}$ with $\Re(\kappa) > 0$, rather than fixing it to a physical spatial dimension. This avoids the need for explicit double-pole evaluations in intermediate steps. As the resulting expression defines an entire function of κ, the final result can be analytically continued to all κ, including integer and half-integer values corresponding to the physically relevant dimensions.

Since the derivation closely parallels that in Sect. B.3, we outline only the main steps. For $\Im\kappa \neq 0$, the integrand has simple poles at $s = 0$ (from $\Gamma(s)$), at $s = \frac{1}{2}$ (from $\zeta(2s)$), and at $s = \kappa - n$ with $n \in \mathbb{N}_0$ (from $\Gamma(s-\kappa)$). By contour deformation to the left, one obtains

$$\begin{aligned}I &= \frac{\sqrt{\pi}}{2}\frac{\Gamma\left(\frac{1}{2}-\kappa\right)}{(\pi z)} - \frac{\Gamma(-\kappa)}{2} + \frac{1}{(\pi z)^{2\kappa}}\left\{\sum_{n=0}^{N-1}\frac{(-1)^n}{n!}\,\zeta(2\kappa-2n)\Gamma(\kappa-n)(\pi z)^{2n} + R_N\right\}, \\ R_N &= \frac{1}{2\pi i}\int_{\sigma_N-i\infty}^{\sigma_N+i\infty}\zeta(2s)\Gamma(s)\Gamma(s-\kappa)(\pi z)^{-2s}\,\mathrm{d}s,\end{aligned} \tag{3.3.14}$$

where $\Re\kappa - N < \sigma_N < \Re\kappa + 1 - N$. For clarity, the poles originating from $\Gamma(s-\kappa)$ have been made explicit in the sum, even though this obscures the ordering by pole strength. Consequently, the truncation index should not be chosen as $N < \kappa$, since the contour displacement to $\sigma < 0$ already includes these residues.

The remainder term is easily estimated as $R_N = O(z^{2N-1})$, confirming that the series is at least asymptotic. Apparent singularities at integer and half-integer κ in (3.3.14) are removable by extracting the corresponding term from the series and taking suitable limits.

Returning to the interpretation of κ as a spatial dimension necessitates separate treatments for integer and non-integer values. For fractional κ, the singularity arising from the first term in Eq. (3.3.14) is cancelled by the term with $n = \lfloor\kappa\rfloor$ in the sum. To see this, set $n = \lfloor\kappa\rfloor$ and consider the limit $\kappa \to \kappa - \epsilon$. Then

$$\begin{aligned}&\lim_{\epsilon\to 0}\left\{\frac{\sqrt{\pi}}{2}\,\frac{\Gamma\left(\frac{1}{2}-\kappa+\epsilon\right)}{\pi z}+\frac{1}{\pi z}\,\frac{(-1)^{\lfloor\kappa\rfloor}}{\lfloor\kappa\rfloor!}\,\zeta(2\kappa-2\epsilon-2\lfloor\kappa\rfloor)\,\Gamma(\kappa-\epsilon-\lfloor\kappa\rfloor)\,(\pi z)^{2\epsilon}\right\}\\&=\frac{1}{\sqrt{\pi}\,z}\,\frac{(-1)^{\lfloor\kappa\rfloor}}{\lfloor\kappa\rfloor!}\left[\frac{H_{\lfloor\kappa\rfloor}}{2}-\log(2\pi z)\right],\end{aligned}\tag{3.3.15}$$

where Eqs. (2.1.9) and (2.2.5) have been used.

For integer κ, one finds analogously that the singularities from the second term and the $n = \kappa$ term in Eq. (3.3.14) cancel. Setting $n = \kappa$ and taking the limit $\kappa \to \kappa - \epsilon$ gives

$$\begin{aligned}&\lim_{\epsilon\to 0}\left\{-\frac{\Gamma(\epsilon-\kappa)}{2}+\frac{(-1)^{\kappa}}{\kappa!}\,\zeta(-2\epsilon)\,\Gamma(-\epsilon)\,(\pi z)^{2\epsilon}\right\}\\&=\frac{(-1)^{\kappa}}{\kappa!}\left[\gamma-\frac{H_{\kappa}}{2}+\log\left(\frac{z}{2}\right)\right].\end{aligned}\tag{3.3.16}$$

Collecting all terms and restricting κ to values corresponding to physical spatial dimensions, Eq. (3.3.14) may be written in the unified form

$$\begin{aligned}I&=\frac{1}{2\pi i}\int_{\sigma-i\infty}^{\sigma+i\infty}\zeta(2s)\,\Gamma(s)\,\Gamma(s-\kappa)\,(\pi z)^{-2s}\,\mathrm{d}s\\&=\frac{1}{(\pi z)^{2\kappa}}\sum_{0\le n<\kappa}\frac{(-1)^n}{n!}\,\Gamma(\kappa-n)\,\zeta(2\kappa-2n)\,(\pi z)^{2n}\\&\quad+\begin{cases}-\dfrac{1}{2}\Gamma(-\kappa)+\dfrac{(-1)^{\lfloor\kappa\rfloor}}{\lfloor\kappa\rfloor!}\left[\dfrac{H_{\lfloor\kappa\rfloor}}{2}-\log(2\pi z)\right]\dfrac{1}{\sqrt{\pi}\,z}, & \text{fractional } \kappa,\\[2ex] \dfrac{\Gamma\left(\frac{1}{2}-\kappa\right)}{2\sqrt{\pi}\,z}+\dfrac{(-1)^{\kappa}}{\kappa!}\left[\gamma-\dfrac{H_{\kappa}}{2}+\log\left(\dfrac{z}{2}\right)\right], & \text{integer } \kappa,\end{cases}\\&\quad+\frac{1}{\sqrt{\pi}\,z^{2\kappa}}\sum_{n>\kappa}^{\infty}\frac{(-1)^n}{n!}\,\Gamma\left(n-\kappa+\tfrac{1}{2}\right)\zeta(2n-2\kappa+1)\,z^{2n}.\end{aligned}\tag{3.3.17}$$

We note that the tail sum over $n > \kappa$ converges absolutely for $|z| \le 1$. Indeed, the large-n behaviour of the summand is controlled by the quotient of gamma functions (cf. Example A.4.13), requiring $|z| \le 1$ for absolute convergence. Alternatively, as the summand decays at least as fast as in the case $\kappa = 2$, convergence follows from the derivation performed in Sect. B.

For $|z| > 1$, the series ceases to converge, as the individual terms grow with n. This loss of convergence is directly related to the situation of the first pole of the Bose-Einstein integral in Eq. (3.3.2). Consequently, the asymptotic expansion in the complementary region of a must be derived by contour displacement to the right, as discussed in Sect. 3.3.3.

Specialising to our case $\kappa = 2$ in (3.3.17) and direct evaluation of (3.3.9) gives

$$\begin{aligned}\overline{P}_3(a) = &-2\pi^4\left\{\frac{1}{90} - \frac{1}{6}z^2 + \frac{2}{3}z^3 + 2z^4\left[\frac{1}{4}\log\frac{z}{2} + \frac{\gamma}{4} - \frac{3}{16}\right]\right\} \\ &- 2\pi^{\frac{7}{2}}\sum_{k=3}^{\infty}\frac{\Gamma\left(k-\frac{3}{2}\right)}{\Gamma(k+1)}\zeta(2k-3)(-1)^k z^{2k},\end{aligned} \tag{3.3.18}$$

$$\begin{aligned}P_3(a) = &-\frac{\pi^2}{\beta^4}\left\{\frac{1}{90} - \frac{1}{6}z^2 + \frac{2}{3}z^3 + 2z^4\left[\frac{1}{4}\log\frac{z}{2} + \frac{\gamma}{4} - \frac{3}{16}\right]\right\} \\ &- \frac{\pi^{\frac{3}{2}}}{\beta^4}\sum_{k=3}^{\infty}\frac{\Gamma\left(k-\frac{3}{2}\right)}{\Gamma(k+1)}\zeta(2k-3)(-1)^k z^{2k},\end{aligned} \tag{3.3.19}$$

This expansion converges absolutely for $|z| \leq 1$. Returning to $d = 3$ yields exact agreement with the results of Dolan and Jackiw (see (B.1.1)), thereby confirming the consistency of both the residue calculation and the contour integration method. Since the series converges absolutely for small z, the corresponding expansion of $\overline{D}_d(a)$ follows directly by differentiation with respect to a^2.

Finally, we remark that series representations of the form (3.3.11), together with their integral formulation (3.3.9) and asymptotic structure (3.3.17), closely resemble starting points in deriving asymptotic expansions of the Riemann zeta function within the critical strip. Indeed, by proceeding analogously to Eq. (3.3.14) and solving for the pole contribution $\zeta(2\kappa)$ in terms of the integral I and the remaining regular terms, one obtains expressions similar to exponentially smoothed Riemann-Siegel type expansions. For instance, replacing the modified Bessel function of the second kind by normalised incomplete gamma functions led Paris [56] to derive such an exponentially smoothed asymptotic expansion. Nevertheless, we shall not pursue this direction further, as it would require parting the interpretation of κ as a spatial dimension. Moreover, since κ appears in the order of $K_\kappa(2\pi nz)$, the variable z would have to be adjusted to ensure asymptoticity in κ. For $\kappa = \sigma + it$ with $t \to \pm\infty$, however, the Bessel functions would cease to decay exponentially not allowing for a truncation. At best, this would yield a Gram-type formula requiring $O\left(\frac{t}{2\pi}\right)$ evaluations, which is asymptotically inferior to Riemann-Siegel formulas scaling as $O\left(\sqrt{\frac{t}{2\pi}}\right)$.

3.3.3 Exponential Asymptotic Expansion

Seemingly, contour displacement approaches are limited exclusively to algebraic-type Poincaré expansions. Moreover, the MB integral in (3.3.9) does not possess singularities to the right of the contour. Consequently, the strategy of successive evaluation of the residues fails to produce a meaningful expansion. This suggests that the pressure expansion for large z is of exponential type (cf. Example A.2.1). Nevertheless, we derive an asymptotic expansion using inverse factorial expansions to introduce artificial singularities, whose evaluation gives rise to exponential asymptotic contributions. Since the MB representation (3.3.9) has no singularities for $\sigma > \kappa = \frac{d+1}{2}$, the contour may be shifted freely to the right, ensuring that $|s|$ is large throughout. In this regime one may combine Euler's reflection formula (2.1.10) with the asymptotic expansion for the quotient of gamma functions (A.4.13), yielding

$$\begin{aligned}\Gamma(s)\Gamma(s-\kappa) = (2\pi)^{1/2}2^{1+\kappa-2s}\Bigg[&\sum_{j=0}^{M-1}(-1)^j c_j\,\Gamma\Big(2s-\kappa-\tfrac{1}{2}-j\Big)\\ &+\rho_M(s)\,\Gamma\Big(2s-\kappa-\tfrac{1}{2}-M\Big)\Bigg],\end{aligned} \tag{3.3.20}$$

where $\rho_M(s) = O(1)$ as $|s| \to \infty$ in $|\arg(s)| < \pi$ and M is a positive integer. The coefficients c_j are given by

$$c_j = \frac{(-1)^j}{j!\,8^j}\prod_{r=1}^{j}\left[(2\kappa)^2-(2r-1)^2\right] = \frac{\Gamma\Big(j+\kappa+\frac{1}{2}\Big)\,\Gamma\Big(j-\kappa+\frac{1}{2}\Big)}{2^j\,j!\,\Gamma\Big(\kappa+\frac{1}{2}\Big)\,\Gamma\Big(\frac{1}{2}-\kappa\Big)}, \tag{3.3.21}$$

see also Paris and Kaminski [30]. Assuming $|s|$ large with $\sigma > \frac{\kappa+M}{2} + \frac{1}{4}$ allows us to write

$$\frac{1}{2\pi i}\int_{\sigma-i\infty}^{\sigma+i\infty}\zeta(2s)\Gamma(s)\Gamma\left(s-\kappa\right)(\pi z)^{-2s}\mathrm{d}s = \sum_{n=1}^{\infty}\frac{1}{2\pi i}\int_{\sigma-i\infty}^{\sigma+i\infty}\Gamma(s)\Gamma\left(s-\kappa\right)(n\pi z)^{-2s}\mathrm{d}s \tag{3.3.22}$$

and, termwise, expand each integral:

$$\begin{aligned}&= \frac{1}{2\pi i}\int_{\sigma-i\infty}^{\sigma+i\infty}\Gamma(s)\Gamma\left(s-\kappa\right)(n\pi z)^{-2s}\mathrm{d}s\\ &= (2\pi)^{1/2}2^{1+\kappa}\Bigg\{\sum_{j=0}^{M-1}(-1)^j c_j\frac{1}{2\pi i}\int_{\sigma-i\infty}^{\sigma+i\infty}\Gamma\left(2s-\kappa-\frac{1}{2}-j\right)(2\pi n z)^{-2s}\mathrm{d}s\\ &\qquad+\frac{1}{2\pi i}\int_{\sigma-i\infty}^{\sigma+i\infty}\rho_M(s)\Gamma\left(2s-\kappa-\frac{1}{2}-M\right)(2\pi n z)^{-2s}\mathrm{d}s\Bigg\}.\end{aligned} \tag{3.3.23}$$

Using the Cahen-Mellin integral (2.1.3) yields

$$\begin{aligned} &= \frac{1}{2\pi i}\int_{\sigma-i\infty}^{\sigma+i\infty} \Gamma(s)\Gamma\left(s-\kappa\right)(n\pi z)^{-2s}\mathrm{d}s \\ &= (2\pi)^{1/2}2^{\kappa}\left[\sum_{j=0}^{M-1}(-1)^j c_j \frac{\mathrm{e}^{-2\pi nz}}{(2\pi nz)^{\kappa+\frac{1}{2}+j}} + R_M(n,z)\right] \end{aligned} \tag{3.3.24}$$

with the remainder

$$\begin{aligned} R_M(n,z) &= \frac{1}{\pi i}\int_{\sigma-i\infty}^{\sigma+i\infty} \rho_M(s)\Gamma\left(2s-\kappa-\frac{1}{2}-M\right)(2\pi nz)^{-2s}\mathrm{d}s \\ &= O\left(|z|^{-\left(\kappa+\frac{1}{2}+M\right)}\mathrm{e}^{-2\pi nz}\right), \end{aligned} \tag{3.3.25}$$

whereby the estimate readily follows from the existence of a constant K such that $\rho_M(s) < K$ for $|s| \to \infty$.

Finally, insertion into (3.3.22) yields the exponential asymptotic expansion

$$\frac{1}{2\pi i}\int_{\sigma-i\infty}^{\sigma+i\infty} \zeta(2s)\Gamma(s)\Gamma\left(s-\kappa\right)(\pi z)^{-2s}\mathrm{d}s \sim (2\pi)^{1/2}2^{\kappa}\sum_{n=1}^{\infty}\sum_{j=0}^{\infty}(-1)^j c_j \frac{\mathrm{e}^{-2\pi nz}}{(2\pi nz)^{\kappa+\frac{1}{2}+j}} \tag{3.3.26}$$

valid as $z \to \infty$ in the sector $|\arg z| < \frac{\pi}{2}$. Evaluating the inner sum over n leads to

$$\mathrm{Li}_{\kappa+\frac{1}{2}+j}(\mathrm{e}^{-a}) = \sum_{n=1}^{\infty}\frac{\mathrm{e}^{-na}}{n^{\kappa+\frac{1}{2}+j}}, \tag{3.3.27}$$

where we identified the *polylogarithm function* $\mathrm{Li}_s(x)$. Ultimately, we obtain the asymptotic representations (valid for $a \to \infty$ in the sector $|\arg a| < \frac{\pi}{2}$)

$$\overline{P}_d(a) \sim -\frac{\Gamma\left(\frac{d}{2}\right)}{2}(2a)^{\kappa-\frac{1}{2}}\sum_{j=0}^{\infty}(-1)^j c_j \frac{\mathrm{Li}_{\kappa+\frac{1}{2}+j}(\mathrm{e}^{-a})}{a^j}, \tag{3.3.28}$$

$$P_d(a) \sim -\frac{1}{\beta}\left(\frac{a}{2\pi\beta^2}\right)^{d/2}\sum_{j=0}^{\infty}(-1)^j c_j \frac{\mathrm{Li}_{\kappa+\frac{1}{2}+j}(\mathrm{e}^{-a})}{a^j}, \tag{3.3.29}$$

with c_j given in (3.3.21) and $\kappa = \frac{d+1}{2}$.

By Stirling's approximation (2.1.16) and the quotient expansion (A.4.13) from Example A.4.1,

the coefficients c_j in (3.3.21) exhibit super-exponential growth,

$$c_j \sim \sqrt{\frac{2\pi}{j}} \frac{1}{\Gamma\left(\kappa+\frac{1}{2}\right)\Gamma\left(\kappa-\frac{1}{2}\right)} \left(\frac{j}{2e}\right)^j \qquad (j \to \infty)\,, \tag{3.3.30}$$

implying that the asymptotic series (3.3.28) and (3.3.29) are divergent for all a. In the sense of Poincaré (cf. Def. A.2.3), this divergence does not detract from their validity as asymptotic representations as $a \to \infty$.

In contrast to the previous asymptotic expansion, we cannot simply differentiate term by term to obtain the asymptotic expansion of

$$\overline{D}_d(a) = 2\partial_{a^2}\overline{P}_d(a).$$

This approach is generally invalid in asymptotic expansions, as it requires specific conditions to be met for term-by-term differentiation to be justified [57]. However, by leveraging the recurrence relation given in identity (3.3.1), we can directly infer the asymptotic expansion of $\overline{D}_d(a)$ from that of $\overline{P}_{d-2}(a)$. This effectively bypasses the need for the differential approach, circumventing the need for the additional criteria usually required in asymptotic expansions. For an independent verification, we obtain the same asymptotics by using Laplace's method on the integral representation (A.4.36) in Example A.4.2.

In summary, in this section we developed asymptotic representations of the one-loop pressure in different parameter regimes. For small values of the scaling parameter z, an algebraic-type Poincaré asymptotic expansion was obtained by displacing the MB contour to the left and evaluating the resulting series of residues. In contrast, the MB representation is free of singularities to the right of the contour, which at first excludes any direct residue-based expansion for the regime $z \to \infty$. We resolved this by introducing inverse factorial expansions that generate artificial poles. Their evaluation yields exponentially suppressed contributions, and from this we derived a complete exponential asymptotic expansion valid for large z in the sector $|\arg z| < \frac{\pi}{2}$.

3.4 Fixed Points and Asymptotic Solutions of the Mass ODE

Having established the asymptotic expansions of $\overline{D}_d(a)$ in the previous section, we now return to the mass differential equation (3.2.1). Its fixed points occur at $a = 0$ and $a \to \infty$, corresponding respectively to the high- and low-temperature limits of the theory. We analyse both regimes in turn.

Employing the identity (3.3.1), the derivative function $\overline{D}(a)$ is given by

$$\overline{D}_3(a) = \frac{\pi^2}{6} - \frac{\pi}{2}a - \frac{a^2}{4}\Big[\gamma - \tfrac{1}{2} + \log\Big(\frac{a}{4\pi}\Big)\Big] + \pi^{3/2}\sum_{k=2}^{\infty}\frac{(-1)^k}{k!}\,\Gamma\Big(k-\tfrac{1}{2}\Big)\,\zeta(2k-1)\Big(\frac{a}{2\pi}\Big)^{2k} \qquad (|a| \le 2\pi). \tag{3.4.1}$$

In the relativistic limit $a \to 0$, the leading term of (3.4.1) is $\overline{D}(a) \simeq \frac{\pi^2}{6}$. Inserting this into (3.2.1) yields the first-order differential equation

$$-1 = \frac{\lambda^3}{4(2\pi)^4}\,\big(\lambda\,\partial_\lambda a + a\big)a. \tag{3.4.2}$$

Introducing $u = \lambda^3 a^2$ and using $\lambda\partial_\lambda = \partial_{\log\lambda}$ leads to the analytic solution

$$a^2(\lambda) = \frac{8(2\pi)^4}{\lambda^3}\left[1 - \frac{\lambda}{\lambda_i}\left(1 - \frac{\lambda_i^3 a_i^2}{8(2\pi)^4}\right)\right], \tag{3.4.3}$$

with initial condition $a(\lambda_i) = a_i \ll 1$.

For $\lambda \ll \lambda_i$, using $a = 4\pi e\,\lambda^{-3/2}$ from (3.1.3), the solution approaches a plateau of the effective coupling

$$e \simeq \sqrt{8}\,\pi,$$

signalling an approximately scale-invariant regime at high temperatures. The negative sign in (3.2.1) implies that this small-a approximation inevitably breaks down as λ decreases.

Restoring factors of Planck's quantum of action $\hbar$, the constancy of $e = \sqrt{8\pi^2/\hbar}$ at high temperature implies that the Euclidean action of a just-not-resolved (anti) caloron of unit topological charge and characteristic size $\rho \sim |\phi|^{-1}$ equals $\hbar$. Hence, the constancy of $\hbar$ may be viewed as a consequence of the near constancy of e up to a logarithmically narrow pole (to be discussed in the next subsection). This perspective motivates an interpretation of Yang–Mills vertices as manifestations of topologically non-trivial field configurations of unit charge, each contributing $\hbar$ through their centre's action. Hence, expansions in Feynman diagrams, and thus quantum corrections, correspond to successive local insertions of such (anti)calorons. The requirement that these configurations remain unresolved ensures that each contribution stays finite, thereby guaranteeing the finiteness of loop integrals in perturbative expansions.

In the opposite, Boltzmann-suppressed limit $a \to \infty$, $\overline{D}_3(a)$ is exponentially suppressed. Using the expansion from Example A.4.2, we obtain

$$\overline{D}_3(a) \sim \sqrt{2a} \sum_{r=0}^{\infty} \binom{\frac{1}{2}}{r} \frac{\Gamma\left(\frac{3}{2}+r\right)}{(2a)^r} \operatorname{Li}_{\frac{3}{2}+r}(\mathrm{e}^{-a}) \qquad (a \to \infty). \tag{3.4.4}$$

To determine the critical temperature λ_c (the point where the mass diverges), we proceed as follows. Equation (3.2.1) requires initial data (λ_0, a_0). For sufficiently large λ_0, the small-a expansion (3.4.3) is accurate, allowing us to set

$$a_0^2(\lambda_0) = \frac{8(2\pi)^4}{\lambda_0^3}. \tag{3.4.5}$$

For $a < 2\pi$, $\overline{D}(a)$ is computed via its convergent small-a expansion (3.4.1). Once a reaches 2π, we switch to the optimally truncated large-a asymptotic expansion (3.4.4), whose error is proved to be exponentially small in Example A.4.2. The optimal truncation order $r_{\mathrm{opt}} = \lfloor 2a \rfloor$ minimises the remainder (Fig. A.2).

For validation, $\overline{D}(a)$ is also evaluated from its integral representation (A.4.36) (denoted D_{int}). As demonstrated in Example A.4.2, the optimally truncated asymptotic expansion achieves exponential accuracy, whilst the numerical integration of (A.4.36) maintains a fixed error bound. Consequently, both D_{asym} and D_{int} agree to within plotting resolution across the entire range shown in Fig. 3.1, confirming the high accuracy of the asymptotic representation throughout the evolution.

Integrating (3.2.1) along this composite approximation reveals a divergence of $a(\lambda)$ at a finite value λ_c. Repeating the procedure for different λ_0 confirms rapid saturation toward the critical value

$$\lambda_c = 13.867.$$

At λ_c, the effective gauge coupling e diverges, signalling the onset of the preconfining phase of SU(2) Yang–Mills theory. While the one-loop approximation for $e(T)$ does not account for the radiatively induced generation of non-trivial holonomy in calorons and their subsequent dissociation into magnetic monopoles, it does correctly describe the screening of magnetic test charges. At the critical temperature, this screening becomes sufficiently strong to render the associated monopoles both massless and effectively chargeless, thereby enabling their condensation into a magnetically dominated ground state and marking the onset of the preconfining phase, in which the thermal quasiparticles decouple.

To conclude this chapter, we derive a semi-analytic estimate for the critical temperature λ_c based on the large-a asymptotics of $\overline{D}(a)$. In the regime $a \to \infty$, the exponential decay

$$\overline{D}(a) \sim \sqrt{\frac{\pi}{2}}\, a^{1/2} \mathrm{e}^{-a}$$

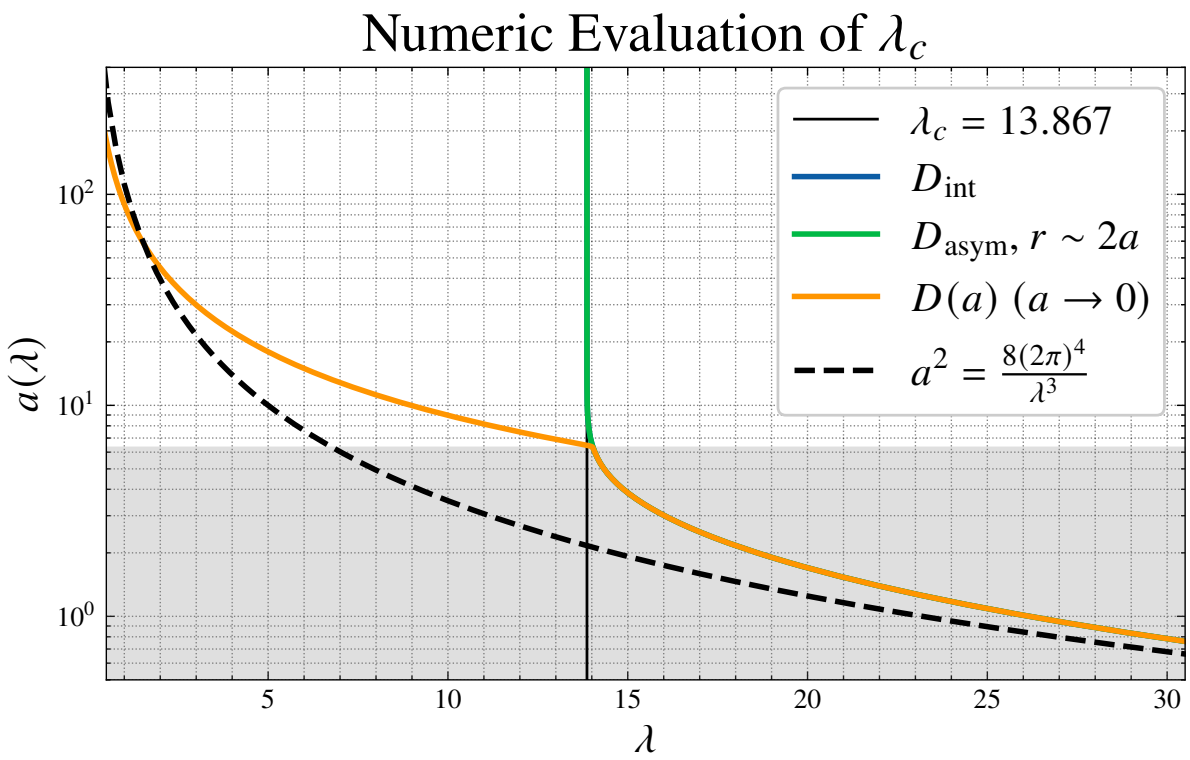

Figure 3.1: Solution of Eq. (3.2.1) using the small-a series for $a < 2\pi$ and, subsequently, the optimally truncated large-a expansion (3.4.4). The analytic solution (3.4.3) (dashed line) is shown for comparison, as well as the small-a series (3.4.1). The shaded region marks the boundary $a = 2\pi$. The curve labelled D_{int} corresponds to the integral representation (A.4.36). Its difference from the asymptotic evaluation D_{asym} is smaller than the plotting resolution. The mass diverges at $\lambda_c \approx 13.867$. Initial data: $\lambda_0 = 300$, a_0 from (3.4.5).

dominates the behaviour of the flow equation. Substituting this asymptotic form into (3.2.1) and noting that the denominator may be neglected, since $a(\lambda)$ diverges only logarithmically, whereas $\overline{D}(a)$ is exponentially suppressed, we obtain the separable equation

$$\partial_a \lambda = -\frac{3\,\lambda^4}{(2\pi)^{11/2}}\, a^{3/2} \mathrm{e}^{-a}. \tag{3.4.6}$$

Integrating from (λ_0, a_0) to (λ_c, ∞),

$$\frac{1}{\lambda_c^3} = \frac{1}{\lambda_0^3} + \frac{9}{(2\pi)^{11/2}} \Gamma\left(\tfrac{5}{2},\, a_0\right), \tag{3.4.7}$$

where $\Gamma(s, x)$ is the *upper incomplete gamma function*. Setting $a_0 = 2\pi$ and $\lambda_0 = 14.040$ (the radius of convergence and the numerically extracted onset value, respectively), gives

$$\lambda_c = 13.868$$

in excellent agreement with the full computation above.

Chapter 4

Logarithmic Expansion of the Effective Potential

In 1921, Hardy and Littlewood [37] proved that there are infinitely many zeros of the Riemann zeta function $\zeta(s)$ on the critical line $\Re(s) = \frac{1}{2}$. Although not technically demanding, this result marked a significant milestone in the study of the zeta function. Subsequent research refined Hardy's method, showing that there are at least $KT \log T$ zeros on the critical line for some positive constant K and all sufficiently large T [58, 59].

The essence of Hardy's argument lies in exploiting the essential singularity of *Jacobi's theta function* to draw conclusions about the coefficients of the moments of the Riemann xi function on the critical line. This is achieved via Mellin inversion of Eq. (A.3.27) together with an expansion in powers of $\log(u)$:

$$G(u) - 1 - \frac{1}{u} = \frac{1}{2\pi i} \int_{\sigma - i\infty}^{\sigma + i\infty} \frac{2\,\xi(s)}{s(s-1)}\, u^{s-1}\, \mathrm{d}s \qquad (0 < \sigma < 1). \tag{4.0.1}$$

Specialising to $\sigma = \frac{1}{2}$ yields

$$\begin{aligned} u^{\frac{1}{2}} \left[G(u) - 1 - \frac{1}{u} \right] &= \sum_{n=0}^{\infty} c_n \big(i \log(u) \big)^n, \\ c_n &= \frac{-1}{\pi n!} \int_{-\infty}^{\infty} \frac{\xi\left(\frac{1}{2} + it\right)}{\frac{1}{4} + t^2}\, t^n \, \mathrm{d}t. \end{aligned} \tag{4.0.2}$$

However, this line of reasoning cannot be generalised to the entire critical strip, since it relies essentially on the fact that xi is real-valued on the critical line, which no longer holds off the line (cf. the functional equation $\xi(s) = \xi(1 - s)$ (2.2.9)).

Comparison with Eq. (3.3.11) suggests that a similar approach may produce similar results. To this end, we expand the mass parameter z in powers of $\log(z)$, thereby obtaining weighted

moments of the zeta function in the critical strip. Evidently, as the Bessel functions possess branch cuts along the negative reals axis, the expansion is valid only within the sector $|\log z| < \pi$ (cf. (3.3.11)). In particular, this sector is determined by the smallest distance to the nearest singularity, which, by the branch cut for negative z, lies at $|\arg z| = |\Im \log z| = \pi$. To this end, we expect the emerging coefficients c_n to scale super-exponentially with n, such that the logarithmic expansion converges within this sector. Crucially, the integral representation (3.3.2) used in the analysis is only valid for $|\arg z| < \frac{\pi}{2}$, and thus the convergence of the series is constrained to $|\log z| < \frac{\pi}{2}$. Hence, this represents a shrinking of the convergence radius from $|\log z| < \pi$ to $|\log z| < \frac{\pi}{2}$, reflecting the limitations imposed by the valid range of the integral representation and ultimately on the choice of contour C.

The emerging coefficients c_n will then be evaluated explicitly by means of Parseval's identity. In this way, we arrive at two distinct representations of the coefficients c_n-one explicit and one in integral form-whose comparison allows us to infer properties of the zeta function.

A major challenge lies in obtaining well-controlled asymptotic expansions of the coefficients c_n as $n \to \infty$. This difficulty arises from the weighted representation involving t^n, whose contribution is dominated by large values of t in the critical strip.

In our setting, termwise integration of the logarithmic pressure expansion is justified by the exponential decay of the gamma functions, by virtue of Eq. (2.1.19),

$$\begin{aligned} P_3(a) &= -\frac{\pi^2}{\beta^4} \sum_{n=0}^{\infty} c_n \frac{(2\log(z))^n}{n!}, \\ c_n &= \frac{1}{2\pi i} \int_{\sigma-i\infty}^{\sigma+i\infty} \zeta(2s)\Gamma(s)\Gamma(s-2)\pi^{-2s}(2-s)^n \mathrm{d}s \qquad (2 < \sigma)\,, \end{aligned} \tag{4.0.3}$$

provided $|\log z| < \frac{\pi}{2}$.

In Sect. 4.1, we derive explicit expressions for the coefficients c_n in terms of double sums involving Touchard polynomials and modified Bessel functions. To demonstrate explicitly that the coefficients do not depend on the choice of σ, we evaluate them both outside and inside the critical strip. In Sect. 4.2, we lift the restriction $\kappa = 2$ and generalise the analysis to arbitrary spatial dimensions d. We show that naive contour displacement fails to produce meaningful asymptotic information. We interpret this failure as the obstruction to generating super-exponential growth by simple analytic continuation. In Sect. 4.3, we derive preliminary upper bounds on the coefficients c_n by applying Hölder's inequality and explicitly evaluating known MB integrals, yielding bounds expressed in terms of number-theoretic functions. This motivates the application of the method of steepest descents, carried out in Sect. 4.4, where we obtain well-controlled and uniform asymptotic expansions of the coefficients c_n in the limit $n \to \infty$.

4.1 Direct Logarithmic Pressure Expansion

4.1.1 Evaluation Outside the Critical Strip

Consider the logarithmic pressure expansion with coefficients

$$c_n = \frac{1}{2\pi i}\int_{\sigma-i\infty}^{\sigma+i\infty}\Big[\Gamma(s)\zeta(2s)\pi^{-s}\Big]\Big[(2-s)^n\Gamma(s-2)\Big]\pi^{-s}\,\mathrm{d}s \quad (n\in\mathbb{N}_0,\ \sigma>2). \tag{4.1.1}$$

Absolute convergence follows from the asymptotics of $\Gamma(s)$ along vertical lines (cf. Eq. (2.1.19)). We now identify the factors as Mellin transforms of explicit functions. First, by the Cahen-Mellin integral [60] together with the Mellin derivative property (Eq. (A.3.33)), we may set

$$G(s) \coloneqq (-s)^n\Gamma(s) = \int_0^\infty x^{s-1}(x\partial_x)^n\mathrm{e}^{-x}\,\mathrm{d}x, \tag{4.1.2}$$

valid for ($\sigma>0$ if $n=0$, $\sigma>-1$ if $n\geq 1$). Second, Example A.3.3 demonstrates that

$$F(s) \coloneqq \Gamma(s)\zeta(2s)\pi^{-s} = \int_0^\infty \psi(x)\,x^{s-1}\,\mathrm{d}x \qquad (\sigma>\tfrac{1}{2}), \tag{4.1.3}$$

where $\psi(x)$ is a variant of Jacobi's theta function (Eq. (A.3.19)). Applying Parseval's identity for Mellin transforms (Eq. (A.3.47)), with F and G as above and setting $u=\pi$ in Eq. (A.3.47) to account for the extra π^{-s} in (4.1.1), we obtain

$$\frac{1}{2\pi i}\int_{\sigma-i\infty}^{\sigma+i\infty} F(s)\,G(s-2)\,\pi^{-s}\,\mathrm{d}s = \int_0^\infty \psi\left(\tfrac{\pi}{x}\right)\Big[(x\partial_x)^n\mathrm{e}^{-x}\Big]\frac{\mathrm{d}x}{x^3}. \tag{4.1.4}$$

The hypotheses of Theorem A.3.1 are met since $F(\sigma+it)\in L(-\infty,\infty)$ and $x^{\sigma-3}\exp(-x)\in L(-\infty,\infty)$ for $\sigma>2$. The operator $(x\partial_x)^n$ naturally introduces the *Touchard polynomials* $T_n(z)$ [61], defined by

$$T_n(z) = \mathrm{e}^{-z}\Big(z\frac{\mathrm{d}}{\mathrm{d}z}\Big)^n\mathrm{e}^{z} = \sum_{k=0}^{n}\left\{{n\atop k}\right\}z^k = \mathrm{e}^{-z}\sum_{k=0}^{\infty}\frac{k^n}{k!}z^k, \tag{4.1.5}$$

where $\left\{{n\atop k}\right\}$ are *Stirling numbers of the second kind*. Expanding and invoking the functional equation of $\psi(x)$ (Eq. (A.3.64)) yields

$$\int_0^\infty\Big[(x\partial_x)^n\mathrm{e}^{-x}\Big]\psi\left(\tfrac{\pi}{x}\right)\frac{\mathrm{d}x}{x^3} = \sum_{r=0}^{n}\left\{{n\atop r}\right\}(-1)^r\int_0^\infty x^{r-3}\mathrm{e}^{-x}\left[\sqrt{\tfrac{x}{\pi}}\,\psi\left(\tfrac{x}{\pi}\right)+\tfrac{1}{2}\left(\sqrt{\tfrac{x}{\pi}}-1\right)\right]\mathrm{d}x. \tag{4.1.6}$$

Evaluating the first term in (4.1.6) recovers the *Epstein zeta function* we consider in Example A.3.7 and evaluate using Poisson summation

$$\int_0^\infty x^{r-3}\mathrm{e}^{-x}\left[\sqrt{\frac{x}{\pi}}\psi\left(\frac{x}{\pi}\right)\right]\mathrm{d}x = \frac{\Gamma(r-2)}{2} - \frac{\Gamma\left(r-\frac{3}{2}\right)}{2\sqrt{\pi}} + \frac{2\pi^r}{\pi^2}\sum_{\nu\in\mathbb{N}}\nu^{r-2}K_{2-r}(2\pi\nu), \tag{4.1.7}$$

whereby the first two contributions cancel the divergent part of the second term in (4.1.6)

$$\int_0^\infty x^{r-3}\mathrm{e}^{-x}\,\tfrac{1}{2}\left(\sqrt{\tfrac{x}{\pi}}-1\right)\mathrm{d}x = \frac{\Gamma\left(r-\frac{3}{2}\right)}{2\sqrt{\pi}} - \frac{\Gamma(r-2)}{2} \qquad (r>2). \tag{4.1.8}$$

Ultimately, we arrive at the result

$$c_n = \frac{2}{\pi^2}\sum_{r=0}^{n}\left\{{n \atop r}\right\}(-\pi)^r\sum_{\nu\in\mathbb{N}}\nu^{r-2}K_{2-r}(2\pi\nu), \tag{4.1.9}$$

with K_ν the modified Bessel function of the second kind. For small n, this representation is particularly useful for evaluating the coefficients c_n numerically. For $r > 2$, the inner sum can be precisely approximated using Euler-Maclaurin summation (cf. Sect. A.4.4), effectively replacing the sum with an integral over the real numbers, modulo correction terms. In the complementary range, this approximation no longer holds, and the sum must be evaluated directly. Anticipating a vanishing contribution from small r, it becomes necessary to distinguish the dominant r-terms by considering the interplay between the Stirling numbers and the Bessel function sum. Therefore, this representation is not immediately suitable for calculating the coefficients in the limit $n \to \infty$.

Nevertheless, Eq. (4.1.9) provides an explicit formula for the coefficients c_n and is especially useful for demonstrating σ independence, as we will now show.

4.1.2 Evaluation Inside the Critical Strip

We displace the contour of the integral in Eq. (4.1.1) into the critical strip $0 < \Re(s) < \frac{1}{2}$, picking up the residues at the poles $s = 2$, $s = 1$, and $s = \frac{1}{2}$, and then evaluating the remaining integral. Observing Eq. (4.1.1), the pole at $s = 2$, denoted R_2, arises from $(2-s)^n\Gamma(s-2)$ and vanishes for $n \neq 0$. The residue at $s = 1$, R_1, also comes from the same factor, and the

residue at $s = \frac{1}{2}$, $R_{1/2}$, arises from $\zeta(2s)$. Using Eq. (2.1.9) and Eq. (2.2.5), we have

$$R_2 = \frac{1}{90}\,\delta_{n,0}, \tag{4.1.10}$$

$$R_1 = -\frac{1}{6}, \tag{4.1.11}$$

$$R_{1/2} = \frac{2}{3}\left(\frac{3}{2}\right)^n. \tag{4.1.12}$$

Hence,

$$\begin{aligned} c_n = {} & \frac{2}{3}\left(\frac{3}{2}\right)^n - \frac{1}{6} + \frac{1}{90}\delta_{n,0} \\ & + \frac{1}{2\pi i}\int_{\sigma-i\infty}^{\sigma+i\infty}\Big[\Gamma(s)\zeta(2s)\pi^{-s}\Big]\Big[(2-s)^n\Gamma(s-2)\Big]\pi^{-s}\,\mathrm{d}s \qquad (0<\sigma<1/2). \end{aligned} \tag{4.1.13}$$

Evaluating the integral in the critical strip requires careful treatment. The Cahen-Mellin integral for $G(s)$ is now closed differently, using a rectangular contour with vertices at $\sigma \pm iT$ and $2 + \sigma \pm iT$ ($T \to \infty$). By the residue theorem, we recover

$$\frac{1}{2\pi i}\int_{\sigma-i\infty}^{\sigma+i\infty}\Gamma(s-2)x^{-s}\,\mathrm{d}s = \mathrm{e}^{-x} + x - 1 \qquad (0<\sigma<1). \tag{4.1.14}$$

Accordingly, the Mellin transforms $F(s)$ and $G(s)$ are modified for the critical strip evaluation:

$$F(s) = \Gamma(s)\zeta(2s)\pi^{-s} = \int_0^\infty \Big[G(x) - 1 - \frac{1}{x}\Big]\,x^{-2s}\,\mathrm{d}x, \tag{4.1.15}$$

$$G(s) = (-s)^n\Gamma(s) = \int_0^\infty x^{s-1}\big(x\partial_x\big)^n(\mathrm{e}^{-x} + x - 1)\,\mathrm{d}x. \tag{4.1.16}$$

Since $F(s)$ is evaluated at $s \to 1-2s$, we apply the generalised Parseval variant, Eq. (A.3.48):

$$\frac{1}{2\pi i}\int_{\sigma-i\infty}^{\sigma+i\infty}F(s)G(s-2)\pi^{-s}\,\mathrm{d}s = \frac{1}{2\sqrt{\pi}}\int_0^\infty \Big[G\Big(\sqrt{\frac{x}{\pi}}\Big) - 1 - \sqrt{\frac{\pi}{x}}\Big]\frac{1}{x^{\frac{5}{2}}}\big(x\partial_x\big)^n(\mathrm{e}^{-x} + x - 1)\,\mathrm{d}x. \tag{4.1.17}$$

The exponential term reproduces the Touchard polynomials, analogously to Example 4.1.1, yielding

$$\begin{aligned} &= \int_0^\infty \Big[G\Big(\sqrt{\frac{x}{\pi}}\Big) - 1 - \sqrt{\frac{\pi}{x}}\Big]\sum_{r=0}^{n}\left\{{n \atop r}\right\}(-1)^r x^{r-5/2}\mathrm{e}^{-x}\,\mathrm{d}x \\ &= \sum_{r=0}^{n}\left\{{n \atop r}\right\}(-1)^r\left[\frac{4\pi^r}{\pi^{3/2}}\sum_{\nu\geq 1}\nu^{r-2}K_{2-r}(2\pi\nu) - \Gamma(r-3/2)\right]. \end{aligned} \tag{4.1.18}$$

For the remaining terms, we notice that x has eigenvalue 1 under the power counting operator $x\partial_x$, and that the constant term vanishes unless $n = 0$. Together, they evaluate to

$$\int_0^\infty \left[G(\sqrt{\frac{x}{\pi}}) - 1 - \sqrt{\frac{\pi}{x}}\right]\left[x^{-3/2} - \delta_{n,0}x^{-5/2}\right] \mathrm{d}x = \frac{\sqrt{\pi}}{3} - \frac{\sqrt{\pi}}{45}\delta_{n,0}. \tag{4.1.19}$$

Combining Eqs. (4.1.18) and (4.1.19) and scaling by $1/(2\sqrt{\pi})$, we recover

$$\begin{aligned} &= \frac{1}{2\sqrt{\pi}} \int_0^\infty \left[G(\sqrt{\frac{x}{\pi}}) - 1 - \sqrt{\frac{\pi}{x}}\right] x^{-5/2} (x\partial_x)^n (\mathrm{e}^{-x} + x - 1)\, \mathrm{d}x \\ &= \frac{1}{6} - \frac{\delta_{n,0}}{90} + \sum_{r=0}^{n} \left\{ {n \atop r} \right\} (-1)^r \left[\frac{2\pi^r}{\pi^2} \sum_{\nu \geq 1} \nu^{r-2} K_{2-r}(2\pi\nu) - \frac{\Gamma\left(r - \frac{3}{2}\right)}{2\sqrt{\pi}} \right]. \end{aligned} \tag{4.1.20}$$

Finally, using Legendre's duplication formula (Eq. (2.1.11)) and the Touchard identity (A.4.73), the gamma contributions simplify to

$$\sum_{r=0}^{n} \left\{ {n \atop r} \right\} (-1)^r \Gamma(r - 3/2) = \frac{4\sqrt{\pi}}{3} \left(\frac{3}{2}\right)^n. \tag{4.1.21}$$

Combining all terms reproduces exactly the coefficients c_n in Eq. (4.1.9).

4.2 Generalised Approach

The foregoing analysis directly suggests that the extension to $P_d(a)$ (3.3.9) is trivially achieved by performing the substitution $2 \to \kappa$ in Eq. (4.1.9). This yields the general expression

$$\begin{aligned} c_n &= \frac{1}{2\pi i} \int_{\sigma - i\infty}^{\sigma + i\infty} \Big[\Gamma(s)\zeta(2s)\pi^{-s}\Big]\Big[(\kappa - s)^n \Gamma(s - \kappa)\Big]\pi^{-s}\, \mathrm{d}s \quad (n \in \mathbb{N}_0,\ \sigma > \kappa) \\ &= \frac{2}{\pi^\kappa} \sum_{r=0}^{n} \left\{ {n \atop r} \right\} (-\pi)^r \sum_{\nu \in \mathbb{N}} \nu^{r-\kappa} K_{\kappa - r}(2\pi\nu) \qquad (\kappa \geq 2), \end{aligned} \tag{4.2.1}$$

where $\kappa = \frac{d+1}{2}$ encodes the dimensional dependence. Invoking the reflection principle, it suffices to evaluate the MB integral in the upper half-plane and take the real part of the integrand.

Alternatively, Eq. (4.2.1) may be derived without explicit evaluation of Mellin transforms, by instead relying on the differential identity for the pressure (3.3.1). By definition of the power-

series expansion, one has

$$\begin{aligned} c_n(\kappa) &= \frac{1}{2\pi i}\int_{\sigma-i\infty}^{\sigma+i\infty}\Big[\Gamma(s)\zeta(2s)\pi^{-s}\Big]\Big[(\kappa-s)^n\Gamma(s-\kappa)\Big]\pi^{-s}\,\mathrm{d}s \\ &= \frac{1}{(2\pi)^{2\kappa}}\big(a^2\partial_a^2\big)^n\left[(-1)\,\frac{4\sqrt{\pi}}{\Gamma\left(\frac{d}{2}\right)}\overline{P}_d(a)\right]\Bigg|_{a=2\pi} \\ &= \frac{1}{(2\pi)^{2\kappa}}\big(a^2\partial_a^2\big)^{n-1}\left[a^2\,\frac{4\sqrt{\pi}}{\Gamma\left(\frac{d}{2}-1\right)}\overline{P}_{d-2}(a)\right]\Bigg|_{a=2\pi}. \end{aligned} \tag{4.2.2}$$

Here, the prefactors account for the fact that, in the power-series expansion, all dimensional quantities have already been factored out. Now, each power-counting operation, either the eigenvector a^2 is acted upon, or the dimension of the pressure is essentially reduced by 2, accompanied by an appropriate rescaling and sign reversal. After n iterations, and upon odering terms according to powers of a^2, the number of ways to select r eigenvector operations from n total operations is given exactly by the Stirling numbers of the second kind. Thus,

$$c_n(\kappa) = \frac{(-1)}{(2\pi)^{2\kappa}}\sum_{r=1}^{n}\left\{{n \atop r}\right\}a^{2r}(-1)^r\,\frac{4\sqrt{\pi}}{\Gamma\left(\frac{d}{2}-r\right)}\overline{P}_{d-2r}(a)\Big|_{a=2\pi} \tag{4.2.3}$$

reproduces the compact form (4.2.1) when expressing the pressure in terms of modified Bessel functions of the second kind as in Eq. (3.3.11).

The MB representation suggests deforming the contour to the left over the poles of the integrand, in analogy with Sect. 3.3.2. However, this procedure is not capable of producing an asymptotic expansion: the sequence $(-k)^n$ arising from the residues fails to form an auxiliary sequence (Def. A.2.4), since $(k+1)^n \neq o(k^n)$ as $n \to \infty$, signalling the breakdown of the standard residue-summation approach. Nevertheless, it is instructive to evaluate a finite number of pole contributions explicitly and to express the remainder as an integral in the critical strip $0 < \mathfrak{R}(s) < \frac{1}{2}$.

The poles occur at $s = \kappa - k$ for $k \in \mathbb{N}_0$, $k < \kappa$, due to the gamma function, and at $s = \frac{1}{2}$ due to the zeta function. The former yield

$$\sum_{k=0}^{k<\kappa}\mathrm{Res}_{s=\kappa-k}\big[\Gamma(s)\zeta(2s)\pi^{-2s}(\kappa-s)^n\Gamma(s-\kappa)\big] = \frac{1}{\pi^{2\kappa}}\sum_{k=0}^{k<\kappa}\frac{(-1)^k k^n}{k!}\,\Gamma(\kappa-k)\,\zeta(2\kappa-2k)\,\pi^{2k}. \tag{4.2.4}$$

At $s = \frac{1}{2}$, the structure of the residue depends on whether κ is an integer or not. For integer κ,

the pole is simple and gives

$$\mathrm{Res}_{s=\frac{1}{2}}\left[\Gamma(s)\zeta(2s)\pi^{-2s}(\kappa-s)^n\Gamma(s-\kappa)\right] = \frac{1}{2\sqrt{\pi}}\,\Gamma\!\left(\tfrac{1}{2}-\kappa\right)\left(\kappa-\tfrac{1}{2}\right)^n. \tag{4.2.5}$$

For fractional κ, a double pole arises at $s=\frac{1}{2}$, and one finds

$$\mathrm{Res}_{s=\frac{1}{2}}\left[\Gamma(s)\zeta(2s)\pi^{-2s}(\kappa-s)^n\Gamma(s-\kappa)\right] = \frac{1}{\sqrt{\pi}}\,\frac{(-1)^{\lfloor\kappa\rfloor}}{\lfloor\kappa\rfloor!}\left[\frac{H_{\lfloor\kappa\rfloor}}{2}-\log(2\pi)-\frac{n}{2\kappa-1}\right]\left(\kappa-\tfrac{1}{2}\right)^n. \tag{4.2.6}$$

These results agree with the expansions (3.3.17) obtained earlier by expanding in z and interchanging the order of summation.

Collecting all contributions, we arrive at

$$\begin{aligned} c_n(\kappa) = {} & \frac{1}{\pi^{2\kappa}}\sum_{k=0}^{k<\kappa}\frac{(-1)^k k^n}{k!}\,\Gamma(\kappa-k)\,\zeta(2\kappa-2k)\,\pi^{2k} \\ & + \begin{cases} \frac{1}{2\sqrt{\pi}}\Gamma\!\left(\frac{1}{2}-\kappa\right)\left(\kappa-\frac{1}{2}\right)^n, & \kappa\in\mathbb{N}, \\ \frac{1}{\sqrt{\pi}}\,\frac{(-1)^{\lfloor\kappa\rfloor}}{\lfloor\kappa\rfloor!}\left[\frac{H_{\lfloor\kappa\rfloor}}{2}-\log(2\pi)-\frac{n}{2\kappa-1}\right]\left(\kappa-\frac{1}{2}\right)^n, & \kappa\notin\mathbb{N}, \end{cases} \\ & + \frac{1}{2\pi i}\int_{\sigma-i\infty}^{\sigma+i\infty}\left[\Gamma(s)\zeta(2s)\pi^{-s}\right]\left[(\kappa-s)^n\Gamma(s-\kappa)\right]\pi^{-s}\,\mathrm{d}s \qquad \left(0<\sigma<\tfrac{1}{2}\right), \end{aligned} \tag{4.2.7}$$

underlining our initial claim that expressing the coefficients c_n in terms of a MB integral amounts to evaluating weighted moments of the Riemann zeta function in the critical strip.

For $k>\kappa$, i.e. the residues along the negative real axis, the resulting tail cannot be controlled by an auxiliary sequence. While $c_n(\kappa)$ is finite by construction, termwise evaluation of residues necessarily produces divergent series. These divergences are therefore not intrinsic but arise solely from non-uniform convergence and improper interchange of summation and integration. This observation suggests a different viable approach: namely, to expand the asymptotic series of Eq. (3.3.17), and then renormalise the formally divergent sums that arise, thereby recovering a finite result. We deem this approach less favourable, however, as it would rely on intricate zeta function regularisation techniques, more technically involved as in the approach of Dolan and Jackiw in Sect B.1. A similar phenomenon appears if one expands the Touchard polynomials via their infinite series representation (A.4.71): the resulting sums over incomplete gamma functions converge only after suitable regularisation and are ill-suited for asymptotic analysis.

One might attempt to shift the contour to the right instead, thereby summing over poles introduced by the inverse-factorial expansion (3.3.20), as in Sect. 3.3.3. However, the factor

$(\kappa - s)^n$ spoils any simplification, and the method rapidly becomes unwieldy.

Lastly, asymptotics of coefficients in power series expansions are also commonly derived using Darboux's method [62]. However, the presence of the singularity at negative z prohibits straightforward application of this method here, as a local expansion about the origin is not possible in terms of pure powers.

4.3 Preliminary Analytic Bounds

Before applying the method of steepest descent directly to the coefficient's integral expression, it is convenient to derive general bounds for $c_n(\kappa)$ that follow solely from the analytic structure of the Mellin representation (4.2.1). Separating the arithmetic factor $\Gamma(s)\,\zeta(2s)\,\pi^{-2s}$ from the purely analytic term $(\kappa - s)^n\Gamma(s-2)$, and applying first the triangle inequality and then Cauchy-Schwarz to the vertical contour, we obtain

$$|c_n(\kappa)|^2 \leq \left(\frac{1}{2\pi i}\int_{\sigma-i\infty}^{\sigma+i\infty}\left|\Gamma(s)\,\zeta(2s)\,\pi^{-2s}\right|^2 \mathrm{d}s\right)\left(\frac{1}{2\pi i}\int_{\sigma-i\infty}^{\sigma+i\infty}\left|(\kappa-s)^n\Gamma(s-2)\right|^2 \mathrm{d}s\right), \quad (4.3.1)$$

valid for $(n \in \mathbb{N}_0,\ \sigma > \kappa)$.

Although the first factor in (4.3.1) is irrelevant for the eventual order-of-growth estimates, we compute it here for completeness. Recognising it as the L^2-norm of the Mellin transform of $\psi(x)$, and using that $\psi(x)\,x^{\sigma-1/2}$ is square-integrable for $\sigma > \kappa$, Plancherel's theorem for the Mellin transform (Theorem A.3.1) gives

$$\begin{aligned}\left(\frac{1}{2\pi i}\int_{\sigma-i\infty}^{\sigma+i\infty}\left|\Gamma(s)\,\zeta(2s)\,\pi^{-2s}\right|^2 \mathrm{d}s\right) &= \pi^{-2\sigma}\int_0^\infty |\psi(x)|^2 x^{2\sigma-1}\,\mathrm{d}x \\ &= \frac{1}{\pi^{2\sigma}}\sum_{n,m=1}^{\infty}\int_0^\infty e^{-(n^2+m^2)\pi x}\,x^{2\sigma-1}\,\mathrm{d}x \\ &= \frac{\Gamma(2\sigma)}{\pi^{4\sigma}}\sum_{n,m=1}^{\infty}\frac{1}{(n^2+m^2)^{2\sigma}}.\end{aligned} \quad (4.3.2)$$

The double sum in (4.3.2) is the Epstein zeta function associated with the quadratic form $n^2 + m^2$, i.e.

$$\zeta_Q(s) = \sum_{n,m=1}^{\infty}(n^2+m^2)^{-s}.$$

It can be written as

$$\zeta_Q(s) = \frac{1}{4}\sum_{(a,b)\in\mathbb{Z}^2}{}'\frac{1}{(a^2+b^2)^s} - \zeta(2s) = \frac{1}{4}\sum_{n=1}^{\infty}\frac{r_2(n)}{n^s} - \zeta(2s), \quad (4.3.3)$$

where the prime indicates the omission of the term $(a, b) = (0, 0)$, and

$$r_2(n) = \#\{(a, b) \in \mathbb{Z}^2 : a^2 + b^2 = n\}$$

counts the number of representations of n as a sum of two squares. Jacobi's two-square theorem yields

$$r_2(n) = 4 \sum_{d|n} \chi_{-4}(d),$$

where χ_{-4} is the real primitive Dirichlet character modulo 4.

Using the Cauchy product for Dirichlet series, one finds that

$$\zeta_Q(s) = \zeta(s)\,\beta(s) - \zeta(2s),$$

where

$$\beta(s) = \sum_{n=1}^{\infty} \frac{\chi_{-4}(n)}{n^s} = \sum_{n=0}^{\infty} \frac{(-1)^n}{(2n+1)^s}$$

is the Dirichlet beta function. Substituting $s = 2\sigma$ in (4.3.3) and inserting into (4.3.2) gives the explicit evaluation

$$\frac{1}{2\pi i} \int_{\sigma-i\infty}^{\sigma+i\infty} \left|\Gamma(s)\,\pi^{-2s}\zeta(2s)\right|^2 \mathrm{d}s = \frac{\Gamma(2\sigma)}{\pi^{4\sigma}} \big[\zeta(2\sigma)\beta(2\sigma) - \zeta(4\sigma)\big]. \tag{4.3.4}$$

We now turn to the second factor in (4.3.1), which is dealt with similarly. Using the Cahen-Mellin integral (see (2.1.3)), and applying the operator $(x\,\partial_x)^n$ under the Mellin transform, we obtain

$$\frac{1}{2\pi i} \int_{\sigma-i\infty}^{\sigma+i\infty} \left|\Gamma(s-\kappa)(\kappa-s)^n\right|^2 \mathrm{d}s = \int_0^{\infty} |(x\partial_x)^n e^{-x}|^2\, x^{2(\sigma-\kappa)-1}\, \mathrm{d}x. \tag{4.3.5}$$

Using the Touchard polynomial expansion from Eq. (A.4.71) where $\left\{ {n \atop j} \right\}$ are Stirling numbers of the second kind, we expand the integrand and integrate termwise to obtain

$$\int_0^{\infty} |(x\partial_x)^n e^{-x}|^2\, x^{2(\sigma-\kappa)-1}\, \mathrm{d}x = \sum_{r=0}^{2n} \left(\sum_{j=0}^{r} \left\{ {n \atop j} \right\} \left\{ {n \atop r-j} \right\} \right) (-1)^r\, \frac{\Gamma(r + 2(\sigma-\kappa))}{2^{\,r+2(\sigma-\kappa)}}. \tag{4.3.6}$$

The powers of 2 arise because the integrand contains the factor $\exp(-2x)$.

Combining the evaluations of the two factors yields the bound

$$|c_n(\kappa)|^2 \leq \frac{\Gamma(2\sigma)}{\pi^{4\sigma}}\big[\zeta(2\sigma)\beta(2\sigma) - \zeta(4\sigma)\big] \sum_{r=0}^{2n}\left(\sum_{j=0}^{r} \left\{ n \atop j \right\} \left\{ n \atop r-j \right\}\right)(-1)^r \frac{\Gamma(r+2(\sigma-\kappa))}{2^{r+2(\sigma-\kappa)}}. \tag{4.3.7}$$

Notably, this bound is independent of the choice of σ within the half-plane $\sigma > \kappa$, leaving the freedom to optimise the estimate by varying σ to minimise it.

The leading order is extracted by observing that, for $n \to \infty$, the dominant contribution in the inner sum (4.3.5) arises from the term of highest degree, namely the $r = 2n$ term (4.3.7). Straightforward utilisation of Stirling's approximation gives

$$|c_n(\kappa)| = O\Big(\big(\tfrac{n}{e}\big)^n n^{\sigma-\kappa-\frac{1}{4}}\Big) \qquad (n \to \infty,\ \sigma > \kappa), \tag{4.3.8}$$

with implicit constant depending on σ.

This estimate implies the crude convergence condition $|\log z| < \frac{1}{2}$ for the logarithmic pressure expansion. However, this bound is far from optimal: it neither reproduces the expected radius of convergence $|\log z| < \frac{\pi}{2}$ nor does it provide access to higher-order corrections. Clearly, this is attributed to the use of the inequalities in Eq. (4.3.1), which discard phase information essential for sharper estimates.

4.4 Method of Steepest Descent

We now investigate the large-n behaviour of the coefficients $c_n(\kappa)$ by means of the method of steepest descent. Starting from their integral representation (4.2.1) and performing a shift $s \mapsto \kappa + s$, we have

$$c_n(\kappa) = \frac{(-1)^n}{\pi^{2\kappa}} \sum_{k=1}^{\infty} \frac{1}{k^{2\kappa}} \left[\frac{1}{2\pi i} \int_{\sigma'-i\infty}^{\sigma'+i\infty} \Gamma(s)\,\Gamma(s+\kappa)\, s^n\, (k\pi)^{-2s}\, \mathrm{d}s \right] \quad (\sigma' > 0)\,, \tag{4.4.1}$$

which follows from expressing the Riemann zeta function via its Dirichlet series and interchanging the order of summation and integration, which is valid provided $\sigma > \kappa \geq 2$.

The contour of integration may be deformed freely, provided it terminates in regions where the integrand decays super-exponentially. Such decay is guaranteed by the asymptotic behaviour of the gamma function, cf. Eq. (2.1.7), which dominates in the sectors $\frac{\pi}{2} \leq |\arg s| < \pi$. Along these deformed contours we may assume $|s| \gg 1$, e.g. $|s| \sim n$, and apply Stirling's approximation, Eq. (2.1.13).

With this, the inner integral can be recast as

$$\begin{aligned} I_k(\kappa) &= \frac{1}{2\pi i}\int_{\sigma-i\infty}^{\sigma+i\infty} \Gamma(s)\,\Gamma(s+\kappa)\,s^n\,(k\pi)^{-2s}\,\mathrm{d}s \\ &\sim \frac{1}{i}\int_{\sigma-i\infty}^{\sigma+i\infty} \exp\!\left\{n\left[\frac{2s+\kappa-1}{n}\log s - \frac{2s}{n}\big(1+\log(\pi k)\big) + \log s\right]\right\}\mathrm{d}s, \end{aligned} \tag{4.4.2}$$

where the exponential structure has been made explicit and $\sigma \to \infty$ and we dropped the prime.

4.4.1 Saddle Point Properties

The phase function associated with the saddle points is

$$p(s,\kappa,n,k) = \frac{2s}{n}\log\!\left(\frac{s}{k\pi}\right) + \frac{N}{n}\log s - \frac{2s}{n}, \tag{4.4.3}$$

where $N = n+\kappa-1$. The saddle points are determined by the stationary condition $p^{(1)}(s) = 0$. Suppressing the dependeces on (n,κ,k), differentiation gives

$$p^{(1)}(s) = \frac{2}{n}\log\!\left(\frac{s}{k\pi}\right) + \frac{N}{ns}. \tag{4.4.4}$$

Setting $p^{(1)}(s_*) = 0$ yields

$$s_*\log\!\left(\frac{s_*}{k\pi}\right) = -\frac{N}{2}. \tag{4.4.5}$$

The solutions to $p^{(1)}(s_*) = 0$ can be written in terms of the Lambert W function as

$$s_* = -\frac{N}{2}\frac{1}{W_j(-x)}, \qquad x = \frac{N}{2k\pi}, \tag{4.4.6}$$

where W_j denotes the j-th branch. Each $j \in \mathbb{Z}$ corresponds to a saddle point on a distinct sheet of the Riemann surface of the logarithm. Throughout, we restrict to the principal sheet $|\arg s| < \pi$.

Higher derivatives follow by direct differentiation:

$$p^{(2+m)}(s) = (-1)^m m!\,\frac{2}{ns^{1+m}}\left(1-(m+1)\frac{N}{2s}\right) \qquad (m \geq 0). \tag{4.4.7}$$

Evaluated at a saddle point,

$$p^{(2+m)}(s_*) = m!\frac{-4}{nN}\left(\frac{2W_j(-x)}{N}\right)^m W_j(-x)\left(1+(m+1)W_j(-x)\right). \tag{4.4.8}$$

In particular, $p^{(2)}(s_*) = 0$ if and only if $W_j(-x) = -1$. Since this occurs exclusively at $x = 1/\mathrm{e}$, all other saddle points are simple.

The branch structure of W separates the saddle configuration into three regimes. For $x > 1/\mathrm{e}$, the argument $-x$ lies to the left of the branch point $-1/\mathrm{e}$, and $W_j(-x)$ is complex for all $j \in \mathbb{Z}$. Hence infinitely many complex saddle points exist, all of first order. The symmetry $j \mapsto -(j+1)$ implies that the saddles occur in complex conjugate pairs and are symmetric with respect to the real axis.

To determine their behaviour for $x \to \infty$, we iteratively solve (4.4.5) and obtain

$$\log\left(\frac{s_*}{k\pi}\right) = \log x + i\pi(2j+1) + O(\log\log x)\,. \tag{4.4.9}$$

Consequently,

$$s_* = -\frac{N}{2}\frac{1}{\log x + i\pi(2j+1)} + O\left(\frac{\log\log x}{\log x}\right) \qquad (x \to \infty). \tag{4.4.10}$$

Thus for fixed j one has $|s_*| = O(N)$, whereas increasing $|j|$ reduces the magnitude of the saddle. As x decreases, the saddles rotate toward the positive real axis. The branches $j \in \{-1, 0\}$ intersect the imaginary axis at $x = \pi/2$, where $s_* = \pm\frac{N}{\pi}i$.

At the critical value $x = 1/\mathrm{e}$ the branches $j = 0$ and $j = -1$ coalesce, since $W_0(-1/\mathrm{e}) = W_{-1}(-1/\mathrm{e}) = -1$. The two simple saddles merge into a single saddle at $s_* = N/2$. From (4.4.8) one obtains $p^{(2)}(s_*) = 0$, while

$$p^{(3)}(s_*)\big|_{x=1/\mathrm{e}} = \frac{8}{nN^2} \neq 0, \tag{4.4.11}$$

so that a second-order saddle occurs.

For $0 < x < 1/\mathrm{e}$ only the branches $j \in \{-1, 0\}$ yield real solutions, and both saddles are simple. As $x \to 0^+$, one has $W_0(-x) \to 0^-$ and $W_{-1}(-x) \to -\infty$. Accordingly, the $j = -1$ saddle approaches the origin, whereas the $j = 0$ saddle diverges to infinity. The approach to $s = 0$ is significant for the steepest descent analysis, since the derivation of the phase function assumes large $|s|$. Indeed, as $s \to 0$,

$$\Gamma(s)\Gamma(s+\kappa)s^n(k\pi)^{-2s} \sim s^{n-1}\Gamma(\kappa), \tag{4.4.12}$$

so that the large-$|s|$ asymptotic expansion of the integrand ceases to be valid in this region. By contrast, the $j = 0$ saddle remains within the asymptotic regime.

In summary, the saddle configuration consists of infinitely many simple complex saddles for $x > 1/\mathrm{e}$, a single double saddle at $x = 1/\mathrm{e}$, and two real simple saddles for $0 < x < 1/\mathrm{e}$, of which only the $j = 0$ branch remains within the domain of validity of the asymptotic expansion.

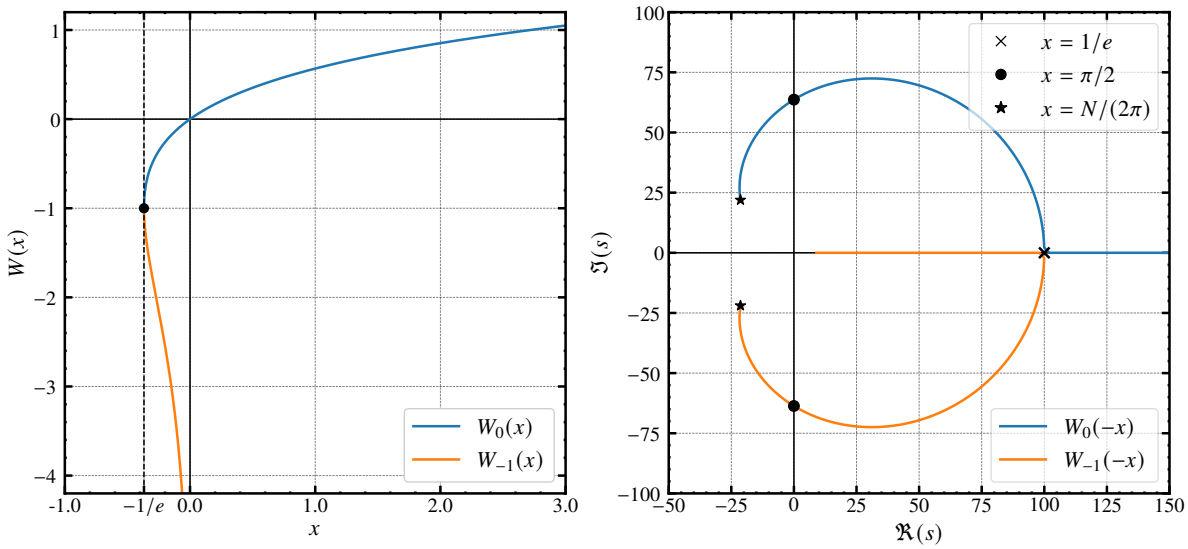

Figure 4.1: Left: principal branches W_0 and W_{-1} of the Lambert W function. Right: Saddle Point Trajectory for diminishing x. Markers indicate $x = \frac{N}{2\pi}$ (star), $x = \frac{\pi}{2}$ (circle) and $x = \frac{1}{\mathrm{e}}$ (cross).

For a visualisation, refere to the right panel of Fig. 4.1.

4.4.2 Dominant Saddle Point Contributions

The contribution of each saddle point to the overall integral is governed by its exponential weight

$$\exp(n\,\Re[p(s_*)])\,,$$

so that the saddle point with the maximal $\Re[p(s_*)]$ dominates the integral. Hence, we seek to evaluate $p(s_*)$ and identify the dominant saddle point for varying j. Insertion of (Eq. (4.4.6)) into Eq. (4.4.3) yields

$$p(s_*) = \frac{N}{n}\left[\frac{1 - W_j(-x)}{W_j(-x)} + W_j(-x) - \log x\right] + \frac{N}{n}\log\frac{N}{2}. \tag{4.4.13}$$

The last term produces a super-exponential growth in the coefficients c_n. We remind the reader that this emergence is due to the branch cut of the modified Bessel functions of the second kind for negative values, restricting the radius of convergence in a logarithmic power series expansion to be less than $|\log z| < \pi$.

Qualitative insight into the dominance structure is obtained by inserting Eq. (4.4.9) into the

phase function $p(s_*)$ given in Eq. (4.4.13). For $x \to \infty$, this gives

$$p(s_*) = \frac{N}{n}\left[\log\left(\frac{N}{2}\right) + i\pi(2j+1) - \log(\log x + i\pi(2j+1)) - 1 + \frac{1}{\log x + i\pi(2j+1)}\right] + O\left(\frac{\log\log(x)}{\log(x)}\right). \tag{4.4.14}$$

For large x, the term last becomes small and can be neglected, leaving us with

$$p(s_*) = \frac{N}{n}\left[\log\left(\frac{N}{2}\right) + i\pi(2j+1) - \log(\log x + i\pi(2j+1)) - 1\right] + O\left(\frac{\log\log(x)}{\log(x)}\right). \tag{4.4.15}$$

We now focus on the part of the phase function that varies with j, which we denote as $g_j(x)$. By Eq. (4.4.13), this is exactly the terms within the brackets

$$g_j(x) = \frac{1 - W_j(-x)}{W_j(-x)} + W_j(-x) - \log x. \tag{4.4.16}$$

Comparison with Eq. (4.4.15) suggests in the same limit $x \to \infty$

$$g_j(x) = i\pi(2j+1) - \log(\log x + i\pi(2j+1)) - 1 + O\left(\frac{\log\log x}{\log x}\right). \tag{4.4.17}$$

The dominant contribution to the integral comes from the saddle point with the maximum real part of $p(s_*)$. This is determined by comparing the real parts of $g_j(x)$ for different values of j. Since $\Re[g_j(x)]$ is dominated by $-\log\log x - 1$, we conclude that the saddle point with the smallest value of $|2j+1|$ will dominate. By the previous established symmetry of $j \mapsto -(j+1)$, the saddle points corresponding to $j = 0$ and $j = -1$ will give the largest contributions. Figure 4.2 numerically confirms this dominance for all $x > 1/\mathrm{e}$, where the real parts of $g_j(x)$ are plotted for several branches j.

To extract the dominant contribution, we investigate the maximum of the phase kernel $g(x)$ defined in Eq. (4.4.16). Differentiating the defining relation $W\mathrm{e}^W = -x$ with respect to x gives

$$W' = -\frac{W}{x(1+W)}. \tag{4.4.18}$$

Applying this to the derivative of the phase kernel yields

$$g'(x) = -\frac{1}{xW}. \tag{4.4.19}$$

Hence, the real part of $g'(x)$ vanishes when W is purely imaginary. By Eq. (4.4.6), this condi-

tion corresponds precisely to the saddle points being located on the imaginary axis. Therefore, the saddle points at $s_* = \pm i\,\frac{N}{\pi}$ for $x = \pi/2$ give the largest contribution to the integral. At this value the real part of the phase attains its maximum:

$$\Re g_0\left(\tfrac{\pi}{2}\right) = \log\left(\frac{2}{\pi e}\right). \tag{4.4.20}$$

In the complementary regime $x \leq 1/\mathrm{e}$ the dominance is unambiguous, since no competition between branches arises. For $x \to 0$, the phase function decays like

$$g_0(x) = -\left[\frac{1}{x} + \log(x) + 1\right] + \mathcal{O}\,(x)\,. \tag{4.4.21}$$

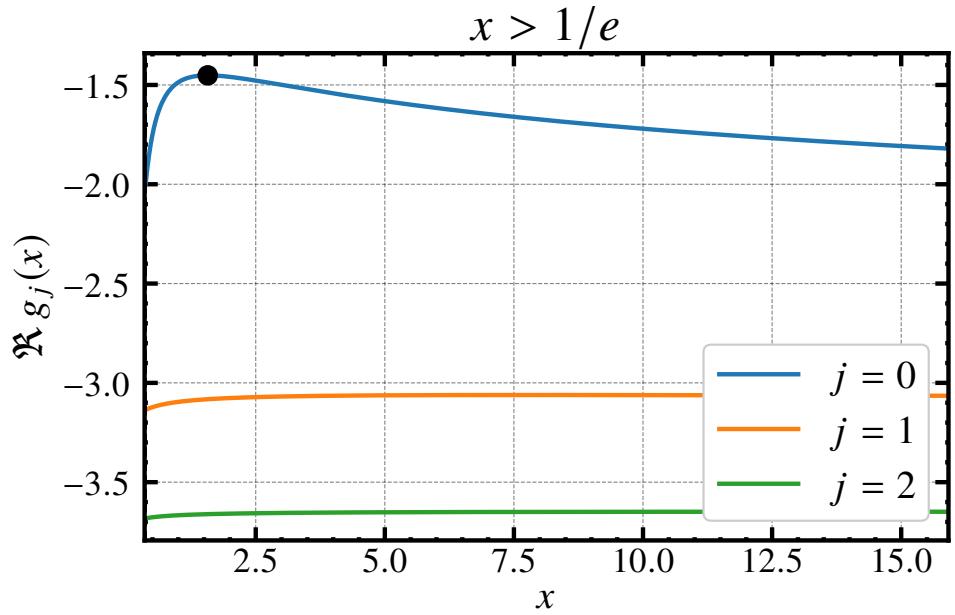

Figure 4.2: Exponential weight contribution at the saddle points (4.4.6), determined by $g_j(x)$ from Eq. (4.4.16). Negative branch indices mirror positive ones under the reflection $j \mapsto -(j+1)$.The black point corresponds to $x = \pi/2$.

4.4.3 Topology of the Steepest Descent Paths

The curves of steepest descent through a saddle point s_* are defined by the condition that the imaginary part of the phase function remains constant,

$$\Im[p(s)] = \Im[p(s_*)]\,, \tag{4.4.22}$$

where s_* solves Eq. (4.4.5).

Writing $s = \sigma + it = re^{i\phi}$ and decomposing the phase as $p(s) = u(\sigma, t) + iv(\sigma, t)$ yields

$$u(\sigma, t) = \frac{2}{n}\left(\sigma \log r - t\phi - \sigma(1 + \log k\pi)\right) + \frac{N}{n}\log r, \tag{4.4.23}$$

$$v(\sigma, t) = \frac{2}{n}\left(\sigma\phi + t\log r - t(1 + \log k\pi)\right) + \frac{N}{n}\phi. \tag{4.4.24}$$

The descent trajectories are characterised by the level sets of v together with the monotonic decrease of u along them.

In the case $x > 1/\mathrm{e}$, the simple saddles occur as complex conjugate pairs. Imposing condition (4.4.22), symmetry allows us to restrict attention to $\phi \to 0$ with $r \to \infty$. Expanding $v(r, \phi)$ gives

$$\begin{aligned} v(r, \phi) &= \frac{2}{n} r\phi \log\frac{r}{k\pi} + \frac{N}{n}\phi + O(\phi^3) \\ &= v(r_*, \phi_*). \end{aligned} \tag{4.4.25}$$

Substituting $t \sim r\phi$ yields the asymptotic form

$$t \sim \frac{v(r_*, \phi_*)}{\log\frac{r}{k\pi}}\frac{n}{2}, \tag{4.4.26}$$

which shows that the trajectories approach the real line as $r \to \infty$. By the definition of the phase function (4.4.3), we infere that these paths are the trajectories of steepest ascent, since the integrand exhibits super-exponential growth due to the gamma factors.

Analogously, for $\phi \to \pi$ and $r \to \infty$ one finds

$$t \sim \frac{r\pi}{\log\frac{r}{k\pi}}. \tag{4.4.27}$$

Thus the steepest descent paths emanate from the logarithmic singularity at the origin and trace curved rays towards infinity in the left half-plane. Complex conjugate branches generate symmetric trajectories in the upper and lower half-planes.

The two descent directions are characterised by the angles

$$\phi = -\frac{\alpha}{2} + \frac{\pi}{2}, \qquad -\frac{\alpha}{2} + \frac{3\pi}{2}, \tag{4.4.28}$$

where $\alpha = \arg\left[p^{(2)}(s_*)\right]$. Employing Eq. (4.4.8), this phase can be expressed as

$$\arg\left[p^{(2)}(s_*)\right] = \arg\left[-W_j(-x)(1 + W_j(-x))\right]. \tag{4.4.29}$$

Contemplating the paths of steepest descent suggests that the original integration contour does not directly deform onto them. The topology of the problem, characterised by the presence of

infinitely many Riemann sheets, allows for contours that wind around the origin an arbitrary number of times, potentially leading to $|\arg s| \to \infty$ and $|s| \to 0$. In such a configuration, the contour could, for instance, originate along the steepest descent trajectory associated with the saddle point $j = -1$, spiral around the origin n times, and subsequently continue along the path for $j = -(n+1)$. A analogous argument holds for the saddles $j = 0$ and $j = n$.

While formally valid, this procedure of tracking the contour across multiple Riemann sheets disguises the real-valued nature of the resulting coefficients. Evidently, a Hankel contour ensures this property directly, as it exploits the symmetry relating complex conjugated sectors. This path is achieved by selecting the branch corresponding to $j = -1$ towards the origin, connecting to the branch for $j = 0$ via an infinitesimal semicircle around the origin, and then following the $j = 0$ branch to $-\infty$. Although the semicircular segment is not itself a path of descent, the asymptotic analysis presented in Fig. 4.2 demonstrates that its contribution is negligible compared to that of the dominant saddle points in the limit of interest. That is, the connecting arc lies deep in the valley of both trajectories.

Therefore, we justify the deformation of the original vertical contour, initially defined by $\Re(s) = \sigma$ (placed sufficiently far to the right to validate the use of Stirling's approximation), onto a path that follows the steepest descent trajectories through the dominant saddle points at $j = 0$ and $j = -1$. Although the deformed contour approaches the origin due to the logarithmic singularity of the phase function, this does not contradict the assumption that $|s|$ is large along the *relevant* part of the contour. The dominant contribution to the integral arises in neighbourhoods of the saddle points, which satisfy this condition. The portion of the contour near $s = 0$ lies deep in the valley of $\Re p$ and contributes only exponentially suppressed terms.

At $x = 1/\mathrm{e}$ the two real saddle points overlap at $s_* = N/2$, producing a second-order saddle. The quadratic term in the local expansion vanishes, and three descent as well as three ascent directions emerge, separated by angles of $2\pi/3$. Evaluating the phase gives

$$p(s_*)\big|_{x=1/\mathrm{e}} = \frac{N}{n}\left[\log\left(\frac{N}{2}\right) - 2\right]. \tag{4.4.30}$$

The descent directions occur at angles $\pm\pi/3$ and π. The direction $\phi = \pi$ connects to the logarithmic singularity at the origin and does not yield an admissible global contour deformation.

For large r, solving $v(r, \phi) = 0$ leads to

$$\phi \cot \phi \sim -\tfrac{1}{2} \log \frac{r}{k\pi}, \tag{4.4.31}$$

which forces $\phi \to \pm\pi$ as $r \to \infty$. Hence admissible descent contours ultimately enter the left half-plane. Near the saddle, the original contour approaches the real axis at angle $-\pi/3$, crosses at $s = N/2$, and leaves at angle $\pi/3$.

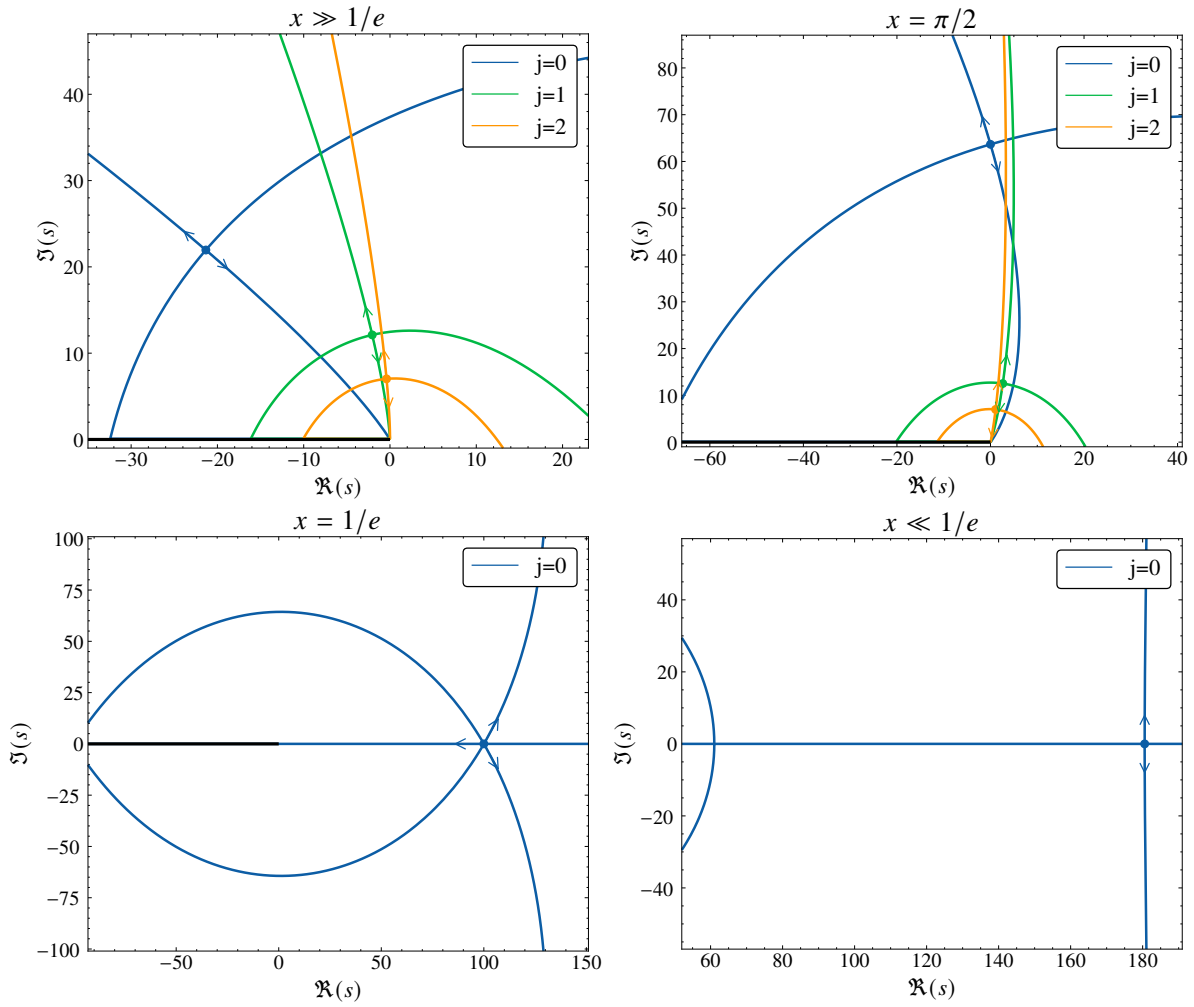

Figure 4.3: Steepest descent trajectories for different x regimes. Each panel visualises the level curve $\Im\, p(s) = \Im\, p(s_*)$ associated with the saddle point on the corresponding Lambert W branch. The arrows mark the directions of steepest descent. Depicted in black is the branch cut.

For $x < 1/\mathrm{e}$, the $j = 0$ saddle point becomes real and diverges to $+\infty$ as $x \to 0$. In this case, the descent directions are parallel to the imaginary axis, because the phase function is real, positive. The admissible global deformation is obtained by following the descent path associated with $j = 0$, which can be continued into the left half-plane and closed at $-\infty$. Topologically, the resulting contour is equivalent to a semicircle.

Fig. 4.3 visualises the saddle points with their associated paths of steepest descents for different regimes in x together with $x = \pi/2$. The latter provides the main contribution to the integral by achieving the maximal real part of the phase function.

4.4.4 Asymptotic Expansion at the Simple Saddle Points

For $x \neq 1/\mathrm{e}$ the saddle points are simple. Moreover, the saddle corresponding to the branch $j = -1$ is the complex conjugate of the one associated with $j = 0$. Since the integrand satisfies the corresponding symmetry, their contributions are complex conjugates as well. It therefore suffices to analyse the trajectory through the $j = 0$ saddle point; the total contribution is obtained by multiplying by 2. In this way, the cases $x < 1/\mathrm{e}$ and $x > 1/\mathrm{e}$ are treated simultaneously.

Having established the steepest descent paths C_j, each passing through a saddle point $s_{*,j}$, we now derive the asymptotic form of the corresponding contour integrals

$$I_k^j(\kappa) \;=\; \int_{C_j} \exp\{\, n\, p(s)\}\, \mathrm{d}s \qquad (j \in \mathbb{Z})\,, \tag{4.4.32}$$

where $p(s) = p(s, \kappa, n, k)$ is the phase function defined in (4.4.3), and the saddles $s_{*,j}$ are determined by (4.4.6) through the choice of branch j.

Each contour C_j originates at $-\infty$ in the left half-plane, passes through the saddle point $s_{*,j}$, and then continues towards the origin $s \to 0$. On the contour we introduce

$$\tau \;=\; p(s_{*,j}) \;-\; p(s), \tag{4.4.33}$$

which is real and nonnegative along C_j. Along the path $I_k^{j<0}(\kappa)$, as s travels from $-\infty$ to the saddle $s_{*,j}$, τ decreases monotonically from $+\infty$ to 0, and then increases back to $+\infty$ as s continues to the origin. The complementary branch $j \mapsto -(j+1)$ behaves analogously. Thus, for each segment of the contour, there are two distinct preimages of the same τ, denoted $s_1(\tau)$ and $s_2(\tau)$: s_1 corresponds to the segment approaching the saddle, while s_2 represents the continuation past the saddle towards the origin.

With this convention, the integral may be expressed as

$$I_k^j(\kappa) = \mathrm{e}^{np(s_{*,j})} \int_0^\infty \left(\frac{\mathrm{d}s_2}{\mathrm{d}\tau} - \frac{\mathrm{d}s_1}{\mathrm{d}\tau} \right) \mathrm{e}^{-n\tau}\, \mathrm{d}\tau. \tag{4.4.34}$$

Expanding the phase function in a Maclaurin series about $s_{*,j}$, we obtain

$$\tau = -\frac{p^{(2)}(s_*)}{2}\,(s - s_{*,j})^2 \left[\sum_{r=0}^{\infty} \frac{2P_m(s_{*,j})}{(2+r)!} (s - s_{*,j})^r \right], \tag{4.4.35}$$

where the normalised coefficients $P_m(s_{*,j})$ are defined by

$$P_m(s_{*,j}) \;=\; \frac{p^{(m+2)}(s_{*,j})}{p^{(2)}(s_{*,j})} \;=\; \Gamma(m+1)\left(\frac{2W_j(-x)}{N}\right)^m \frac{1+(m+1)W_j(-x)}{1+W_j(-x)} \tag{4.4.36}$$

and were derived using Eq. (4.4.8). Inverting this series using the Lagrange inversion theorem leads to two local branches,

$$(s-s_{*,j})_1(\tau) = i\sqrt{\tfrac{2}{p^{(2)}(s_{*,j})}}\sum_{m=0}^{\infty}(-1)^{m+1}\,\frac{d_m}{m+1}\,\tau^{(m+1)/2}, \tag{4.4.37}$$

$$(s-s_{*,j})_2(\tau) = i\sqrt{\tfrac{2}{p^{(2)}(s_{*,j})}}\sum_{m=0}^{\infty}\qquad\quad\frac{d_m}{m+1}\,\tau^{(m+1)/2}, \tag{4.4.38}$$

where the coefficients d_m are given explicitly by

$$m!\,d_m \;=\; \Big(-\tfrac{2}{p^{(2)}(s_{*,j})}\Big)^{m/2}\,\frac{\mathrm{d}^m}{\mathrm{d}s^m}\left[\sum_{r=0}^{\infty}\frac{2P_m(s_{*,j})}{(2+r)!}(s-s_{*,j})^r\right]^{-\frac{m+1}{2}}\Bigg|_{s=s_{*,j}}. \tag{4.4.39}$$

Additionally, the first three coefficients d_{2m} are readily computed from (4.4.39),

$$d_0 = 1, \tag{4.4.40}$$

$$d_2 = \frac{1}{12p^{(2)}}\big(3P_2-5P_1^2\big), \tag{4.4.41}$$

$$d_4 = \frac{1}{864(p^{(2)})^2}\left\{385P_1^4-35\left(6P_1^2-P_2\right)P_2+168P_1P_3-24P_4\right\}, \tag{4.4.42}$$

where for simplicity we suppressed the explicit $s_{*,j}$ dependence.

Crucially, the coefficients d_{2m} inherit a simple scaling structure. From Eq. (4.4.8) the quantities $P_m(s_{*,j})$ scale like N^{-m}. Since d_{2m} are homogeneous polynomials of total degree m in the P_k (cf. Eq. (4.4.39)), their polynomial part scales like N^{-m}. In Eq. (4.4.39) this is multiplied by the prefactor $\big(-2/p^{(2)}(s_{*,j})\big)^{m/2}$, which scales like $(nN)^{m/2}$. Combining both contributions shows that

$$d_{2m} = \left(\frac{n}{N}\right)^{m/2}\widetilde{d}_{2m}(x),$$

where the reduced coefficients $\widetilde{d}_{2m}$ depend only on x. For instance, in the case $m=2$ the prefactor in Eq. (4.4.39) scales like $(nN)^2$, whereas the homogeneous polynomial in the P_k is of total degree 4 and therefore scales like N^{-4}. Together this gives $d_4 \sim (n/N)^2$.

Continuing from Eq. (4.4.34), differentiation of the two local branches and subtraction yields

$$\frac{\mathrm{d}s_2}{\mathrm{d}\tau} - \frac{\mathrm{d}s_1}{\mathrm{d}\tau} = i\sqrt{\frac{2}{p^{(2)}}} \sum_{m=0}^{\infty} d_{2m}\, \tau^{(2m-1)/2}, \tag{4.4.43}$$

so that only the even coefficients d_{2m} remain due to cancellation of the odd terms.

Substituting this expression into (4.4.34) gives

$$I_k^j(\kappa) \sim \mathrm{e}^{np(s_{*,j})}\, i\sqrt{\frac{2}{p^{(2)}(s_{*,j})}} \sum_{m=0}^{\infty} d_{2m} \int_0^{\infty} \tau^{(2m-1)/2}\, \mathrm{e}^{-n\tau}\, \mathrm{d}\tau. \tag{4.4.44}$$

The remaining Laplace integral is evaluated using Watson's Lemma A.4.1, yielding

$$I_k^j(\kappa) \sim \mathrm{e}^{np(s_{*,j})}\, i\sqrt{\frac{2}{p^{(2)}(s_{*,j})}} \sum_{m=0}^{\infty} d_{2m}\, \frac{\Gamma\!\left(m+\frac{1}{2}\right)}{n^{m+\frac{1}{2}}}. \tag{4.4.45}$$

With this representation at hand, we now distinguish the regimes $x > 1/\mathrm{e}$ and $x < 1/\mathrm{e}$.

For $x > 1/\mathrm{e}$ two simple saddle points occur, corresponding to the branches $j = 0$ and $j = -1$, which are complex conjugates of each other. Their contributions are likewise complex conjugate, and therefore the full asymptotic expansion is obtained by taking twice the real part of the $j = 0$ contribution. This yields

$$I_k(\kappa) \sim 2\,\Re\left[\mathrm{e}^{np(s_{*,0})}\sqrt{\frac{2}{p^{(2)}(s_{*,0})}} \sum_{m=0}^{\infty} d_{2m}\, \frac{\Gamma\!\left(m+\frac{1}{2}\right)}{n^{m+\frac{1}{2}}}\right] \qquad (n \to \infty). \tag{4.4.46}$$

Insertion of the saddle-point representation (4.4.13) and of $p^{(2)}(s_{*,0})$ then gives

$$I_k(\kappa) \sim 2\left(\frac{N}{2}\right)^{N+\frac{1}{2}} \Re\left[\exp\{Ng_0(x)\}\sqrt{\frac{-1}{W(1+W)}} \sum_{m=0}^{\infty} \widetilde{d}_{2m}(x)\, \frac{\Gamma\!\left(m+\frac{1}{2}\right)}{N^m}\right], \qquad \left(x > \frac{1}{\mathrm{e}}\right) \tag{4.4.47}$$

where $W = W_0(-x)$ denotes the principal branch of the Lambert function.

For $x < 1/\mathrm{e}$, however, only the saddle corresponding to $j = 0$ contributes. The derivation proceeds identically but without taking the real part and without the additional factor of 2. Since $W = W_0(-x)$ is real and negative on $(-1/\mathrm{e}, 0)$, both $g_0(x)$ and the prefactor are real-valued. Moreover, $-W(1+W) > 0$ in this interval, so that the square root is real. Thus,

$$I_k(\kappa) \sim \left(\frac{N}{2}\right)^{N+\frac{1}{2}} \exp\{Ng_0(x)\}\sqrt{\frac{-1}{W(1+W)}} \sum_{m=0}^{\infty} \widetilde{d}_{2m}(x)\, \frac{\Gamma\!\left(m+\frac{1}{2}\right)}{N^m} \qquad \left(x < \frac{1}{\mathrm{e}}\right). \tag{4.4.48}$$

Ultimately, both cases can be written compactly as

$$I_k(\kappa) \sim \big(1 + \Theta(x - 1/\mathrm{e})\big) \left(\frac{N}{2}\right)^{N+\frac{1}{2}} \times \Re\left[\exp\big\{N g_0(x)\big\} \sqrt{\frac{-1}{W(1+W)}} \sum_{m=0}^{\infty} \widetilde{d}_{2m}(x)\, \frac{\Gamma\big(m+\frac{1}{2}\big)}{N^m}\right], \tag{4.4.49}$$

provided $x \neq 1/\mathrm{e}$ and the real part is taken only in the regime $x > 1/\mathrm{e}$. Here, $\theta(x)$ denotes the Heaviside step function, defined by

$$\theta(x) = \begin{cases} 0, & x < 0, \\ 1, & x \geq 0. \end{cases}$$

Inspection of the denominator in the square-root factor reveals that the above expansion breaks down at $x = 0$ and $x = 1/\mathrm{e}$, where $W_0(0) = 0$ and $W_0(-1/\mathrm{e}) = -1$, respectively. While the singularity at $x = 0$ lies outside the present scaling regime, the one at $x = 1/\mathrm{e}$ reflects the structural change of the saddle-point configuration.

4.4.5 Asymptotic Expansion at the Degenerate Saddle Point

At $x = 1/\mathrm{e}$ the two simple saddle points coalesce into a single saddle of second order located at $s = N/2$ on the positive real axis. From this point three paths of steepest descent emanate (see Fig. 4.3). The original vertical contour is therefore deformed so as to approach the real axis at an angle $-\pi/3$, pass through the saddle point, and leave at an angle $\pi/3$. Along this contour we introduce the local variable

$$\begin{aligned} \tau &= p(N/2) - p(s) \\ &= \frac{N}{n} \sum_{m=3}^{\infty} \frac{(-1)^m}{m} \left(\frac{m-2}{m-1}\right) \left(\frac{2\delta}{N}\right)^m, \end{aligned} \tag{4.4.50}$$

where $\delta = s - N/2$. Reversion of this series yields

$$\delta = \sum_{m=0}^{\infty} A_m \left(\frac{N}{6}\right)^{\frac{2-m}{3}} (n\tau)^{\frac{1+m}{3}}, \tag{4.4.51}$$

where the first few constants are given by

$$A_0 = 3, \qquad A_1 = 1, \qquad A_2 = \frac{1}{10},$$
$$A_3 = -\frac{1}{270}, \qquad A_4 = \frac{4}{14175}, \qquad A_5 = 0.$$

With the substitution $\delta = s - N/2$ and the phase function evaluated at the saddle point in Eq. (4.4.30), the integral at $x = 1/\mathrm{e}$ can be expressed as

$$I \sim \frac{1}{i}\left(\frac{N}{2}\right)^N \mathrm{e}^{-2N} \int_0^\infty \mathrm{e}^{-n\tau}\left\{\frac{\mathrm{d}\delta}{\mathrm{d}\tau}\left(e^{i\pi}\tau\right) - \frac{\mathrm{d}\delta}{\mathrm{d}\tau}\left(e^{-i\pi}\tau\right)\right\}\mathrm{d}\tau. \tag{4.4.52}$$

Here, the factors $e^{\pm i\pi}$ account for the orientation of the two branches along the paths of steepest descent emanating from the cubic saddle.

Differentiating Eq. (4.4.51) gives

$$\frac{\mathrm{d}\delta}{\mathrm{d}\tau}\left(e^{i\pi}\tau\right) - \frac{\mathrm{d}\delta}{\mathrm{d}\tau}\left(e^{-i\pi}\tau\right) = \frac{2i}{3}\left(\frac{N}{6}\right)^{2/3} \sum_{m=0}^{\infty} B_m \left(\frac{N}{6}\right)^{-m/3} \sin\pi\left(\frac{m}{3} + \frac{1}{3}\right) \frac{(n\tau)^{(1+m)/3}}{\tau}, \tag{4.4.53}$$

where we defined $B_m = A_m(m+1)$ for brevity, with the coefficients A_m given in Eq. (4.4.51).

Substituting Eq. (4.4.53) into Eq. (4.4.52) and evaluating the resulting Laplace-type integral using Watson's Lemma A.4.1 yields

$$I \sim \frac{2}{3^{5/3}} \mathrm{e}^{-2N}\left(\frac{N}{2}\right)^{N+2/3} \sum_{m=0}^{\infty} B_m \, \sin\pi\left(\frac{m}{3} + \frac{1}{3}\right) \frac{\Gamma\left(\frac{m}{3} + \frac{1}{3}\right)}{(N/6)^{m/3}}. \tag{4.4.54}$$

Since the exponential scale remains unchanged, the only modification, w.r.t. the expansion in Eq. (4.4.49), is algebraic: the Gaussian $N^{\frac{1}{2}}$ factor is replaced by $N^{\frac{2}{3}}$, yielding an overall enhancement of order $N^{\frac{1}{6}}$.

4.4.6 Numerical Validation of the Asymptotic Expansion

We assess the accuracy of the asymptotic expansions (4.4.49) and (4.4.54) by comparison with direct numerical evaluation of the integral representation (4.4.2). To suppress the dominant superexponential growth of $I_k(\kappa)$, we consider the rescaled quantity

$$\widehat{I}_k(\kappa) = I_k(\kappa)\left(\frac{2}{N}\right)^{N+\frac{1}{2}} \tag{4.4.55}$$

and apply the same rescaling to the corresponding asymptotic expansions.

Table 4.1 lists leading-order approximations (truncation index $m = 0$) for several values of x, together with the associated absolute relative errors with respect to numerical integration. The cases $x = N/(2\pi)$ and $x = \pi/2$ correspond to contributions from a pair of complex conjugate saddles, whereas $x = 1/\mathrm{e}$ is governed by a single degenerate saddle and $x = 1/\pi$ by a single simple saddle.

Overall, for increasing N, the rescaled values $\widehat{I}_k(\kappa)$ decay rapidly, while the relative errors decrease steadily. This behaviour reflects the increasing accuracy of the saddle-point approximation as the saddle locations move away from the origin and Stirling's approximation becomes more effective. For example, at $x = \pi/2$ the relevant saddle lies at $s = iN/\pi$. Thus, for moderate N (e.g. $N = 25$), the integrand is not yet well approximated by its asymptotic form, resulting in a comparatively larger relative error.

The numerical reference values were obtained from the integral representation (4.4.2) by exploiting its invariance under shifts of the contour parameter σ. In practice, the integral was evaluated for a range of σ values and working precisions, and a plateau in the resulting values was identified to ensure σ-stability. According to Stirling's formula, the integrand behaves asymptotically as

$$|t|^{2\sigma+n-1} \exp(-\pi|t|)\,,$$

so that smaller values of σ reduce algebraic growth and improve numerical stability. The reported values were therefore extracted from the stable region at small σ.

	$x = N/(2\pi)$		$x = \pi/2$	
N	$\widehat{I}_{\mathrm{asym}}$	Error	$\widehat{I}_{\mathrm{asym}}$	Error
25	1.43292(-17)	5.813(-01)	2.72993(-17)	2.092(+00)
50	4.32189(-37)	1.869(-01)	-6.19518(-32)	1.193(-02)
75	-4.59322(-59)	8.827(-02)	-1.42449(-48)	7.716(-02)
100	4.93201(-80)	4.419(-02)	1.60953(-63)	2.346(-02)
	$x = 1/e$		$x = 1/\pi$	
N	$\widehat{I}_{\mathrm{asym}}$	Error	$\widehat{I}_{\mathrm{asym}}$	Error
25	6.55446(-22)	2.273(-01)	3.20755(-24)	3.402(-02)
50	1.41901(-43)	1.732(-01)	2.88543(-48)	1.689(-02)
75	3.97172(-66)	1.477(-01)	2.83406(-73)	1.104(-02)
100	5.92527(-87)	1.334(-01)	2.33499(-96)	8.352(-03)

Table 4.1: Leading-order asymptotic value $\widehat{I}_{\mathrm{asym}}$ and absolute relative Error for $\kappa = 2$ ($N = n + 1$).

4.4.7 Asymptotic Representation of the Coefficients

The asymptotic behaviour of the coefficients $c_n(\kappa)$ follows from their representation in (4.4.1) together with the expansion (4.4.49). Recalling that $x = N/(2k\pi)$, we note that the critical value $x = \frac{1}{\mathrm{e}}$ cannot occur for integer k. This leads to the following asymptotic expansion.

$$c_n(\kappa) \sim (-1)^n \left(\frac{N}{2}\right)^{N+\frac{1}{2}-2\kappa} \sum_{m=0}^{\infty} \frac{\Gamma\left(m+\frac{1}{2}\right)}{N^m} \,\Re\left[\sum_{k=1}^{\infty} F_m(x)\right]. \tag{4.4.56}$$

Here the function F_m is given by

$$F_m(x) = x^{2\kappa} \exp\{N g_0(x)\} \sqrt{\frac{-1}{W(1+W)}}\, \widetilde{d}_{2m}(x) \left[1 + \theta\left(x - \tfrac{1}{e}\right)\right], \tag{4.4.57}$$

where $W = W_0(-x)$. For $x < \frac{1}{e}$, the Lambert W function remains real-valued, and the real-part operator may therefore be omitted.

4.4.8 First-Order Upper Bound

We conclude the asymptotic analysis by deriving a simple upper bound on the coefficients $c_n(\kappa)$ using the leading term ($m = 0$) of the expansion (4.4.56). This bound can then be compared with estimates obtained directly from the original integral representation.

Consider the inner sum in (4.4.56). Applying the triangle inequality gives

$$\sum_{k=1}^{\infty} \Re[F_0(x)] \le \sum_{k=1}^{\infty} |F_0(x)|. \tag{4.4.58}$$

Since the summand is monotone in $x = N/(2k\pi)$, the sum can be estimated by a Riemann integral:

$$\sum_{k=1}^{\infty} |F_0(x)| \le \frac{N}{2\pi} \int_0^{\frac{N}{2\pi}} |F_0(x)| \,\frac{\mathrm{d}x}{x^2}. \tag{4.4.59}$$

The dominant contribution to this integral is determined by the behaviour of the phase function $g_0(x)$, with potentially relevant points

$$x \in \left\{0,\ \frac{1}{\mathrm{e}},\ \frac{\pi}{2},\ \frac{N}{2\pi}\right\},$$

corresponding to the lower boundary, the branch-point singularity of the Lambert W function

at $x = 1/\mathrm{e}$, the stationary point of $\Re g_0(x)$ at $x = \pi/2$, and the upper boundary.

As $x \to 0$, the phase function vanishes exponentially (cf. (4.4.21)), suppressing the integrand. At $x = 1/\mathrm{e}$, although the prefactor $\sqrt{-1/(W(1+W))}$ exhibits a mild algebraic singularity of order $(x - 1/\mathrm{e})^{-1/4}$, the exponential term $\exp\{N g_0(x)\}$ contributes a strong suppression $\exp(-2N)$ (cf. (4.4.30)), rendering this point negligible for large N.

At the upper boundary $x = N/(2\pi)$, we have

$$F_0(x) \sim \exp\left[(2\kappa - 2)\log N - (N+1)\log\log N - N\right],$$

which is superexponentially smaller than the interior maximum at $x = \pi/2$, where

$$F_0(\pi/2) \sim \exp\big(-N - N\log(\pi/e)\big).$$

Thus, in the large-N limit, the integral is entirely dominated by the stationary point at $x = \pi/2$, and a Laplace approximation around this point suffices to obtain a sharp first-order bound.

Applying Laplace's method, we obtain

$$\sum_{k=1}^{\infty} |F_0(x)| = O\left(\sqrt{N}\left(\frac{2}{\pi\mathrm{e}}\right)^N\right). \tag{4.4.60}$$

Insertion into (4.4.56) yields

$$c_n(\kappa) = O\left(\left(\frac{N}{\pi\mathrm{e}}\right)^N N^{1-2\kappa}\right) = O\left(N!\, N^{\frac{1}{2}-2\kappa}\pi^{-N}\right) = O\left(\left(\frac{n}{\pi\mathrm{e}}\right)^n n^{-\kappa}\right), \tag{4.4.61}$$

confirming the anticipated super-exponential growth. This also shows that the convergence domain of the logarithmic expansion is bounded by

$$|\log z| < \frac{\pi}{2}, \tag{4.4.62}$$

set by the nearest singularity of the integral representation. Compared to the earlier estimates in Sect. 4.3, this provides a substantial improvement. Importantly, the present expansion is optimal, yielding higher-order corrections while remaining valid throughout the full convergence domain.

4.5 Probing the Zeta Function Through Asymptotic Coefficient Expansions

Having obtained both the MB representation (4.2.7) and the large-n expansion (4.4.56), we now outline how these expressions might be compared. The purpose of this section is thus purely exploratory: rather than establishing definitive results, we investigate how the two representations could interact and what information about zeta in the critical strip *could*, in principle, be extracted.

A first attempt at comparison is to bound $c_n(\kappa)$ directly from the MB integral by controlling the modulus of the integrand. For $s = \sigma + iT$ with $0 < \sigma < \frac{1}{2}$, Lindelöf's estimate (2.2.14) yields

$$\Gamma(s)\,\zeta(2s)\,\pi^{-2s}\,(\kappa - s)^n\Gamma(s-\kappa) = O\Big(T^{2\sigma+\mu(2\sigma)+n-\kappa-1}\,e^{-\pi T}\Big).$$

Using the reflection principle from Sect. 4.2 and bounding the real part of the contour integral by its modulus gives

$$c_n(\kappa) = O\left(\left(\frac{n}{\pi e}\right)^n n^{\,2\sigma+\mu(2\sigma)-\kappa-\frac{1}{2}}\right), \tag{4.5.1}$$

with the implicit constant depending only on σ and κ. This estimate, however, is far from optimal. Consistency with the steepest-descent bound (4.4.61) would require

$$\mu(2\sigma) = \frac{1}{2} - 2\sigma \qquad \left(0 < \sigma < \tfrac{1}{2}\right).$$

It is striking that, for the crude bound (4.5.1) to be compatible with the steepest-descent estimate (4.4.61), one would effectively need to invoke the Lindelöf hypothesis in the regime $0 < \sigma < 1/4$ (accounting for $\zeta(2s)$). This illustrates two key points: first, discarding the phase information in the integrand destroys the delicate cancellations between $\zeta(2s)$ and $(\kappa - s)^n$; second, the asymptotic expansion of $c_n(\kappa)$ derived via the saddle-point analysis is exceptionally sharp, and its precise scaling cannot be captured by such simple modulus-based estimates. In other words, absolute-value bounds on the MB integral are insufficient to reproduce the subtle asymptotic behaviour of the coefficients.

Indeed, the steepest-descent asymptotics provide a more informative perspective. For large n, the dominant contribution to the integral (4.2.7) arises from a neighbourhood of

$$T_{\max} \sim \frac{n}{\pi},$$

where the integrand attains its maximum. Expanding the logarithm of the integrand to quadratic order shows that the width of this neighbourhood scales as $\sqrt{n}$. Thus, the contour contribution is concentrated in an increasingly narrow interval around $T_{\max}$, while the height grows like

$\left(\frac{n}{\pi e}\right)^n$. In this sense, n acts as a *resolution parameter*: as n increases, the MB representation probes $\zeta(2s)$ in an ever tighter region of the critical strip.

This localisation suggests a possible mechanism for detecting the influence of non-trivial zeros. If a zero of $\zeta(2s)$ lies within the localisation region, the MB integral would be strongly suppressed. Should such a suppression conflict with the independently derived asymptotic expansion (4.4.56), one could, in principle, rule out the presence of a zero in that region. This is analogous to Watson's lemma: the vanishing of an integrand at a critical point can drastically reduce the size of the corresponding asymptotics.

For this approach to yield constraints, n must be sufficiently large that

$$T_{\max} \sim \frac{n}{\pi}$$

probes heights beyond the current numerical verification of the RH ($T \lesssim 10^{13}$). At the same time, the asymptotic expansion (4.4.56) becomes increasingly accurate as $n \to \infty$, sharpening the potential comparison.

Although no concrete bounds on zeros are obtained here, this analysis outlines a possible strategy for probing the distribution of non-trivial zeros of $\zeta(2s)$ at heights far beyond present computational reach. A more detailed investigation of this idea is left for future work.

Chapter 5

Summary and Outlook

In this thesis we have investigated the one-loop thermal pressure of SU(2) Yang–Mills theory in its deconfined phase, with particular emphasis on the analytic structures emerging from its dependence on the quasiparticle mass parameter a. We initiated our work by expanding the pressure in both the small- and large-mass regimes, with the results given in Eqs. (3.3.18) and (3.3.29), respectively. Using these expressions, the critical temperature λ_c was determined numerically by solving the thermodynamic self-consistency condition in the form of the first-order differential equation (3.2.1), and the resulting values were found to be in excellent agreement with those obtained semi-analytically from the leading behaviour of the large-a expansion.

A central element of the analysis was the logarithmic mass expansion of the one-loop pressure, Eq. (3.3.9), whose coefficients $c_n(\kappa)$ encode the full analytic continuation of the effective potential. Two complementary representations of these coefficients were established in Chapter 4: a double-sum expression (4.2.1) useful for small n, and a Mellin–Barnes representation (4.2.7) that probes $\zeta(2s)$ inside the critical strip. Starting from the Mellin–Barnes representation and shifting the contour to the right, a uniform large-order asymptotic expansion for $c_n(\kappa)$ was derived in Eq. (4.4.56) using the method of steepest descent. In this regime, the zeta function enters solely through its Dirichlet series representation, thereby permitting termwise evaluation of the contour integrals and avoiding the subtleties associated with the critical strip. Finally, in Sect. 4.5, we explored how the Mellin–Barnes representation and the large-n asymptotics might be compared to shed light on the distribution of non-trivial zeros of the Riemann zeta function.

The results obtained here open several areas for further investigation. A natural first direction concerns the rôle of spatial dimension. The coefficients $c_n(\kappa)$ depend on the parameter $\kappa = \frac{d+1}{2}$, yet in the steepest–descent expansion (4.4.56) this dependence enters only through the shift $n \mapsto n + \kappa$. A deeper understanding of this mild dimensional sensitivity requires a systematic use of the recurrence relation given in Eq. (3.3.1) and its iterative action on the

pressure. Equation (4.2.2) shows explicitly that the coefficients $c_n(\kappa)$ may be expressed as weighted sums of rescaled pressures in lower dimensions, with Stirling numbers of the second kind governing the combinatorics. Clarifying the structural implications of this dimensional coupling, and determining whether a universal pattern persists beyond one-loop, constitutes a promising direction for future work.

A second direction concerns the analytic number theory that entered through $\zeta(2s)$. The exploratory analysis in Sect. 4.5 suggests that, at least in principle, the MB representation may be sensitive to the location of non-trivial zeros due to its sharp localisation at $T_{\max} \sim n/\pi$ for large n. A more rigorous comparison between the contour integral and the asymptotic expansion would require controlling the error terms in Eq. (4.4.56) at arbitrarily large order, as well as understanding how the presence of a hypothetical zero ρ off the critical line–encoded through a factorisation $\zeta(s) = (s-\rho)\, g(s)$ into a zero and a non-vanishing analytic part–manifests itself within the MB resolvent. In the regime of large imaginary part, the zeta function exhibits rapid oscillations and increasingly complicated behaviour [63, 64], making the analysis of its influence on $c_n(\kappa)$ particularly challenging.

Although the comparative analysis between the integral representation and the large-order asymptotic expansion highlights a structural sensitivity to the location of non-trivial zeros, it does not, in its present form, yield unconditional statements about them. Establishing such results would require a level of analytic control that currently lies beyond reach. The present investigation should therefore be regarded as an indication that analytic structures arising in finite-temperature Yang–Mills theory interact in a non-trivial way with the properties of the zeta function, rather than as a route to proving statements about zero locations. Nevertheless, the established framework provides a foundation for more refined analyses, relying on sharper asymptotics or improved integral representations, and may eventually lead to quantitative constraints on the distribution of zeros at heights far beyond current computational limits. Finally, this approach complements already existing connections between number theory and quantum physics, such as those based on random matrix theory and Hamiltonian constructions, by presenting a perspective rooted in thermal SU(2) Yang–Mills theory.

Appendix A

Fundamental Mathematical Methods

This chapter aims to highlight selected techniques in asymptotic analysis and illustrate them through concrete examples, which are essential for understanding the methods used in this work. We present a number of well-known examples from the literature, many of which play a central rôle in the analytic study of the Riemann zeta function, along with several calculations carried out independently by the author, which are crucial for the developments presented in this thesis. For a comprehensive and systematic treatment of asymptotic methods, the reader is referred to the classical references [30, 57, 65, 66].

A.1 Introduction to Asymptotic Analysis

Asymptotic analysis investigates the behaviour of functions, sequences, or series in the vicinity of prescribed points in their domain. The objective is to obtain approximations that are valid within a neighbourhood of the point under consideration. Importantly, the function itself does not necessarily need to be defined for all points in this neighbourhood.

Asymptotic expansion techniques examine contour integral formulations, solutions to differential equations, and series expansions [57]. In many cases, the function is expressed in terms of a truncated series, where the remainder must be of the same order of magnitude as the first neglected term. In most cases, the truncation error cannot simply be expressed as the sum of the remaining tail of the series, as the asymptotic series typically do not converge.

In the case of convergent expansions, it is possible to refine the approximation to arbitrary accuracy by adding more terms. However, their limited radius of convergence renders their accuracy inferior to divergent asymptotic expansions when comparing numerical values close to their boundary and beyond. In contrast, for divergent asymptotic series, the minimal achievable error is limited and dictated by the behaviour of the parameter under consideration [66]. Thus, the strength of asymptotic analysis lies in its ability to provide meaningful approxima-

tions even when exact convergence is not attainable.

A.2 Asymptotic Expansions

Asymptotic expansions are naturally formulated using Bachmann-Landau notation to describe the limiting behaviour of a function. Let x be a real or complex variable, and suppose that $f(x)$ and $g(x)$ are two functions defined and continuous in a domain R such that x_0 lies in the closure $\overline{R}$.

Definition A.2.1 (Landau's Large ''O''[65])**.** We say that f is of order not exceeding g as $x \to x_0$, denoted by

$$f(x) = O(g(x)) \qquad \text{as} \quad x \to x_0, \tag{A.2.1}$$

if there exists a constant $M > 0$ and a neighbourhood N_0 of $x_0 \in \overline{R}$ such that

$$|f(x)| \leq M|g(x)| \qquad \left(\forall x \in N_0 \cap \overline{R}\right). \tag{A.2.2}$$

The least constant M fulfilling the above condition is called the *implied constant*.

Similarly,

Definition A.2.2 (Landau's Small ''o''[65])**.** We say that f is asymptotic to g as $x \to x_0$, denoted by

$$f(x) = o(g(x)) \qquad \text{as} \quad x \to x_0, \tag{A.2.3}$$

if for any $\epsilon > 0$, there exists a neighbourhood N_ϵ of $x_0 \in \overline{R}$ such that

$$|f(x)| \leq \epsilon|g(x)| \qquad \left(\forall x \in N_\epsilon \cap \overline{R}\right). \tag{A.2.4}$$

Example A.2.1 (Topologically Non-Trivial Sector[19])**.** Consider the Euclidean Yang–Mills action for a pure gauge field configuration with non-trivial topology, satisfying the (anti)selfduality condition. The action is given by $S = \frac{8\pi^2|k|}{g^2}$, where g is the coupling constant and $k \in \mathbb{Z}$ is the topological charge.

Let us examine the function

$$f(x) = \begin{cases} 0, & (-\infty < x \leq 0), \\ \exp\left(-\frac{1}{x}\right), & (0 < x \leq \infty), \end{cases} \tag{A.2.5}$$

along with $g(x) = x^m$ for any $m \in \mathbb{C}$.

We compute the limits

$$\lim_{x\to 0^+} \frac{f(x)}{g(x)} = 0, \qquad \lim_{x\to 0^-} \frac{f(x)}{g(x)} = 0. \tag{A.2.6}$$

Therefore, $f(x) = o(x^m)$ as $x \to 0$ for all $m \in \mathbb{C}$.

Such terms are said to be *asymptotic beyond all orders* in x. Hence, the topologically non-trivial sector does not contribute to the action in the perturbative expansion around the vanishing coupling constant g. This observation underlies the claim made in Section 1. The concept of an essential zero is also explored by Hardy and Littlewood [37], who used it to prove the existence of infinitely many zeros of the Riemann zeta function on the critical line $\Re(s) = \frac{1}{2}$.

Asymptotic equality is expressed by the notation $f(x) \sim g(x)$, which denotes the relation $f(x) = g(x)\big(1 + o(1)\big)$ as $x \to x_0$. In short, one writes $f(x) = O(g(x))$ as $x \to x_0$ if the ratio $f(x)/g(x)$ remains bounded, whereas $f(x) = o(g(x))$ as $x \to x_0$ if this ratio tends to zero.

Moreover, if an asymptotic expansion depends on additional parameters and remains valid over a domain in the parameter space, the expansion is said to hold *uniformly* within that domain. For formulas concerning combinations of order relations, see [65].

Up to restrictions concerning the convergence of integrals, order relations and asymptotics may be carried through integration. Differentiation, on the other hand, is generally not permissible. Special cases where it is applicable include complex functions that are holomorphic in a closed annular sector, see also [66].

Definition A.2.3 (Asymptotic Power Series Expansion [67, 68])**.** Let $f(x)$ be defined and continuous on R. Then $f(x)$ is said to have a convergent or divergent asymptotic power series expansion in the sector $S_{\alpha\beta} = \{x \in \mathbb{C} | 0 < |x - x_0|; \alpha < \arg(x - x_0) < \beta\}$ for x_0 finite,

$$f(x) \sim \sum_{n=0}^{\infty} a_n (x - x_0)^n \qquad (x \to x_0 \in S) \tag{A.2.7}$$

provided the following condition holds:

$$\lim_{x\to x_0} \left\{ (x - x_0)^{-N} \left[f(x) - \sum_{n=0}^{N} a_n (x - x_0)^n \right] \right\} = 0 \qquad (\forall N \in \mathbb{N}_0)\,, \tag{A.2.8}$$

which is equivalent to

$$f(x) = \sum_{n=0}^{N} a_n (x - x_0)^n + O(x - x_0)^{N+1} \qquad (x \to x_0 \in S, \forall N \in \mathbb{N}_0)\,. \tag{A.2.9}$$

The definition is then broadened to allow the condition to be satisfied up to $N \in \mathbb{N}$, in which

case f is said to have an asymptotic power series to N terms as $x \to x_0$

$$f(x) = \sum_{n=0}^{N-1} a_n (x - x_0)^n + o(x - x_0)^{N-1} \qquad (x \to x_0)\,. \tag{A.2.10}$$

Moreover, the limit $x \to \infty$ is permissible with respect to the asymptotic sequence $\{x^{-n}\}_{n\in\mathbb{N}_0}$. Generally, *Poincaré-type* expansions allude to expansion in which each summand is a product of a coefficient a_n and an auxiliary scale function, to be introduced in Def. A.2.4. A crucial property of Poincaré-type asymptotic expansions is that their coefficients a_n are uniquely determined by the recursion relation

$$a_n = \lim_{x\to x_0} \left\{ (x - x_0)^{-n} \left[f(x) - \sum_{r=0}^{n-1} a_r (x - x_0)^r \right] \right\} \qquad (n \in \mathbb{N}_0)\,. \tag{A.2.11}$$

If a possibly infinite power series expansion converges to $f(x)$ throughout some neighbourhood of $x = x_0$, powerful methods of complex analysis aid towards the determination of the coefficients a_n recursively as well as of the error estimate $r_R(x)$-obtained by truncating the series after R terms-by use of Cauchy's integral formula and the geometric series as

$$r_R(x) = \sum_{n=R}^{\infty} a_n x^n = \frac{x^R}{2\pi i} \oint_C \frac{f(z)}{z^R (z - x)}\, \mathrm{d}z, \tag{A.2.12}$$

with C positively encircling 0 and x.

Consequently, asymptotic series of single-valued holomorphic functions are convergent and equal $f(x)$ in their disk of convergence by properties of their Laurent series.

Example A.2.2 (Binomial Series)**.** For $z \in \mathbb{C}$, $\nu \in \mathbb{R}_{>0}$, and $R \in \mathbb{N}_0$, the binomial expansion with remainder reads

$$(1 + z)^\nu = \sum_{k=0}^{R-1} \binom{\nu}{k} z^k + r_R(z), \tag{A.2.13}$$

where the coefficients are given by the generalised binomial theorem,

$$\binom{\nu}{k} = \frac{\Gamma(\nu + 1)}{\Gamma(k + 1)\,\Gamma(\nu - k + 1)}, \qquad \nu \in \mathbb{C} \setminus \{-1, -2, \dots\}, \quad k \in \mathbb{N}_0, \tag{A.2.14}$$

with the gamma function introduced in Sect. 2.1. The remainder term can be represented, via Cauchy's integral formula for $|z| < 1$, as

$$r_R(z) = \frac{z^R}{2\pi i} \oint_C \frac{(1 + u)^\nu}{u^R (u - z)}\, \mathrm{d}u, \tag{A.2.15}$$

where C is a circular contour centred at the origin with radius $\rho > |z|$. Estimating the contour integral yields

$$|r_R(z)| \leq \left(\frac{|z|}{\rho}\right)^R \sup_{|u|=\rho} |(1+u)^\nu| = O(z^R), \tag{A.2.16}$$

showing that the remainder is of the same order as the first omitted term.

The binomial series converges absolutely for $|z| < 1$ for all ν, and also for $|z| = 1$ provided $\Re(\nu) > 0$:

$$(1+z)^\nu = \sum_{k=0}^{\infty} \binom{\nu}{k} z^k \qquad \big(|z| < 1 \text{ or } (|z| = 1 \text{ and } \Re(\nu) > 0)\big). \tag{A.2.17}$$

For $|z| > 1$, one may factor out z^ν and re-expand in inverse powers of z.

However, Example A.2.1 demonstrates that power series expansions are not always capable of providing useful asymptotic descriptions. To obtain a more refined qualitative picture, one may introduce an *auxiliary sequence* that serves as a scale against which comparisons are made. It is evident that the choice of auxiliary sequence has a decisive influence on the accuracy of numerical approximations.

Definition A.2.4 (Asymptotic Sequence [24])**.** A sequence of functions $\{\phi_n(x)\}$, $n \in I$, is called an *asymptotic sequence* if

$$\phi_{n+1} = o(\phi_n) \qquad \big(x \to x_0\big), \tag{A.2.18}$$

as long as n and $n+1$ both belong to I.

Remark A.2.1. In literature, the phrasing of asymptotic sequence and asymptotic scale are used interchangeably.

Generalisations of auxiliary asymptotic sequences satisfying similar conditions belong to the class of Poincaré-type asymptotics and are chosen a posteriori to yield sufficient error estimates.

Definition A.2.5 (Poincaré Type Asymptotic Expansion [30])**.** Let $f(x)$ be defined and continuous on the common domain of the asymptotic scale $\{\phi_n\}$. Then $f(x)$ is said to have an (infinite) asymptotic expansion with respect to the asymptotic sequence $\{\phi_n\}$

$$f(x) \sim \sum_{n=0}^{\infty} a_n \phi_n(x) \qquad (x \to x_0)\,, \tag{A.2.19}$$

provided that for any non-negative integer N

$$f(x) = \sum_{n=0}^{N} a_n \phi_n(x) + O\left(\phi_{N+1}(x)\right) \qquad (x \to x_0)\,. \tag{A.2.20}$$

Similar to the coefficients in Def. (A.2.3), the coefficients a_n in Def. (A.2.5) are uniquely determined by the recursive relation

$$a_n = \lim_{x \to x_0} \frac{1}{\phi_n(x)} \left\{ f(x) - \sum_{r=0}^{n-1} a_r \phi_r(x) \right\} \qquad (n \in \mathbb{N}_0)\,. \tag{A.2.21}$$

Remark A.2.2. Asymptotic expansions of Poincaré-type have uniquely defined coefficients a_n. However, the converse does not necessarily hold: two distinct functions can share the same asymptotic expansion. For example, any function $f(x)$ with power series expansion as $x \to \infty$ shares the same expansion as $f(x) + e^{-x}$. Extensions of Definition A.2.5 include *generalised asymptotic expansions* and *compound asymptotic expansions*. These cases are not treated here, since our work relies on the uniqueness of the coefficients a_n, which is no longer guaranteed in the generalised setting.

As our work is founded on the uniqueness principle of analytic continuation, it is important to remark on the *Stokes phenomenon*, which concerns the analytic continuation of a function $f(x)$ and its asymptotic expansion beyond a sector of validity S in the complex plane. It may occur that, across certain rays-*Stokes lines*-the asymptotic expansion ceases to represent the behaviour of $f(x)$. This situation arises in particular when a multivalued function is approximated asymptotically by expressions with a different multivalued structure. When traversing Stokes lines, exponentially small contributions can switch on and come to dominate the asymptotic description, producing a qualitative change that is both smooth and universal in character [69]. This indicates that the chosen asymptotic scale is insufficient to reflect the behaviour of the function outside its initial sector of validity.

Example A.2.3 (Modified Bessel Functions of the Second Kind $K_\nu(z)$ [69, 70])**.** Consider the large-z asymptotic sequence

$$u_\pm(z) = \left(\frac{\pi}{2z}\right)^{1/2} e^{\pm z} \sum_{r=0}^{\infty} (\mp 1)^r \, a_r(\nu) \, (2z)^{-r}, \tag{A.2.22}$$

where $a_0(\nu) = 1$ and, for $r \geq 1$,

$$a_r(\nu) = \frac{\left(4\nu^2 - 1^2\right)\left(4\nu^2 - 3^2\right) \cdots \left(4\nu^2 - (2r-1)^2\right)}{r!\, 2^{2r}}. \tag{A.2.23}$$

The modified Bessel function of the second kind admits the decomposition

$$K_\nu(z) = A\,u_+(z) + B\,u_-(z) \qquad (z \to \infty). \tag{A.2.24}$$

By comparing the exponential factors, one finds that the Stokes lines are located at

$$\theta = \arg(z) = \pm\pi,\ \pm 2\pi,\ \ldots \tag{A.2.25}$$

and thus

$$K_\nu(z) \sim u_-(z) \qquad \big(|z| \to \infty,\ -\pi < \theta < \pi\big). \tag{A.2.26}$$

Using the connection formula [23]

$$K_\nu(z) = 2\cos(\pi\nu)\,K_\nu\big(ze^{-i\pi}\big) - K_\nu\Big(ze^{-2i\pi}\Big), \tag{A.2.27}$$

we also have

$$K_\nu(z) \sim u_-(z) + 2i\cos(\pi\nu)\,u_+(z) \qquad \big(|z| \to \infty,\ \pi < \theta < 2\pi\big). \tag{A.2.28}$$

This shows that the multiplier A undergoes a discontinuous jump as a Stokes line is crossed. Berry [69] demonstrated, via Borel summation of the remainder, that this jump is in fact a smooth, yet rapid transition.

In the literature, a slightly wider validity range is also given [23]:

$$K_\nu(z) \sim u_-(z) \qquad \big(|\arg z| \le \tfrac{3}{2}\pi\big), \tag{A.2.29}$$

$$K_\nu(z) \sim u_-(z) + 2i\cos(\pi\nu)\,u_+(z) \qquad \big(|\arg z| \le \tfrac{3}{2}\pi\big). \tag{A.2.30}$$

Lastly, we examine the *optimal truncation* of the asymptotic series (A.2.22). Since the coefficients (A.2.23) grow factorially, the series is divergent. To minimise the truncation error, we choose $N(z)$ so that the magnitude ratio of successive terms is about one:

$$\left|\frac{a_N(\nu)}{a_{N-1}(\nu)}\right| = \left|\frac{4\nu^2 - (2N-1)^2}{4N}\right| \approx 2\,|z|. \tag{A.2.31}$$

Hence $N\,(1 + o(1)) \approx 2\,|z|$, so that the optimal truncation index is

$$N_{\text{opt}} = \lfloor 2\,|z| \rfloor + 1, \tag{A.2.32}$$

where $\lfloor \cdot \rfloor$ denotes the integer part.

A.3 Mellin Transforms

Although not formally a member of the class of *h-transforms*, the Mellin transform plays an invaluable rôle in asymptotic analysis due to its analytic properties. It is particularly indispensable when studying the asymptotic behaviour of functions that are defined through integrals. By shifting the contour of integration in the complex plane, contributions from subsets of singularities in the integrand arise, thereby contributing to asymptotic expansions in either ascending or descending order, depending on the direction of contour displacement.

More precisely, closure on the left half-plane leads to descending series expansions with respect to the relevant parameter, whereas closure on the right half-plane produces ascending power series expansions, to be explained later.

Formally, the Mellin transform $\mathcal{M}[f;s]$ of a locally integrable function $f(t)$ on the interval $\mathbb{R}_>$, evaluated at $s \in \mathbb{C}$, is given by the bilateral Laplace transform:

$$\mathcal{M}[f;s] = \int_0^\infty f(t)t^{s-1}\mathrm{d}t. \tag{A.3.1}$$

The complex variable $s = \sigma + it$ is the standard notation, introduced in the work of Riemann [33], who was the first to apply Mellin transformations.

From Eq. (A.3.1), it follows that the Mellin transform converges absolutely and defines a holomorphic function in the *strip of analyticity* $\alpha < \Re(s) < \beta$, where

$$\alpha = \inf\left\{\alpha^* \mid f = O(t^{-\alpha^*}),\ t \to 0^+\right\}, \tag{A.3.2}$$

$$\beta = \sup\left\{\beta^* \mid f = O(t^{-\beta^*}),\ t \to \infty\right\}. \tag{A.3.3}$$

The canonical example is the Mellin pair consisting of e^{-t} and $\Gamma(s)$, cf. Eq. (2.1.2) and Eq. (2.1.3). The inversion formula for Mellin transforms is given by

$$f(t) = \frac{1}{2\pi i}\int_{\sigma-i\infty}^{\sigma+i\infty} t^{-s}\mathcal{M}[f;s]\,\mathrm{d}s \qquad (\alpha < \sigma < \beta)\,. \tag{A.3.4}$$

Mellin transforms can be analytically continued beyond their domains $\alpha < \Re(s) < \beta$ by expanding the integrand $f(t)$ into a power series of the form $f(t) = f_n(t) + r_n(t)$, with remainder term $r_n(t)$. The Mellin transform then decomposes into $\mathcal{M}[f;s] = \mathcal{M}[f_n;s] + \mathcal{M}[r_n;s]$. Depending on the asymptotic behaviour of f encoded in f_n, the Mellin transform can either be holomorphic or meromorphic; see Bleistein and Handelsman [65, Chapter 4] for a detailed discussion.

For example, $\Gamma(s) = \mathcal{M}\left[e^{-t};s\right]$ (see Eq. (2.1.2)), which initially requires $0 < \Re(s) < \infty$, admits an analytic continuation to a meromorphic function defined over the entire complex

plane, except at the simple poles $\mathbb{C} \setminus \mathbb{Z}_{\leq}$.

In general, the limiting behaviour of f determines the continuation properties of its Mellin transform [65]:

(a) $\mathcal{M}[f;s]$ is holomorphic in a right half-plane if f decays exponentially as $t \to \infty$.

(b) $\mathcal{M}[f;s]$ can be analytically continued into a right half-plane as a holomorphic function if f is oscillatory as $t \to \infty$.

(c) $\mathcal{M}[f;s]$ can be analytically continued into a right half-plane as a meromorphic function if f decays algebraically and monotonically as $t \to \infty$.

By symmetry, analogous continuation results hold for the left half-plane by examining the limiting behaviour as $t \to 0$. Thus, a Mellin transform of f may exist in a generalised sense even if $\alpha > \beta$.

Example A.3.1 (Beta Function as Generalised Mellin Transform)**.** Consider the function

$$f(t) = t(t^2 - a^2)^{\nu} \qquad (\Re(\nu) > 0, a > 0)\,. \tag{A.3.5}$$

Since $f(t) \sim t^{1+2\nu}$ as $t \to \infty$ and $f(t) \sim t$ as $t \to 0^+$, we obtain the growth exponents $\alpha = -1$ and $\beta = -1 - 2\Re(\nu)$ so that $\mathcal{M}[f;s]$ does not exist in the ordinary sense.

To overcome this, we split f into two parts according to the domain

$$f_1(t) = \begin{cases} t(t^2 - a^2)^{\nu}, & (0 \leq t < a)\,, \\ 0, & (a \leq t < \infty)\,, \end{cases} \tag{A.3.6}$$

$$f_2(t) = \begin{cases} 0, & (0 \leq t < a)\,, \\ t(t^2 - a^2)^{\nu}, & (a \leq t < \infty)\,, \end{cases} \tag{A.3.7}$$

from which we can define the generalised Mellin transform $\mathcal{M}[f;s] = \mathcal{M}[f_1;s] + \mathcal{M}[f_2;s]$.

The integral defining $\mathcal{M}[f_1;s]$ converges in the half-plane $\Re(s) > -1$, while $\mathcal{M}[f_2;s]$ converges for $\Re(s) < -1 - 2\Re(\nu)$. Thus, each part is initially defined only in a complementary strip of the complex plane. To obtain the generalised Mellin transform, we must analytically continue $\mathcal{M}[f_1;s]$ to the left half-plane and $\mathcal{M}[f_2;s]$ to the right half-plane.

As both functions decay algebraically, we expect meromorphic continuations with poles at $s = 1, 3, 5, \cdots$ and $s = 2\nu + 1, 2\nu - 1, 2\nu - 3, \cdots$. Specifically, comparison with (2.1.24)

yields after substitution

$$\mathcal{M}[f_1; s] = \frac{(-1)^\nu}{2} a^{1+2\nu+s} B\left(\nu+1, \frac{s+1}{2}\right) \qquad (\Re(s) > -1) \tag{A.3.8}$$

$$\mathcal{M}[f_2; s] = \frac{1}{2} a^{1+2\nu+s} B\left(\nu+1, -\frac{s+2\nu+1}{2}\right) \qquad (\Re(s) < -1-2\Re(\nu))\,. \tag{A.3.9}$$

Since the beta function admits a meromorphic continuation via the gamma function, both $\mathcal{M}[f_1; s]$ and $\mathcal{M}[f_2; s]$ extend to meromorphic functions on the entire complex plane. Moreover, the pole structure agrees with that expected. Finally, we obtain

$$\mathcal{M}[f; s] = \frac{a^{1+2\nu+s}}{2} \Gamma(\nu+1) \left\{ \frac{\Gamma\left(-\frac{s+2\nu+1}{2}\right)}{\Gamma\left(\frac{1-s}{2}\right)} + \frac{(-1)^\nu \Gamma\left(\frac{1+s}{2}\right)}{\Gamma\left(\frac{3}{2}+s+\nu\right)} \right\}. \tag{A.3.10}$$

Example A.3.2 (Functional Equation of the Riemann Zeta Function [33, 41])**.** We begin with the Mellin transform of the exponential (the gamma function definition):

$$\int_0^\infty e^{-nx}\, x^{s-1}\, \mathrm{d}x = \frac{\Gamma(s)}{n^s} \qquad (\Re(s) > 0,\ n \in \mathbb{N}). \tag{A.3.11}$$

Summing (A.3.11) over $n \geq 1$ and interchanging sum and integral (justified by absolute convergence for $\Re(s) > 1$) gives

$$\Gamma(s)\, \zeta(s) = \int_0^\infty \frac{x^{s-1}}{e^x - 1}\, \mathrm{d}x \qquad (\Re(s) > 1). \tag{A.3.12}$$

To continue analytically, we consider the keyhole (Hankel) contour $\mathcal{H}$ encircling the positive real axis and the origin. This leads to the definition

$$I(s) := \int_{\mathcal{H}} \frac{x^s}{e^x - 1} \frac{\mathrm{d}x}{x},$$

where x^s uses the principal branch.

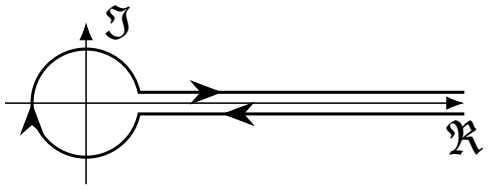

Figure A.1: Hankel Contour $\mathcal{H}$

Since the singularity at the origin vanishes for $\Re(s) > 1$, the circle around the origin may be shrunk to zero. Traversing just above and just below the positive real axis, we find

$$\begin{aligned} I(s) &= \left(e^{2\pi i s} - 1\right) \int_0^\infty \frac{x^{s-1}}{e^x - 1}\, \mathrm{d}x \\ &= \frac{2\pi i e^{i\pi s}}{\Gamma(1-s)} \zeta(s). \end{aligned} \tag{A.3.13}$$

Alternatively, we can evaluate $I(s)$ by adding asymptotic circles enclosing the poles of the integrand at $x = 2\pi in$, $n \in \mathbb{Z} \setminus \{0\}$, and letting their radii tend to infinity. As $I(s)$ is an integral function in any finite s-domain, this step is permissible and allows taking the limits of radii by the boundedness of the integrand provided $\Re(s) < 0$. Evaluating the residues at these poles yields for $\Re(s) < 0$

$$\begin{aligned} I(s) &= -(2\pi i) \sum_{n=1}^{\infty} \left[(2\pi in)^{s-1} + (-2\pi in)^{s-1} \right] \\ &= -(2\pi)^s i\zeta(1-s) \left[e^{\frac{\pi}{2} i(s-1)} + e^{\frac{3}{2}\pi i(s-1)} \right] \\ &= -(2\pi)^s i\zeta(1-s) e^{i\pi(s-1)} (-2) \sin\left(\frac{\pi}{2} s\right) \\ &= 2i(2\pi)^s e^{\pi i s} \zeta(1-s) \sin\left(\frac{\pi}{2} s\right). \end{aligned} \tag{A.3.14}$$

Note that the minus sign originates in the clockwise orientation of the contour around the poles.

Ultimately, equating (A.3.13) and (A.3.14) gives the functional equation

$$\zeta(s) = 2^s \pi^{s-1} \sin\left(\frac{\pi s}{2}\right) \Gamma(1-s)\zeta(1-s) \qquad (s \in \mathbb{C}). \tag{A.3.15}$$

Equivalently, by the reflection formula (2.1.10), we obtain the symmetric form

$$\pi^{-s/2}\Gamma\left(\frac{s}{2}\right)\zeta(s) = \pi^{-(1-s)/2}\Gamma\left(\frac{1-s}{2}\right)\zeta(1-s) \quad (s \in \mathbb{C}). \tag{A.3.16}$$

The sine in Eq. (A.3.16) explicitly demonstrates the locations of the trivial zeros of the zeta function at $s = -2n$ for $n \in \mathbb{N}$. Moreover, Eq. (A.3.16) underlines the location of the pole at $s = 1$, with approximation near $s = 1$ given by

$$\zeta(s) = \frac{1}{s-1} + \gamma + O(|s-1|), \tag{A.3.17}$$

consult Titchmarsh [42] for more details.

Example A.3.3 (Riemann Xi Function via Mellin Transforms [33, 41])**.** In his work, Riemann [33] introduced the Mellin transform of Jacobi's theta function to derive the functional equation for the Riemann zeta function. For $s = \sigma + it$ with $\sigma > \frac{1}{2}$, one has

$$\zeta(2s)\Gamma(s)\pi^{-s} = \int_0^{\infty} \psi(x)\, x^{s-1}\, \mathrm{d}x, \tag{A.3.18}$$

where

$$\psi(u) = \sum_{n=1}^{\infty} e^{-\pi n^2 u} \qquad (\Re(u) > 0) \tag{A.3.19}$$

denotes the first half of Jacobi's theta function.

Equivalently, the Riemann Xi function admits the Mellin representation

$$\frac{2\xi(s)}{s(s-1)} = \int_0^\infty \left[G(u) - \frac{1}{u}\right] u^{-s}\,\mathrm{d}u \qquad (1 < \Re(s)), \tag{A.3.20}$$

where

$$G(u) = 1 + 2\psi(u^2) = \sum_{n=-\infty}^{\infty} e^{-\pi n^2 u^2} \qquad \left(\Re(u^2) > 0\right) \tag{A.3.21}$$

is precisely Jacobi's theta function, which satisfies the modular relation $uG(u) = G(1/u)$ (the functional equation for this relation is derived in Example A.3.6). From this symmetry it follows that

$$G(u) - \frac{1}{u} = \frac{1}{u}\left[G\left(\tfrac{1}{u}\right) - 1\right], \tag{A.3.22}$$

which together with Example A.2.1 implies exponential decay of itself and all its derivatives as $u \to 0^+$. Moreover,

$$G(u) - \frac{1}{u} = [G(u) - 1] + \left[1 - \frac{1}{u}\right], \tag{A.3.23}$$

confirming that the abscissa of convergence in (A.3.20) is $1 < \Re(s)$. Substituting $s \mapsto 1 - s$ in (A.3.20), the expression resembles the Mellin transform as defined in Eq. (A.3.1). Before performing explicit analytic continuation, one can infer from the asymptotics of the integrand as $u \to \infty$ that the Mellin transform possesses simple poles at $s = 0, 1$; see also [65, Lemma 4.3.3]. Although this is evident from the left-hand side of (A.3.20), when only given the right-hand side, it is a non-trivial conclusion.

Indeed, applying the substitution $u \mapsto 1/u$ yields

$$\frac{2\xi(s)}{s(s-1)} = \int_0^\infty \big[G(u) - 1\big] u^{-s}\,\mathrm{d}u \qquad (\Re(s) < 0). \tag{A.3.24}$$

Interpolating between (A.3.20) and (A.3.24), we use

$$\begin{aligned} \int_0^1 \frac{\mathrm{d}x}{x^{s+1}} &= -\frac{1}{s} \quad (\Re(s) < 0), \\ \int_1^\infty \frac{\mathrm{d}x}{x^{s+1}} &= +\frac{1}{s} \quad (\Re(s) > 0), \end{aligned} \tag{A.3.25}$$

to obtain

$$\frac{2\xi(s)}{s(s-1)} = \int_0^\infty \left[G(u) - 1 - \frac{1}{u} \right] u^{-s} \, \mathrm{d}u \qquad (0 < \Re(s) < 1). \tag{A.3.26}$$

Combining the three representations, we arrive at

$$\frac{2\xi(s)}{s(s-1)} = \begin{cases} \displaystyle\int_0^\infty \left[G(u) - 1 \right] u^{-s} \, \mathrm{d}u, & (\Re(s) < 0), \\ \displaystyle\int_0^\infty \left[G(u) - 1 - \tfrac{1}{u} \right] u^{-s} \, \mathrm{d}u, & (0 < \Re(s) < 1), \\ \displaystyle\int_0^\infty \left[G(u) - \tfrac{1}{u} \right] u^{-s} \, \mathrm{d}u, & (\Re(s) > 1), \end{cases} \tag{A.3.27}$$

which provides an analytic continuation of the Mellin representation of $\xi(s)$ to the entire complex plane, with simple poles only at $s = 0$ and $s = 1$.

Of fundamental importance in asymptotic analysis is Parseval's identity, which connects the integral of two products to a complex contour integral involving their Mellin transforms.

Theorem A.3.1 (Parseval's Formula for Mellin Transforms [63])**.** *Let $F(s)$ and $G(s)$ denote the Mellin transforms of $f(t)$ and $g(t)$, respectively. If either of the following conditions holds:*

(a) $t^{k-1} f(t) \in L(0, \infty)$ and $G(1 - k - it) \in L(-\infty, \infty)$, or

(b) $F(k + it) \in L(-\infty, \infty)$ and $t^{-k} g(t) \in L(0, \infty)$,

then

$$\frac{1}{2\pi i} \int_{k-i\infty}^{k+i\infty} F(s) G(1 - s) \, \mathrm{d}s = \int_0^\infty f(t) g(t) \, \mathrm{d}t. \tag{A.3.28}$$

Proof. Substituting the definition of the Mellin transform (Eq. (A.3.1)) into the left-hand side gives

$$\begin{aligned} \frac{1}{2\pi i} \int_{k-i\infty}^{k+i\infty} F(s) G(1 - s) \, \mathrm{d}s &= \frac{1}{2\pi i} \int_{k-i\infty}^{k+i\infty} F(s) \left[\int_0^\infty g(t) t^{-s} \, \mathrm{d}t \right] \mathrm{d}s \\ &= \int_0^\infty g(t) \left[\frac{1}{2\pi i} \int_{k-i\infty}^{k+i\infty} F(s) t^{-s} \, \mathrm{d}s \right] \mathrm{d}t. \end{aligned} \tag{A.3.29}$$

The interchange of the order of integration is justified by the Cauchy-Schwarz inequality together with the integrability conditions stated in the theorem and Fubini's theorem. Applying the inverse Mellin transform (Eq. (A.3.4)) to the inner integral yields

$$\int_0^\infty f(t) g(t) \, \mathrm{d}t, \tag{A.3.30}$$

which completes the proof. □

Remark A.3.1. The above statement presents one particular set of sufficient conditions for the applicability of Parseval's formula. Alternative sets of conditions also exist in the literature, [30, 63, 65], but are not included here.

By virtue of Parseval's identity (Theorem A.3.1), kernel transforms can be rewritten as complex contour integrals, which may then be displaced over their residues to yield asymptotic series.

Furthermore, by elementary arithmetical manipulations applied to the Mellin transform definition in Eq. (A.3.1), a number of useful translational and scaling properties can be derived [60, 63]. These are collected below:

$$\mathcal{M}[f(at);s] = a^{-s}\,\mathcal{M}[f;s], \qquad (a>0), \tag{A.3.31}$$

$$\mathcal{M}[t^{\nu}f;s] = \mathcal{M}[f;s+\nu], \tag{A.3.32}$$

$$\mathcal{M}[f(t^{-\nu});s] = \frac{1}{\nu}\,\mathcal{M}\left[f;-\tfrac{s}{\nu}\right], \qquad (\nu>0), \tag{A.3.33}$$

$$\mathcal{M}[f(t^{\nu});s] = \frac{1}{\nu}\,\mathcal{M}\left[f;\tfrac{s}{\nu}\right], \qquad (\nu>0), \tag{A.3.34}$$

$$\mathcal{M}[(\log t)^n f;s] = \mathcal{M}^{(n)}[f;s], \qquad (n\in\mathbb{N}), \tag{A.3.35}$$

$$\mathcal{M}\left[\left(t\frac{\mathrm{d}}{\mathrm{d}t}\right)^n f;s\right] = (-s)^n\,\mathcal{M}[f;s], \qquad (n\in\mathbb{N}), \tag{A.3.36}$$

$$\mathcal{M}\left[\left(\frac{\mathrm{d}}{\mathrm{d}t}\right)^n f;s\right] = (-1)^n\,\frac{\Gamma(s)}{\Gamma(s-n)}\,\mathcal{M}[f;s-n], \qquad (n\in\mathbb{N}), \tag{A.3.37}$$

An exhaustive account on transform properties and tables on Mellin transforms is given in Oberhettinger [60].

Example A.3.4 (Modified Bessel Functions [30])**.** Mellin transforms are frequently used to solve differential equations by converting differential operators into algebraic recursions. As an illustrative case, consider the modified Bessel differential equation

$$z^2\frac{\mathrm{d}^2w}{\mathrm{d}z^2} + z\frac{\mathrm{d}w}{\mathrm{d}z} - (z^2+\nu^2)w = 0 \quad (\nu\in\mathbb{C})\,. \tag{A.3.38}$$

By property (A.3.36) and (A.3.32), its Mellin transform satisfies the recurrence relation

$$(4s^2-\nu^2)\mathcal{M}[w;s] = \mathcal{M}[w;s+1]. \tag{A.3.39}$$

A general solution to this recurrence takes the form

$$\mathcal{M}[w;s] = C2^{2s}\Gamma\left(s-\tfrac{\nu}{2}\right)\Gamma\left(s+\tfrac{\nu}{2}\right)p(s), \tag{A.3.40}$$

where $p(s)$ is an arbitrary periodic function of unit period and C is a normalisation constant. Performing Mellin inversion then gives

$$w(z) = \frac{C}{2\pi i}\int_{\sigma-i\infty}^{\sigma+i\infty} \Gamma\left(s+\tfrac{\nu}{2}\right)\Gamma\left(s-\tfrac{\nu}{2}\right) p(s)\left(\tfrac{1}{2}z\right)^{-2s}\,\mathrm{d}s, \tag{A.3.41}$$

where $2\sigma > |\Re\nu|$ ensures that the integration contour lies to the left of all poles.

Example A.3.5 (Mellin Transform of the Cosine and Sine Functions)**.** The Mellin transforms of $\cos(kt)$ and $\sin(kt)$ are significant in the analytic continuation of the zeta function (see e.g. [63]) and will become important in later sections. For $k > 0$ one has, by analytic continuation of the gamma integral,

$$\int_0^\infty t^{s-1}e^{-ikt}\,\mathrm{d}t = e^{-i\frac{\pi s}{2}}\,\Gamma(s)\,k^{-s} \qquad (0 < \Re(s) < 1). \tag{A.3.42}$$

Taking real and imaginary parts in (A.3.42) yields the Mellin transforms of cosine and sine:

$$\mathcal{M}[\cos(kt); s] = \Gamma(s)\,k^{-s}\cos\left(\tfrac{\pi s}{2}\right) \qquad (0 < \Re(s) < 1) \tag{A.3.43}$$

$$\mathcal{M}[\sin(kt); s] = \Gamma(s)\,k^{-s}\sin\left(\tfrac{\pi s}{2}\right) \qquad (0 < \Re(s) < 1). \tag{A.3.44}$$

The identities (A.3.43) and (A.3.44) are initially valid in the strip $0 < \Re(s) < 1$; outside this strip the right-hand sides define analytic continuations as meromorphic functions of the Mellin transforms, whose pole structure is predicted by the discussion below Eq. (A.3.4). The inverse representation reads

$$\cos(kt) = \frac{1}{2\pi i}\int_{\sigma-i\infty}^{\sigma+i\infty} \Gamma(s)\cos\left(\tfrac{\pi s}{2}\right) k^{-s}\,t^{-s}\,\mathrm{d}s \qquad (0 < \sigma < 1)\,. \tag{A.3.45}$$

An analogous representation holds for $\sin(kt)$ using $\sin(\frac{\pi s}{2})$.

Corollary A.3.1 (Convolution Variants of Parseval's Formula [60])**.** *Applying the properties of Eq.* (A.3.31) *together with Eq.* (A.3.33) *to Parseval's identity in Eq.* (A.3.28) *yields*

$$\frac{1}{2\pi i}\int_{\sigma-i\infty}^{\sigma+i\infty} \mathcal{M}[f;s]\mathcal{M}[g;s]u^{-s}\,\mathrm{d}s = \int_0^\infty f\left(\frac{u}{t}\right) g(t)\frac{\mathrm{d}t}{t}. \tag{A.3.46}$$

Next, shifting the argument by means of Eq. (A.3.32)

$$\frac{1}{2\pi i}\int_{\sigma-i\infty}^{\sigma+i\infty} \mathcal{M}[f;s]\mathcal{M}[g;s-2]u^{-s}\,\mathrm{d}s = \int_0^\infty f\left(\frac{u}{t}\right) g(t)\frac{\mathrm{d}t}{t^3}. \tag{A.3.47}$$

Finally, by scaling the argument of $\mathcal{M}[f;s]$ *with* $s \to 2s$ *and subsequent* $s \to 1-s$ *by*

Eq. (A.3.32) *and Eq.* (A.3.33)

$$\frac{1}{2\pi i}\int_{\sigma-i\infty}^{\sigma+i\infty}\mathcal{M}[f;1-2s]\mathcal{M}[g;s-2]u^{-s}\,\mathrm{d}s=\frac{1}{2\sqrt{u}}\int_0^\infty f\left(\sqrt{\frac{t}{u}}\right)g(t)\frac{\mathrm{d}t}{t^{\frac{5}{2}}}. \tag{A.3.48}$$

A.3.1 Poisson Summation

The *Poisson summation formula* provides a connection between sums in position space and their counterparts in frequency space. In this thesis, we employ it as a tool to analytically continue certain expressions obtained in our analysis.

Rather than deriving the identity directly from Fourier theory by restricting first to the class of *Schwartz functions* and then extending the result by successive relaxation of the conditions, we instead make use of Mellin transforms to establish the formula. For classical proofs based on Fourier analysis, the reader is referred to references such as [42, 71].

Theorem A.3.2 (Poisson Summation Formula [72, 73])**.** *Let $\phi(s)$ be a function of $s=\sigma+it$ satisfying the following conditions:*

(a) $\phi(s)$ is analytic, except possibly for poles, in the strip $-b\le\sigma\le 1+c$ with $b,c>0$;

(b) the only pole in this strip is a simple pole at $s=0$, where the residue is ϕ_0;

(c) there exist constants M, t_0, and $\eta>\max(b,c)$ such that

$$|\phi(\sigma+it)|<M|t|^{\frac{1}{2}\sigma-\frac{3}{2}-\frac{1}{2}\eta} \tag{A.3.49}$$

whenever $|t|>t_0$ and $-b\le\sigma\le 1+c$.

Let $f(x)$ denote the inverse Mellin transform of $\phi(s)$. Then

$$\frac{1}{2}f(0^+)+\sum_{n=1}^{\infty}f(n)=\int_0^\infty f(x)\,\mathrm{d}x+2\sum_{n=1}^{\infty}\int_0^\infty f(x)\cos(2\pi nx)\,\mathrm{d}x. \tag{A.3.50}$$

Proof. By definition of the inverse Mellin transform,

$$f(x)=\frac{1}{2\pi i}\int_{\sigma-i\infty}^{\sigma+i\infty}\phi(s)x^{-s}\,\mathrm{d}s\qquad(0<\sigma\le 1+c). \tag{A.3.51}$$

Standard contour shifts yield the asymptotics

$$f(x)\sim\begin{cases}O(x^{1-c}), & x\to\infty,\\ \phi_0+O(x^b), & x\to 0,\end{cases} \tag{A.3.52}$$

showing that $\sum_{n=1}^{\infty} f(n)$ converges absolutely. Thus,

$$\sum_{n=1}^{\infty} f(n) = \sum_{n=1}^{\infty} \frac{1}{2\pi i} \int_{1+c-i\infty}^{1+c+i\infty} \phi(s) n^{-s} \, \mathrm{d}s \tag{A.3.53}$$

$$= \frac{1}{2\pi i} \int_{1+c-i\infty}^{1+c+i\infty} \phi(s)\zeta(s) \, \mathrm{d}s. \tag{A.3.54}$$

By condition (iii), the contour may be shifted to $\Re(s) = -b$. In doing so, we cross two simple poles: the first at $s = 0$, from $\phi(s)$, contributing $-\frac{1}{2}\phi_0$, and the second at $s = 1$, from $\zeta(s)$, contributing $\phi(1)$.

Applying the functional equation of $\zeta(s)$, we obtain

$$\sum_{n=1}^{\infty} f(n) = -\tfrac{1}{2}\phi_0 + \phi(1) + \frac{1}{2\pi i} \int_{-b-i\infty}^{-b+i\infty} \frac{\pi^{s-\frac{1}{2}}\Gamma(\frac{1}{2} - \frac{s}{2})}{\Gamma(\frac{s}{2})} \phi(s)\zeta(1-s) \, \mathrm{d}s. \tag{A.3.55}$$

Expanding $\zeta(1 - s)$ into its Dirichlet series and interchanging summation with integration (justified by absolute convergence, using condition (iii)), we find

$$\sum_{n=1}^{\infty} f(n) = -\tfrac{1}{2}\phi_0 + \phi(1) + \frac{1}{2\pi i} \sum_{n=1}^{\infty} \int_{-b-i\infty}^{-b+i\infty} \frac{\pi^{s-\frac{1}{2}}\Gamma(\frac{1}{2} - \frac{s}{2})}{\Gamma(\frac{s}{2})} \phi(s) n^{s-1} \, \mathrm{d}s. \tag{A.3.56}$$

Substituting the Mellin representation (A.3.51) for $\phi(s)$ and interchanging the order of integration gives

$$\int_0^{\infty} f(x) \left[\frac{1}{2\pi i} \int_{-b-i\infty}^{-b+i\infty} \frac{\pi^{s-\frac{1}{2}}\Gamma(\frac{1}{2} - \frac{s}{2})}{\Gamma(\frac{s}{2})} (nx)^{s-1} \, \mathrm{d}s \right] \mathrm{d}x. \tag{A.3.57}$$

The inner integral is recognised (via the Mellin transform of the cosine, see Example A.3.5 together with Euler's reflection formula (2.1.10)) as $2\cos(2\pi nx)$. Hence,

$$\sum_{n=1}^{\infty} f(n) = -\tfrac{1}{2}\phi_0 + \phi(1) + 2\sum_{n=1}^{\infty} \int_0^{\infty} f(x) \cos(2\pi nx) \, \mathrm{d}x. \tag{A.3.58}$$

Finally, we note that $\phi(1) = \int_0^{\infty} f(x) \, \mathrm{d}x$ and $-\frac{1}{2}\phi_0 = -\frac{1}{2} f(0^+)$, yielding the identity (A.3.50). □

Example A.3.6 (Functional Equation of the Jacobi Theta Function [41])**.** Riemann employed the functional equation of the Jacobi theta function to analytically continue the zeta function beyond the half-plane $\Re(s) > 1$. Thus, the theta function is fundamental to the theory of the zeta function and its relatives (see also Example A.3.3). The Poisson summation formula in

Eq. (A.3.50) is especially suited for the function $\psi(u)$ defined in Eq. (A.3.19). Identifying $f(x) = \exp(-\pi u x^2)$, one verifies from Eq. (2.1.2) and Eq. (A.3.33) that the Mellin transform $\phi(s)$ of $f(x)$ satisfies the conditions imposed in Theorem A.3.2. Accordingly, Eq. (A.3.50) yields

$$\tfrac{1}{2} + \psi(u) = \int_0^\infty e^{-\pi u x^2}\,\mathrm{d}x + \sum_{n=1}^{\infty} \int_{-\infty}^{\infty} e^{-\pi u x^2 + 2\pi i n x}\,\mathrm{d}x. \tag{A.3.59}$$

The first integral evaluates to the standard Gaussian integral

$$\int_0^\infty e^{-\pi u x^2}\,\mathrm{d}x = \tfrac{1}{2}\sqrt{\tfrac{1}{u}}. \tag{A.3.60}$$

For the second term, completing the square and substituting $y = x - i\frac{n}{u}$ gives

$$\begin{aligned}
\int_{-\infty}^{\infty} e^{-\pi u x^2 + 2\pi i n x}\,\mathrm{d}x &= e^{-\pi n^2/u} \int_{in/u-\infty}^{in/u+\infty} e^{-\pi u y^2}\,\mathrm{d}y && \text{(A.3.61)}\\
&= e^{-\pi n^2/u} \int_{-\infty}^{\infty} e^{-\pi u y^2}\,\mathrm{d}y && \text{(A.3.62)}\\
&= \frac{1}{\sqrt{u}}\, e^{-\pi n^2/u}, && \text{(A.3.63)}
\end{aligned}$$

where in the penultimate step the contour has been shifted back to the real axis, justified by the vanishing contributions at infinity, and in the last step the Gaussian integral was evaluated. Consequently, we obtain the functional equation

$$\tfrac{1}{2} + \psi(u) = \frac{1}{\sqrt{u}}\Big(\tfrac{1}{2} + \psi(1/u)\Big). \tag{A.3.64}$$

As a final remark, the function $G(u)$ introduced in Eq. (A.3.21), which can be expressed as

$$G(u) = 1 + 2\psi(u^2) = \sum_{n=-\infty}^{\infty} e^{-\pi n^2 u^2} \qquad \Big(\Re(u^2) > 0\Big), \tag{A.3.65}$$

is precisely Jacobi's theta function and satisfies the modular relation

$$G(u) = \frac{1}{u}\, G\Big(\tfrac{1}{u}\Big). \tag{A.3.66}$$

Example A.3.7 (Inhomogeneous Epstein-Hurwitz Zeta Function)**.** Consider the Dirichlet-type series

$$S_a(z) = \sum_{n=1}^{\infty} \frac{1}{(n^2 + z^2)^a} \qquad \Big(\Re(a) > \tfrac{1}{2},\ z^2 \notin \mathbb{Z}_{\leq}\Big). \tag{A.3.67}$$

We obtain an analytic continuation of $S_a(z)$ by applying Poisson summation to the function $f(x; z, a) = (x^2 + z^2)^{-a}$.

The Mellin transform of f is given by

$$\phi(s) = \mathcal{M}\left[(x^2 + z^2)^{-a}; s\right] \tag{A.3.68}$$

$$= \frac{1}{2} z^{s-2a} B\left(\tfrac{s}{2}, a - \tfrac{s}{2}\right). \tag{A.3.69}$$

Initially this identity holds under the sector of absolute convergence $\Re(a) > \frac{\Re(s)}{2} > 0$. However, by analytic continuation, the right-hand side provides the correct extension to all $s \in \mathbb{C}$, except at the poles of the beta function. Hence, ϕ is admissible for the Poisson summation Theorem A.3.2.

The first integral term in Eq. (A.3.50) is

$$\int_0^\infty \frac{dx}{(x^2 + z^2)^a} = \frac{\sqrt{\pi}}{2} \frac{\Gamma\left(a - \frac{1}{2}\right)}{\Gamma(a)} z^{1-2a}, \qquad \left(\Re(a) > \tfrac{1}{2}, \Re(z^2) > 0\right). \tag{A.3.70}$$

The second integral is identified with Basset's integral, which yields the modified Bessel function of the second kind $K_\nu(x)$ (cf. Sect. 2.3 and [23]):

$$\int_{-\infty}^\infty \frac{\cos(2\pi n x)}{(x^2 + z^2)^a} dx = \frac{2\pi^a}{\Gamma(a)} z^{\frac{1}{2}-a} n^{a-\frac{1}{2}} K_{\frac{1}{2}-a}(2\pi n z) \qquad \left(\Re(a) > 0, |\arg(z)| < \tfrac{\pi}{2}\right). \tag{A.3.71}$$

Substituting into Poisson summation gives

$$\tfrac{1}{2} z^{-2a} + \sum_{n=1}^\infty \frac{1}{(n^2 + z^2)^a} = \frac{\sqrt{\pi}}{2} \frac{\Gamma\left(a - \frac{1}{2}\right)}{\Gamma(a)} z^{1-2a} + \frac{2\pi^a}{\Gamma(a)} z^{\frac{1}{2}-a} \sum_{n=1}^\infty n^{a-\frac{1}{2}} K_{\frac{1}{2}-a}(2\pi n z). \tag{A.3.72}$$

This identity provides an analytic continuation of $S_a(z)$ in the parameter a to the whole complex plane in terms of an exponentially decreasing power series, provided $z^2 \geq 0$, with the exception of the poles at $a = \frac{1}{2} - k$, $k \in \mathbb{N}_0$.

A.4 Asymptotic Expansion Techniques

A.4.1 Watson's Lemma

A fundamental tool in the theory of asymptotic expansions is Watson's lemma. It applies to functions that can be represented as a Laplace transform of the form

$$F(z) = \int_0^\infty f(t)\, e^{-zt}\, \mathrm{d}t, \tag{A.4.1}$$

where $z \to \infty$ in an appropriate sector of the complex plane. The central idea underlying Watson's lemma is that the main contribution to the integral emanates from the neighbourhood of $t \to 0$, as the exponential kernel suppresses the vicinity. Therefore, by expanding the integrand $f(t)$ into a power series around $t = 0$ and interchanging the order of summation and integration, an asymptotic expansion with gamma function coefficients is expected. Although conceptually simple, most other theorems are founded on this powerful principle.

Lemma A.4.1 (Watson's Lemma [74])**.** *Let*

$$F(z) = \int_0^\infty f(t) e^{-zt}\, \mathrm{d}t. \tag{A.4.2}$$

Suppose the following conditions hold:

(i) $f(t)$ *is analytic for* $|t| \leq a + \delta$*, where* $a > 0$ *and* $\delta > 0$*, except possibly at a branch point at the origin, and for* $|t| \leq a$*, it admits the expansion*

$$f(t) = \sum_{m=1}^{\infty} a_m t^{\frac{m}{r}-1} \qquad (r > 0). \tag{A.4.3}$$

(ii) For $t \geq a$*,* $|f(t)| \leq K e^{bt}$*, where* K *and* b *are constants independent of* t*.*

(iii) The argument of z *satisfies*

$$|\arg(z)| \leq \frac{\pi}{2} - \Delta \qquad (\Delta > 0). \tag{A.4.4}$$

(iv) The magnitude of z *is sufficiently large.*

Then $F(z)$ *has the following complete asymptotic expansion:*

$$F(z) \sim \sum_{m=1}^{\infty} a_m \Gamma\left(\frac{m}{r}\right) z^{-\frac{m}{r}}. \tag{A.4.5}$$

Proof. If M is any fixed integer, we have

$$|f(t) - \sum_{m=1}^{M-1} a_m t^{\frac{m}{r}-1}| < K_1 t^{\frac{M}{r}-1} e^{bt} \tag{A.4.6}$$

throughout the range of integration, where K_1 is some number independent of t. Hence

$$\int_0^\infty f(t)e^{-zt}\,\mathrm{d}t = \sum_{m=1}^{M-1} a_m \int_0^\infty t^{\frac{m}{r}-1} e^{-zt}\,\mathrm{d}t + R_M, \tag{A.4.7}$$

where

$$R_M < K_1 \int_0^\infty t^{\frac{M}{r}-1} e^{bt} |e^{-zt}|\,\mathrm{d}t < K_1 \Gamma\left(\frac{M}{r}\right) (\Re(z) - b)^{-\frac{M}{r}}, \tag{A.4.8}$$

provided that $\Re(z) > b$, which is the case when $|z|$ is sufficiently large. Since $(\Re(z) - b)^{-1} = O\left(\frac{1}{z}\right)$ for the range of values of z under consideration, we have

$$F(z) = \sum_{m=1}^{M-1} a_m \Gamma\left(\frac{m}{r}\right) z^{-\frac{m}{r}} + O\left(z^{-\frac{M}{r}}\right), \tag{A.4.9}$$

and so the integral possesses the complete asymptotic expansion, which is of Poincaré-type. □

In summary, the asymptotic expansion of $f(t)$ as $t \to 0$ dictates the asymptotic behaviour of its Laplace transform as $z \to \infty$. Watson's lemma, however, only yields the order of the error term rather than a precise error bound. Clearly, the conditions raised on the expansion on $f(t)$ as $t \to 0$ do only account for algebraic singularities at the origin. Examining the proof and contemplating the Mellin transform property (A.3.35), asymptotic power series expansions involving logarithmic terms can be included, which are discussed in [57, 65]. For generalisations of Watson's lemma along rays in the complex contour integral, we refer to [62].

Example A.4.1 (Quotient of Gamma Functions [75])**.** The integral representation of the quotient of two gamma functions follows from the definition of the beta function in Eq. (2.1.24)

$$\frac{\Gamma(z+a)}{\Gamma(z+b)} = \frac{1}{\Gamma(b-a)} \int_0^\infty (1-e^{-t})^{b-a-1} e^{-(z-a)t}\mathrm{d}t \qquad (\Re(z-a) > 0, \Re(b-a) > 0)\,. \tag{A.4.10}$$

Setting $f(t) = (1-e^{-t})^{b-a-1} e^{at}$, the conditions of Watson's Lemma A.4.1 are clearly satisfied.

Introducing the generalised Bernoulli polynomials [23] via

$$\left(\frac{t}{e^t-1}\right)^{\ell} e^{xt} = \sum_{n=0}^{\infty} B_n^{(\ell)}(x)\,\frac{t^n}{n!} \qquad (|t|<2\pi)\,, \tag{A.4.11}$$

allows for the expansion

$$f(t) = \sum_{n=0}^{\infty} (-1)^n B_n^{(a+1-b)}(a)\frac{t^{n+b-a-1}}{n!} \qquad (|t|<2\pi)\,. \tag{A.4.12}$$

Accordingly, by Watson's Lemma

$$\frac{\Gamma(z+a)}{\Gamma(z+b)} \sim z^{a-b}\sum_{n=0}^{\infty}\frac{G_n(a,b)}{z^n}, \tag{A.4.13}$$

as $|z|\to\infty$ in $|\arg z|<\pi$ with coefficients

$$G_n(a,b) = \binom{a-b}{n} B_n^{(a-b+1)}(a). \tag{A.4.14}$$

The condition $\Re(b-a)>0$ originates from the singularity of $f(t)$ at $t=0$.

Comparison with Example A.3.2 suggests to consider

$$I(s) = \int_{\mathcal{H}} f(t)e^{-zt}\mathrm{d}t \qquad (\Re(z-a)>0)\,, \tag{A.4.15}$$

where the Hankel contour $\mathcal{H}$ starts at $+\infty$, encircling the origin counterclockwise, and returning to $+\infty$ (see Fig. A.1).

Because $(1-e^{-t})^{b-a-1}$ is non-singular for $\Re(b-a)>0$, the circle $|t|=\epsilon$ can be shrunk to zero, giving

$$I(s) = \left(e^{2\pi i(b-a)}-1\right)\Gamma(b-a)\frac{\Gamma(z+a)}{\Gamma(z+b)}. \tag{A.4.16}$$

However, Eq. (A.4.15), defining $I(s)$, is uniformly convergent in any finite region of the s-plane. This implies the validity of Eq. (A.4.13) without restriction on $\Re(b-a)$.

A.4.2 Laplace's Method

Laplace's method [76] is a classical technique for deriving asymptotic expansions of integrals of the form

$$I(z) = \int_a^b q(t)e^{-zp(t)}\,\mathrm{d}t \qquad (z \to \infty), \tag{A.4.17}$$

where $z > 0$ is a parameter, while the limits a, b and the functions p, q are independent of z. The essential idea is that, for large z, the dominant contribution comes from a global minimum of $p(t)$ inside the integration range. Without loss of generality, suppose that $p(t)$ has a unique minimum at $t = a$, otherwise split the interval of integration into finite segments with minima at the boundary. By monotonicity of $p(t)$ in the neighbourhood of its minimum, the substitution $y = p(t) - p(a)$ is one-to-one. This reduces the analysis to the setting of Watson's lemma.

In detail, as $t \to a^+$, assume that $p(t)$ and $q(t)$ admit the following asymptotic expansions:

$$p(t) \sim p(a) + \sum_{n=0}^{\infty} a_n (t-a)^{n+\mu}, \tag{A.4.18}$$

$$q(t) \sim \sum_{n=0}^{\infty} b_n (t-a)^{n+\alpha-1}, \tag{A.4.19}$$

$$p'(t) \sim \sum_{n=0}^{\infty} a_n (n+\mu)(t-a)^{n+\mu-1}, \tag{A.4.20}$$

with $\mu > 0$ and $\Re(\alpha) > 0$.

Theorem A.4.1 (Extended Laplace Formula [57])**.** *Let*

$$I(z) = \int_a^b q(t)e^{-zp(t)}\,\mathrm{d}t. \tag{A.4.21}$$

Suppose that $p(t) > p(a)$ for all $t \in (a, b)$, with $\inf_{t\in(a,b)}(p(t) - p(a)) > 0$. Further assume that $p'(t)$ and $q(t)$ are continuous in (a, c) for some $c \in (a, b)$, that the expansions (A.4.18) *to* (A.4.20) *hold, and that $I(z)$ converges absolutely for all sufficiently large z. Then*

$$I(z) \sim e^{-zp(a)} \sum_{n=0}^{\infty} \Gamma\left(\tfrac{n+\alpha}{\mu}\right) \frac{c_n}{z^{(n+\alpha)/\mu}} \qquad (z \to \infty), \tag{A.4.22}$$

where the coefficients c_n are expressible in terms of $\{a_n\}$ and $\{b_n\}$. The first three coefficients

are explicitly given by

$$c_0 = \frac{b_0}{\mu a_0^{\frac{\alpha}{\mu}}}, \tag{A.4.23}$$

$$c_1 = \left\{ \frac{b_1}{\mu} - \frac{(\alpha+1)a_1 b_0}{\mu^2 a_0} \right\} \frac{1}{a_0^{\frac{\alpha+1}{\mu}}}, \tag{A.4.24}$$

$$c_2 = \left[\frac{b_2}{\mu} - \frac{(\alpha+2)a_1 b_1}{\mu^2 a_0} + \left\{ (\alpha+\mu+2)a_1^2 - 2\mu a_0 a_2 \right\} \frac{(\alpha+2)b_0}{2\mu^3 a_0^2} \right] \frac{1}{a_0^{\frac{(\alpha+2)}{\mu}}}. \tag{A.4.25}$$

Proof. By continuity of $p'(t)$ and $q(t)$ near a, there exists $c \in (a, b)$ such that both are continuous on (a, c), with $p'(t) > 0$ there. Set $Y = p(c) - p(a)$ and introduce the new variable

$$y = p(t) - p(a). \tag{A.4.26}$$

Since $p(t)$ is increasing on (a, c), we can write

$$e^{zp(a)} \int_a^c q(t) e^{-zp(t)} \, \mathrm{d}t = \int_0^Y f(y) e^{-zy} \, \mathrm{d}y, \tag{A.4.27}$$

where

$$f(y) = \frac{q(t)}{p'(t)} \qquad \text{with } t = p^{-1}(y + p(a)). \tag{A.4.28}$$

Substituting the expansion (A.4.18) into (A.4.26) and reverting the resulting series yields

$$t - a \sim \sum_{n=1}^{\infty} \alpha_n y^{n/\mu} \qquad (y \to 0^+). \tag{A.4.29}$$

The existence of the coefficients α_n is verified by Brümann's theorem [24]. Inserting (A.4.29) into (A.4.28) gives

$$f(y) \sim \sum_{n=0}^{\infty} c_n y^{(n+\alpha-\mu)/\mu} \qquad (y \to 0^+). \tag{A.4.30}$$

Applying Watson's lemma (Lemma A.4.1) to (A.4.27) then yields

$$\int_a^c q(t) e^{-zp(t)} \, \mathrm{d}t \sim e^{-zp(a)} \sum_{n=0}^{\infty} \Gamma\left(\tfrac{n+\alpha}{\mu}\right) \frac{c_n}{z^{(n+\alpha)/\mu}} \qquad (z \to \infty). \tag{A.4.31}$$

It remains to estimate the remainder $\int_c^b q(t) e^{-zp(t)} \, \mathrm{d}t$. Let z_0 be such that $I(z)$ is absolutely

convergent for $z \geq z_0$, and define

$$\epsilon = \inf_{t\in(c,b)} \big(p(t) - p(a)\big) > 0. \tag{A.4.32}$$

Then, for $z \geq z_0$,

$$|e^{zp(a)} \int_c^b q(t) e^{-zp(t)}\, \mathrm{d}t| \leq M e^{-\epsilon z}, \tag{A.4.33}$$

with

$$M = e^{z_0(\epsilon+p(a))} \int_c^b |q(t)| e^{-z_0 p(t)}\, \mathrm{d}t < \infty. \tag{A.4.34}$$

Combining (A.4.31) and (A.4.33) proves (A.4.22). □

Remark A.4.1. The condition (A.4.20) assumes that $p(t)$ can be differentiated termwise in its asymptotic expansion. This restriction excludes some classes of functions $p(t)$, as noted below the Example A.2.1.

Example A.4.2 (Asymptotic Expansion of $\overline{D}_d(a)$)**.** The function $\overline{D}_d(a)$, closely related to the pressure-like quantity $\overline{P}_d(a)$ through

$$\overline{D}_d(a) = 2\partial_{a^2} \overline{P}_d(a), \tag{A.4.35}$$

will prove invaluable in the following chapter. We restrict to spatial dimensions $d \in \mathbb{N}_{>2}$, $a \in \mathbb{R}$ and begin with the integral representation

$$\overline{D}_d(a) = \int_0^\infty \frac{x^{d-1}}{\sqrt{x^2+a^2}} \frac{\mathrm{d}x}{\exp\big(\sqrt{x^2+a^2}\big) - 1}. \tag{A.4.36}$$

Expanding the Bose-Einstein denominator into its geometric series and interchanging summation and integration-justified by comparison with the convergent case $a = 0$-gives

$$\begin{aligned} \overline{D}_d(a) &= \frac{1}{a} \sum_{n=1}^\infty \int_0^\infty \mathrm{d}x\, \frac{x^{d-1}}{\sqrt{1+(x/a)^2}}\, e^{-na\sqrt{1+(x/a)^2}} \\ &= 2^{\frac{d-2}{2}} a^{d-1} \sum_{n=1}^\infty e^{-na} \int_0^\infty \mathrm{d}x\, x^{\frac{d-2}{2}} \Big(1+\frac{x}{2}\Big)^{\frac{d-2}{2}} e^{-nax}. \end{aligned} \tag{A.4.37}$$

Applying the generalised binomial expansion (cf. Example A.2.2) and identifying the polylog-

arithm

$$\mathrm{Li}_s(x) = \sum_{n=1}^{\infty} \frac{x^n}{n^s}, \tag{A.4.38}$$

we obtain the asymptotic expansion

$$\overline{D}_d(a) \sim (2a)^{\frac{d-2}{2}} \sum_{r=0}^{\infty} \binom{\frac{d-2}{2}}{r} \frac{\Gamma\left(\frac{d}{2}+r\right)}{(2a)^r} \mathrm{Li}_{\frac{d}{2}+r}(e^{-a}) \qquad (a \to \infty). \tag{A.4.39}$$

Introducing the convenient parameter $\kappa = \frac{d+1}{2}$, this becomes

$$\overline{D}_d(a) \sim (2a)^{\kappa-\frac{3}{2}} \sum_{r=0}^{\infty} \binom{\kappa-\frac{3}{2}}{r} \frac{\Gamma\left(\kappa-\frac{1}{2}+r\right)}{(2a)^r} \mathrm{Li}_{\kappa-\frac{1}{2}+r}(e^{-a}) \qquad (a \to \infty). \tag{A.4.40}$$

For $\mathrm{Re}(s) > 1$, the polylogarithm satisfies $\mathrm{Li}_s(e^{-a}) \sim e^{-a}$ as $a \to \infty$, implying that the sequence $\{\mathrm{Li}_{\kappa-\frac{1}{2}+r}(e^{-a})/a^r\}_r$ forms a valid asymptotic hierarchy. For half-integer κ, the binomial coefficient terminates the series at finite order. Otherwise, the tail diverges superexponentially (cf. Example A.4.1).

It is convenient to define the individual terms and truncated series as

$$d_r(a) = (2a)^{\kappa-\frac{3}{2}} \binom{\kappa-\frac{3}{2}}{r} \frac{\Gamma\left(\kappa-\frac{1}{2}+r\right)}{(2a)^r} \mathrm{Li}_{\kappa-\frac{1}{2}+r}(e^{-a}), \tag{A.4.41}$$

$$S_N(a) = \sum_{r=0}^{N-1} d_r(a), \tag{A.4.42}$$

such that $\overline{D}_d(a) \sim S_N(a)$ for large a. The relative accuracy of the truncated expansion can then be quantified by

$$\Delta D = \left| S_N(a) - \overline{D}_d(a) \right| \tag{A.4.43}$$

where $\overline{D}_d(a)$ denotes the numerical evaluation of Eq. (A.4.36).

The optimal truncation index r_{opt} is estimated by imposing $|d_{r+1}(a)/d_r(a)| = 1$, yielding

$$r_{\mathrm{opt}} \sim 2a, \tag{A.4.44}$$

which is largely independent of κ. This behaviour is illustrated in Fig. A.2, while Fig. A.3 compares the truncated sums $S_N(a)$ to the numerical integral for representative a values. Both reveal the asymptotic (rather than convergent) nature of the expansion: adding more terms

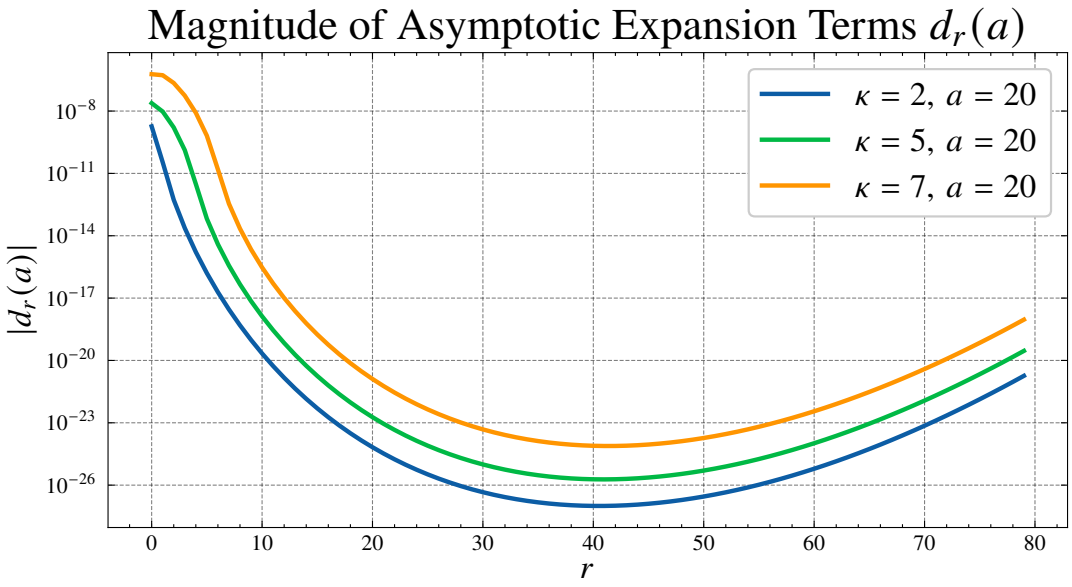

Figure A.2: Magnitude of the summands $|d_r(a)|$ in Eq. (A.4.39) for various κ. The minimal term appears near $r_{\text{opt}} \approx 2a$.

beyond r_{opt} does not improve accuracy.

The error at optimal truncation is given by the summand in (A.4.41) evaluated at r_{opt}. From Example A.4.1 and Stirling's formula (2.1.13), one infers the asymptotic behaviour

$$d_{2a}(a) = O(a^{-\frac{1}{2}} e^{-3a}), \tag{A.4.45}$$

showing that it is exponentially small in a.

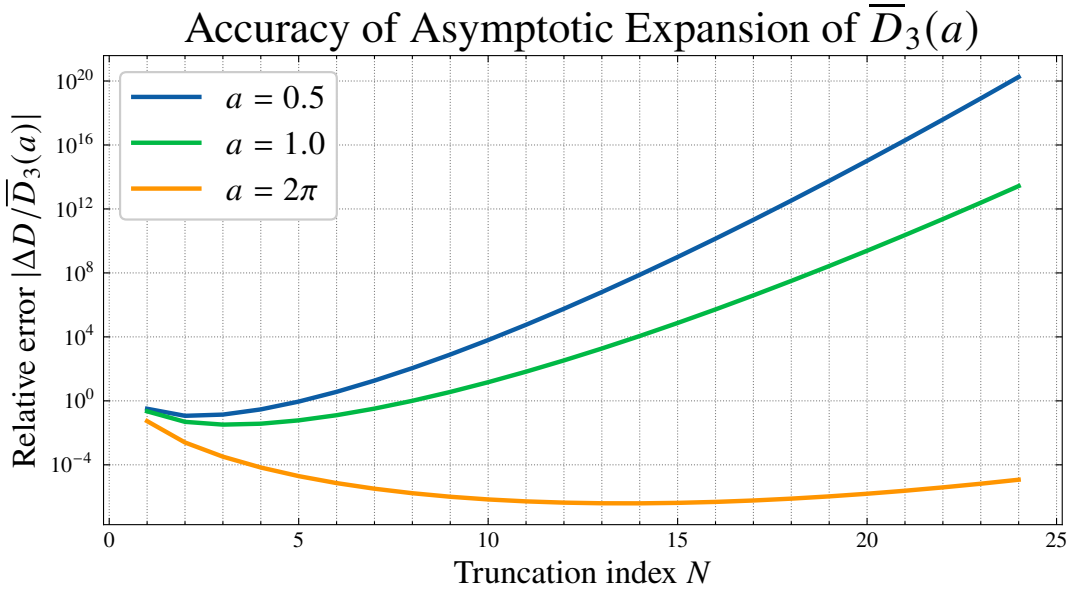

Figure A.3: Relative error of the truncated series $S_N(a)$ compared to the numerical integral (A.4.36). For small a, the asymptotic expansion becomes inaccurate.

As an explicit example, for $\kappa = 2$ ($d = 3$), the leading-order term reads

$$\overline{D}_3(a) \sim \sqrt{\frac{\pi}{2}}\, a^{\frac{1}{2}}\, \mathrm{Li}_{\frac{3}{2}}(e^{-a})\,. \tag{A.4.46}$$

This asymptotic expansion will be crucial in determining the critical temperature of the deconfining SU(2) Yang–Mills theory in Chapter 3.

Example A.4.3 (A Contour Integral Related to Touchard Polynomials)**.** Consider the integral

$$I_k(z) = \frac{\Gamma(n)e^{-z}}{2\pi i} \int_{C_k} e^{\,n\psi(t)}\, \mathrm{d}t, \tag{A.4.47}$$

where the contour C_k follows a path of constant imaginary part of $\psi(t)$ and passes through a saddle point t_k at which $\Re\psi(t)$ attains a local maximum. The derivatives of ψ evaluated at t_k are assumed to satisfy

$$\psi(t_k) = \frac{1}{t_k} - \ln t_k, \tag{A.4.48}$$

$$\psi^{(n)}(t_k) = \frac{1}{t_k} + (-1)^n \frac{\Gamma(n)}{t_k^n} \qquad (n > 0). \tag{A.4.49}$$

Introducing the local variable

$$\tau := -\big[\psi(t_k) - \psi(t)\big], \tag{A.4.50}$$

the integral takes the form applicable to Laplace's extended formula (A.4.22),

$$I_k(z) = \frac{\Gamma(n)e^{-z+n\psi(t_k)}}{2\pi i} \int_0^{\infty} \left(\frac{\mathrm{d}t_1}{\mathrm{d}\tau} - \frac{\mathrm{d}t_2}{\mathrm{d}\tau}\right) e^{\,n\tau}\, \mathrm{d}\tau, \tag{A.4.51}$$

where t_1 denotes the parametrization along C_k starting from the saddle, and t_2 corresponds to the opposite direction. The difference of Jacobians reflects the reversal of orientation.

Expanding τ around t_k gives

$$\tau = -\tfrac{1}{2}\psi^{(2)}(t_k)(t - t_k)^2 \left[\sum_{m=0}^{\infty} \frac{2}{(m+2)!} \frac{\psi^{(m+2)}(t_k)}{\psi^{(2)}(t_k)} (t - t_k)^m\right]. \tag{A.4.52}$$

Taking the square root yields

$$\tau^{1/2} = \pm\sqrt{\tfrac{-\psi^{(2)}(t_k)}{2}}\, (t - t_k) \left[\sum_{m=0}^{\infty} \frac{2}{(m+2)!} \frac{\psi^{(m+2)}(t_k)}{\psi^{(2)}(t_k)} (t - t_k)^m\right]^{1/2}. \tag{A.4.53}$$

The correct branch of $\arg \psi^{(2)}(t_k)$ is chosen such that

$$\left| 2 \arg \psi^{(2)}(t_k) + \omega_0 \right| \leq \tfrac{\pi}{2}, \qquad \omega_0 = \lim_{t \to t_k} \arg(t - t_k),$$

ensuring convergence along the contour.

By Lagrange's inversion theorem one obtains the expansions

$$t_1 - t_k = i \sqrt{\frac{2}{\psi^{(2)}(t_k)}} \sum_{m=0}^{\infty} \frac{c_m}{m+1} \tau^{\frac{m+1}{2}}, \tag{A.4.54}$$

$$t_2 - t_k = i \sqrt{\frac{2}{\psi^{(2)}(t_k)}} \sum_{m=0}^{\infty} (-1)^{m+1} \frac{c_m}{m+1} \tau^{\frac{m+1}{2}}, \tag{A.4.55}$$

valid for sufficiently small τ. The coefficients are given by

$$m!\, c_m = \left(\frac{-2}{\psi^{(2)}(t_k)} \right)^{m/2} \frac{\mathrm{d}^m}{\mathrm{d}t^m} \left[\sum_{m=0}^{\infty} \frac{2}{(m+2)!} \frac{\psi^{(m+2)}(t_k)}{\psi^{(2)}(t_k)} (t - t_k)^m \right]^{-\frac{m+1}{2}} \Bigg|_{t=t_k}. \tag{A.4.56}$$

Note that the first-order factor was extracted to make all coefficients c_{2m} real valued, with the explicit factor of i written separately.

Inserting these series into Eq. (A.4.51) and evaluating the resulting gamma integrals yields the asymptotic expansion

$$I_k(z) \sim \frac{\Gamma(n) e^{-z + n\psi(t_k)}}{\sqrt{2\pi\, \psi^{(2)}(t_k)}} \sum_{m=0}^{\infty} \frac{c_{2m}}{n^{m+\frac{1}{2}}} \frac{\Gamma\left(m + \frac{1}{2}\right)}{\Gamma\left(\frac{1}{2}\right)}. \tag{A.4.57}$$

Finally, using the explicit form of $\psi(t_k)$ this can be written as

$$I_k(z) \sim \frac{\Gamma(n) e^{-z + n t_k}}{\sqrt{2\pi (1 + t_k)}\, t_k^{n-1}} \sum_{m=0}^{\infty} \frac{c_{2m}}{n^{m+\frac{1}{2}}} \frac{\Gamma\left(m + \frac{1}{2}\right)}{\Gamma\left(\frac{1}{2}\right)}. \tag{A.4.58}$$

The first coefficients are (A.4.23)

$$c_0 = 1, \tag{A.4.59}$$

$$c_2 = \frac{3\, \psi^{(2)}(t_k) \psi^{(4)}(t_k) - 5 \left(\psi^{(3)}(t_k) \right)^2}{12 \left(\psi^{(2)}(t_k) \right)^3}. \tag{A.4.60}$$

A.4.3 The Method of Steepest Descent

The method of steepest descent provides a systematic approach to evaluate contour integrals of the form

$$I(\lambda) = \int_C g(z)\, e^{\lambda f(z)}\, \mathrm{d}z, \tag{A.4.61}$$

where $f(z)$ and $g(z)$ are analytic in a domain D containing the contour C, and $\lambda \to \infty$ is a large parameter. The central idea is to identify the *critical points* of the integrand and to deform the contour into one that passes through them in directions where the exponential factor decays most rapidly.

Critical points arise as:

- saddle points of $f(z)$, i.e. solutions to $f'(z_0) = 0$,
- singularities of $f(z)$ or $g(z)$,
- and, if present, endpoints of the contour C.

In practice, saddle points are of primary interest. Writing $z = x + iy$ and $f(z) = u(x, y) + i\, v(x, y)$, the Cauchy-Riemann equations imply that a point z_0 with $f'(z_0) = 0$ corresponds to a stationary point of $u(x, y)$. Because $u(x, y)$ is harmonic, such a point is necessarily a saddle in the (x, y, u)-surface. The curves along which the imaginary part remains constant, $v(x, y) = v(x_0, y_0)$, are the *steepest descent* or *steepest ascent* trajectories through z_0.

Definition A.4.1 (Directions of Descent and Ascent [65])**.** Let $z_0 = x_0 + iy_0 \in D$. A direction away from z_0 in which $u(x, y)$ decreases from $u(x_0, y_0)$ is called a direction of descent; a direction in which u increases is called a direction of ascent. The corresponding curves along which the rate of decrease (increase) is maximal are the steepest descent (ascent) trajectories.

Topologically, the local surface $u(x, y)$ near a saddle point can be divided into adjacent valleys ($u < u(x_0, y_0)$) and hills ($u > u(x_0, y_0)$), separated by boundaries along which $u(x, y) = u(x_0, y_0)$. Steepest descent directions are precisely those that penetrate into the valleys, while steepest ascent directions lead into the hills.

Lemma A.4.2. *Let $f = u(x, y) + i\, v(x, y)$ be analytic in a domain of $\mathbb{C}$. Then the steepest descent and ascent trajectories through $z_0 = x_0 + iy_0$ are exactly the curves in the (x, y)-plane along which the imaginary part is constant:*

$$v(x, y) = v(x_0, y_0). \tag{A.4.62}$$

Proof. Let γ be a smooth curve in the (x, y)–plane passing through (x_0, y_0), parametrised by arc length $s \mapsto (x(s), y(s))$ with $s = 0$ at (x_0, y_0). Then

$$\big(x'(s)\big)^2 + \big(y'(s)\big)^2 = 1$$

and we may write $x' = \cos\theta,\ \ y' = \sin\theta$, where θ is the angle between the tangent and the x-axis.

The rate of change of the real part u along γ is

$$\frac{\mathrm{d}u}{\mathrm{d}s} = u_x(x, y)\, x'(s) + u_y(x, y)\, y'(s) = u_x \cos\theta + u_y \sin\theta.$$

We seek directions θ for which this directional derivative is extremal. Differentiating with respect to θ and setting to zero yields the stationarity condition

$$\frac{\mathrm{d}}{\mathrm{d}\theta}\Big(u_x \cos\theta + u_y \sin\theta\Big) = -u_x \sin\theta + u_y \cos\theta = 0,$$

or equivalently

$$u_x \sin\theta = u_y \cos\theta. \tag{A.4.63}$$

Now use the Cauchy-Riemann relations for the analytic function f:

$$u_x = v_y, \qquad u_y = -v_x.$$

Substituting these into (A.4.63) gives

$$v_y \sin\theta - v_x \cos\theta = 0 \quad \Longleftrightarrow \quad v_x \cos\theta + v_y \sin\theta = 0.$$

The left-hand side is precisely the directional derivative of v in the tangent direction of γ:

$$\frac{\mathrm{d}v}{\mathrm{d}s} = v_x \cos\theta + v_y \sin\theta.$$

Hence $\frac{\mathrm{d}v}{\mathrm{d}s} = 0$ at a stationary direction of $\frac{\mathrm{d}u}{\mathrm{d}s}$. Because the curves are connected, $\frac{\mathrm{d}v}{\mathrm{d}s} = 0$ along the entire trajectory, so v is constant on γ:

$$v(x(s), y(s)) \equiv v(x_0, y_0).$$

Conversely, if v is constant along a curve then $\frac{\mathrm{d}v}{\mathrm{d}s} = 0$, which by the Cauchy-Riemann relations implies that the directional derivative $\frac{\mathrm{d}u}{\mathrm{d}s}$ is stationary with respect to the tangent direction; the sign of the second derivative of u along the curve then distinguishes steepest ascent from

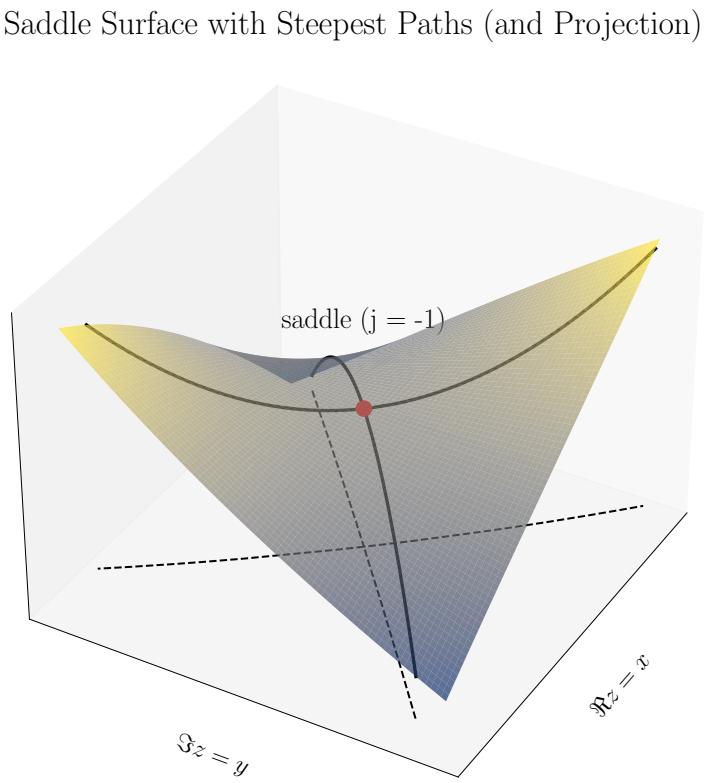

Figure A.4: Local structure of a first-order saddle point with steepest descent and ascent trajectories. The plane is divided into alternating valleys and hills.

steepest descent. Therefore, the curves on which v is constant are exactly the directions of steepest ascent and descent of u, as claimed. □

If f has a saddle of order $n-1$ at z_0, i.e. the first $n-1$ derivatives vanish at z_0, the directions of descent and ascent can be expressed in closed form.

Theorem A.4.2 (Directions of Steepest Descent and Ascent [65])**.** *Suppose*

$$\left.\frac{\mathrm{d}^q f}{\mathrm{d}z^q}\right|_{z=z_0} = 0, \quad q = 1, \dots, n-1 \qquad \left.\frac{\mathrm{d}^n f}{\mathrm{d}z^n}\right|_{z=z_0} = a e^{i\alpha}. \tag{A.4.64}$$

Writing $z - z_0 = \rho e^{i\theta}$, the directions are given by

$$\begin{aligned} \textit{steepest descent:} \quad & \theta = -\tfrac{\alpha}{n} + (2p+1)\tfrac{\pi}{n}, && p = 0, \dots, n-1, \\ \textit{steepest ascent:} \quad & \theta = -\tfrac{\alpha}{n} + 2p\tfrac{\pi}{n}, && p = 0, \dots, n-1, \\ \textit{constant } u\textit{:} \quad & \theta = -\tfrac{\alpha}{n} + \left(p + \tfrac{1}{2}\right)\tfrac{\pi}{n}, && p = 0, \dots, 2n-1. \end{aligned}$$

Once the local descent directions are known, Cauchy's integral theorem permits the deformation of the original contour C into one that follows steepest descent trajectories through the relevant saddles. While the exact topology of these trajectories can be difficult to determine

explicitly, it suffices to know their asymptotic directions and their qualitative structure. Importantly, any two descent contours lying in the same valley are *asymptotically equivalent*, in the sense that they yield the same asymptotic expansion of $I(\lambda)$.

Assume z_0 is a saddle point of order $n-1$, and that C can be deformed into a steepest descent trajectory through z_0, along which $u(x,y) \to -\infty$. Introducing the variable

$$\tau = -\big[f(z) - f(z_0)\big], \tag{A.4.65}$$

the integral becomes

$$I(\lambda) = e^{\lambda f(z_0)} \int_0^\infty G(\tau)\, e^{-\lambda\tau}\, \mathrm{d}\tau, \tag{A.4.66}$$

where

$$G(\tau) = g(z)\frac{\mathrm{d}z}{\mathrm{d}\tau} = -\frac{g(z)}{f'(z)}\Big|_{z=f^{-1}(f(z_0)-\tau)}. \tag{A.4.67}$$

The integral in Eq. (A.4.66) is now of Laplace-type and Watson's Lemma (cf. Lemma A.4.1) applies. If

$$G(\tau) \sim \sum_{m=1}^{\infty} a_m \tau^{\frac{m}{r}-1} \qquad r > 0, \tag{A.4.68}$$

then

$$I(\lambda) \sim e^{\lambda f(z_0)} \sum_{m=0}^{\infty} a_m\, \Gamma\!\left(\tfrac{m}{r}\right) \lambda^{-\frac{m}{r}}. \tag{A.4.69}$$

In particular, if z_0 is a simple saddle point and g is regular at z_0, one obtains the classical approximation

$$I(\lambda) \sim g(z_0) \sqrt{\frac{\pi}{2\lambda|f''(z_0)|}}\, \exp\!\Big[\lambda f(z_0) + i\Big(\tfrac{2p+1}{2}\pi - \tfrac{\alpha}{2}\Big)\Big], \quad p = 0, 1; \tag{A.4.70}$$

which coincides with the leading term of the extended Laplace method (Theorem A.4.1). The coefficients of higher order terms are given in Eq. (A.4.23). Equivalently to the case of Laplace-type integrals, the asymptotic expansion of $G(\tau)$ can be broadened to include logarithmic singularities. For a detailed account, refer to the work of Bleistein and Handelsman[65].

Examples of the method are often either deceptively simple-thus falling short of indicating common pitfalls-or excessively detailed, making them unsuitable as introductory illustrations. Here, we briefly summarise on the uniform asymptotic analysis of the Touchard polynomials carried out by Paris [77], which is directly relevant to our later discussion in Sec. 4.

Example A.4.4 (Asymptotics of the Touchard Polynomials [77])**.** The Touchard polynomials $T_n(z)$ [61] are defined by

$$T_n(z) = e^{-z}\left(z\frac{\mathrm{d}}{\mathrm{d}z}\right)^n e^z = \sum_{k=0}^{n} \left\{ n \atop k \right\} z^k = e^{-z}\sum_{k=0}^{\infty} \frac{k^n}{k!} z^k, \tag{A.4.71}$$

where $\left\{ n \atop k \right\}$ denote Stirling numbers of the second kind. Their generating function is

$$\exp\left[z\left(e^t - 1\right)\right] = \sum_{n=0}^{\infty} T_n(z)\frac{t^n}{n!}. \tag{A.4.72}$$

For later analysis, we also cite the identity [78]

$$\sum_{k=0}^{n} \left\{ n \atop k \right\} (x)_k = x^n, \tag{A.4.73}$$

where $(x)_k = x(x-1)\cdots(x-k+1)$ denotes the falling factorial. Our interest lies in the asymptotic behaviour of $T_n(z)$ as $n \to \infty$, where $|z|$ may be finite or of order $O(n)$.

From the reflection property

$$T_n(\overline{z}) = \overline{T_n(z)}, \tag{A.4.74}$$

it suffices to consider $0 \le \arg z \le \pi$. By Cauchy's theorem, $T_{n-1}(z)$ admits the contour integral representation

$$T_{n-1}(z) = \frac{\Gamma(n)e^{-z}}{2\pi i}\oint \frac{e^{ze^t}}{t^n}\,\mathrm{d}t, \tag{A.4.75}$$

where the contour encircles the origin counterclockwise. Since $\exp(t)$ decays rapidly in $\Re t < 0$, one may deform the contour to a Hankel path beginning and ending at $-\infty$ and encircling the origin.

Setting $\mu = \frac{n}{x}$ with $x = |z|$, $\theta = \arg z \in [0, \pi]$, we obtain the standard saddle point form

$$T_{n-1}(z) = \frac{\Gamma(n)e^{-z}}{2\pi i}\int_{-\infty}^{(0+)} e^{n\psi(t;\mu,\theta)}\,\mathrm{d}t, \tag{A.4.76}$$

$$\psi(t;\mu,\theta) = \frac{e^{t+i\theta}}{\mu} - t. \tag{A.4.77}$$

Saddles occur when $\psi'(t) = 0$, i.e.

$$te^t = \mu e^{-i\theta}, \tag{A.4.78}$$

with solutions $t_k = W_k\left(\mu e^{-i\theta}\right)$ given by the branches of Lambert's W function.

For concreteness, and because this structure reappears in Sect. 4.4, we restrict to negative real $z = x < 0$ ($\theta = \pi$). Three distinct cases occur:

- $0 < \mu < 1/e$: two distinct real saddles on the negative axis.
- $\mu = 1/e$: a double saddle at $t = -1$ (degenerate case).
- $\mu > 1/e$: saddles occur in complex-conjugate pairs.

Higher derivatives at the saddles follow from

$$\psi^{(n)}(t_k) = \frac{1}{t_k} + (-1)^n \frac{\Gamma(n)}{t_k^n}. \tag{A.4.79}$$

The logarithmic form of (A.4.78) leads to the transcendental equation

$$t + \ln t = \ln \mu + i(2\pi k - \theta), \tag{A.4.80}$$

which admits the asymptotic form

$$t_k \approx \ln \mu - \tfrac{1}{2} \ln\left[\ln^2 \mu + (2\pi k - \theta)^2\right] + i\left(2\pi k - \theta - \arctan\tfrac{2\pi k - \theta}{\ln \mu}\right). \tag{A.4.81}$$

As $|k| \to \infty$, the saddles satisfy

$$t_k \sim \ln \mu - \ln\left(2\pi|k| \mp \theta\right) + i\left(2\pi k - \theta \mp \tfrac{\pi}{2}\right), \tag{A.4.82}$$

i.e. their real parts decrease logarithmically, while imaginary parts separate by 2π.

The steepest descent/ascent paths are determined by the condition

$$\Im\psi(t) = \Im\psi(t_k), \tag{A.4.83}$$

which in coordinates $t = x + iy$ becomes

$$\frac{e^x}{\mu} \sin y + \arctan \frac{y}{x} = \left(\tfrac{1}{|t_k|} - |t_k|\right) \sin \arg(t_k) + (2\pi k + \pi). \tag{A.4.84}$$

These paths either terminate in $\Re(t) < 0$ or, for $x \to \infty$, approach horizontal asymptotes $y = 2k\pi$ (descent) or $y = (2k-1)\pi$ (ascent). They can be determined by evaluating the initial directional angle, given in Theorem A.4.2

Figure A.5 illustrates these paths for representative μ values. For $\mu < 1/e$, the contour C_k is deformed from $-\infty$ below the branch cut, passes through t_0, follows its descent path to $+\infty$, and returns along the conjugate path above the cut, so that non-descent contributions cancel.

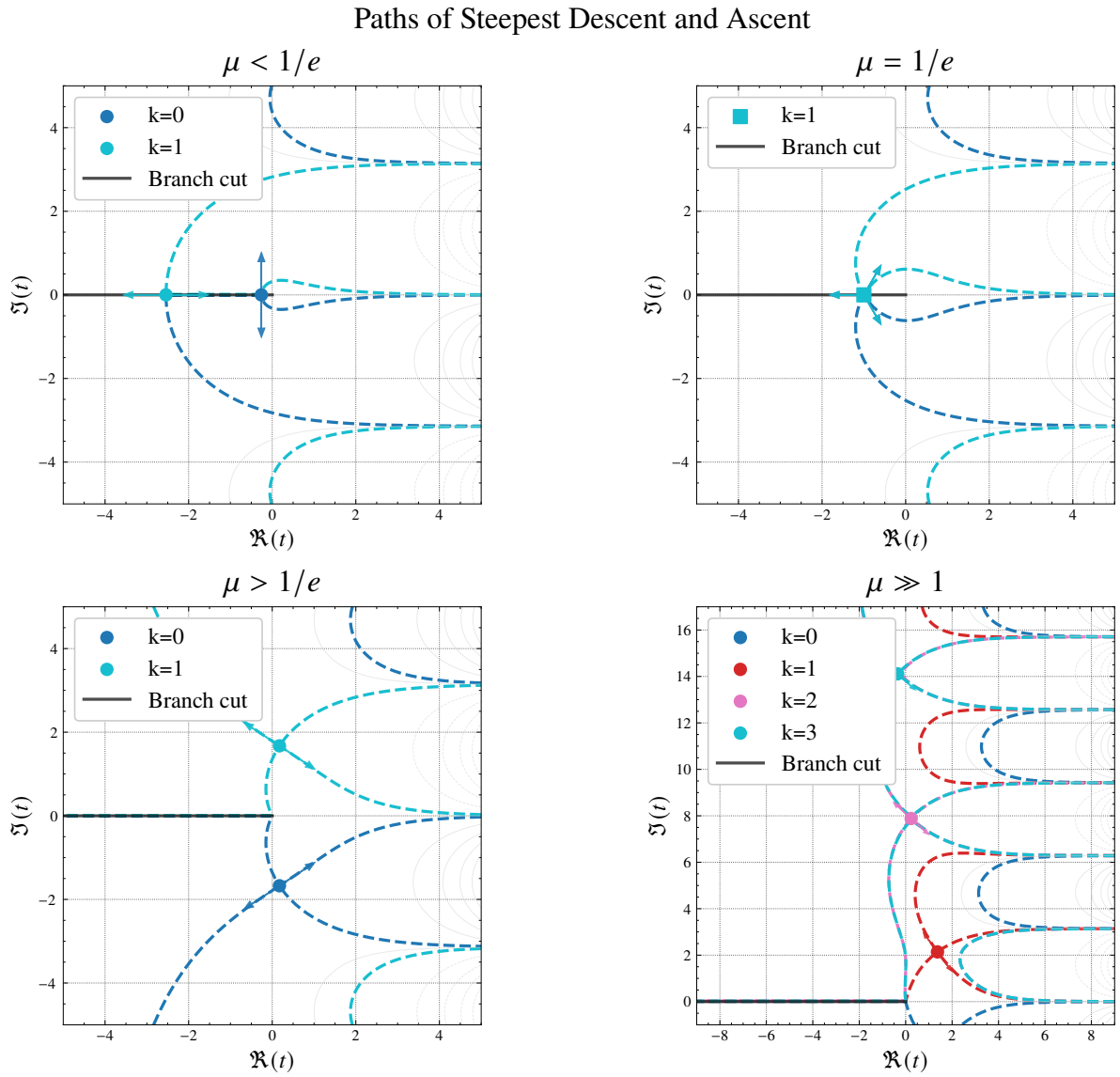

Figure A.5: Steepest descent (with arrows) and ascent (without) paths of the phase function (A.4.76) for $\theta = \pi$ and various μ. For $\mu < 1/e$, saddles lie on the negative real axis. At $\mu = 1/e$, they merge at $t = -1$ to form a double saddle. For $\mu > 1/e$, saddles appear as complex conjugate pairs, with dominance governed by $k = 0, 1$.

Moreover, this cancellation removes the contribution of the $k = 0$ saddle. At $\mu = 1/e$, the saddles coalesce at $t = -1$. For $\mu > 1/e$, the contour is deformed through the contributing conjugate pair of saddles (typically $k = 0, 1$), with further saddles accessible as μ increases.

Having established the contour representation and identified the dominant saddle points, the asymptotic expansion of the integral in (A.4.76) follows by applying the method of steepest descent and subsequently summing over the relevant contributions. In particular, for large n

one obtains

$$T_{n-1}(-x) \sim \begin{cases} \Re\left[\dfrac{\sqrt{2}\,\Gamma(n)\,e^{x+x/t_0}}{\sqrt{\pi(1+t_0)}\,t_0^{n-1}} \displaystyle\sum_{m=0}^{\infty} \frac{c_{2m}(t_0)\,\Gamma\left(m+\frac{1}{2}\right)}{n^{m+\frac{1}{2}}\,\Gamma\left(\frac{1}{2}\right)}\right], & \left(\mu > \tfrac{1}{e}\right), \\ \dfrac{\Gamma(n)\,e^{x+x/t_0}}{\sqrt{2\pi(1+t_0)}\,t_0^{n-1}} \displaystyle\sum_{m=0}^{\infty} \frac{c_{2m}(t_0)\,\Gamma\left(m+\frac{1}{2}\right)}{n^{m+\frac{1}{2}}\,\Gamma\left(\frac{1}{2}\right)}, & \left(0 < \mu < \tfrac{1}{e}\right), \end{cases} \tag{A.4.85}$$

where t_0 denotes the saddle point corresponding to the principal branch $k = 0$ of (A.4.78).

The distinction between the two cases reflects the saddle point geometry:

- For $0 < \mu < 1/e$, the expansion is governed by a single real saddle point $t_0 < 0$.
- For $\mu > 1/e$, the dominant contribution arises from a complex-conjugate pair of saddles, which combine to yield the real part in (A.4.85).

In both cases, the coefficients $c_{2m}(t_0)$ are determined locally by the expansion of the phase function at t_0. Their general form is given in (A.4.56), with the first few listed explicitly in (A.4.23).

A.4.4 Euler-Maclaurin Summation

The Euler-Maclaurin summation formula provides a way to estimate sums by corresponding integrals, with error terms expressible as finite sums involving products of the summand values at the boundaries and Bernoulli polynomials (see [79] and references therein). In what follows, we give a brief summary of the essential properties of Bernoulli polynomials relevant to our work. For a comprehensive account, the reader is referred to the standard reference [23].

Definition A.4.2 (Bernoulli Polynomials)**.** The Bernoulli polynomials $B_\nu(x)$ are uniquely defined by either of the equivalent relations:

$$\int_x^{x+1} B_\nu(t)\,\mathrm{d}t = x^\nu, \tag{A.4.86}$$

$$\frac{te^{xt}}{e^t - 1} = \sum_{\nu=0}^{\infty} B_\nu(x)\,\frac{t^\nu}{\nu!} \qquad (|t| < 2\pi). \tag{A.4.87}$$

for all values of x.

Remark A.4.2. The evaluations $B_\nu := B_\nu(0)$ are called the *Bernoulli numbers*. They are crucial for the error estimate in the Euler-Maclaurin formula, whilst also expressing special values of the Riemann zeta function.

Proposition A.4.1 (Zeta Values and Bernoulli Numbers)**.** *For $n \in \mathbb{N}_0$, the Riemann zeta function satisfies*

$$\zeta(-n) = (-1)^n \frac{B_{n+1}}{n+1}. \tag{A.4.88}$$

In particular,

$$\zeta(0) = -\tfrac{1}{2}, \tag{A.4.89}$$

$$\zeta(-2n) = 0 \qquad n \in \mathbb{N}, \tag{A.4.90}$$

where (A.4.90) *identifies the trivial zeros of the zeta function. Moreover, evaluating the functional equation at negative odd integers yields*

$$\zeta(2n) = (-1)^{n+1} \frac{(2\pi)^{2n}}{2(2n)!} B_{2n} \qquad (n \in \mathbb{N}) \,. \tag{A.4.91}$$

Proof. Insert Eq. (A.4.87) into Eq. (A.3.13)

$$\begin{aligned} \zeta(-n) &= \frac{e^{i\pi n}\Gamma(1+n)}{2\pi i} \sum_{\nu=0}^{\infty} \frac{B_\nu}{\nu!} \int_{|x|=1} x^{m-n-2} \, \mathrm{d}x \\ &= e^{i\pi n}\Gamma(1+n) \sum_{\nu=0}^{\infty} \frac{B_\nu}{\nu!} \delta_{\nu,n+1} \\ &= (-1)^n \frac{B_{n+1}}{n+1}. \end{aligned} \tag{A.4.92}$$

From which we deduce Eq. A.4.89. The location of the trivial zeros in Eq. (A.4.90) follows directly from the vanishing of all Bernoulli numbers with odd index greater than one, see the upcoming Corollary A.4.1 and Eq. (A.4.95). Eq. (A.4.91) is computed by evaluating $\zeta(1-2n)$ by means of the functional equation (2.2.7). □

Corollary A.4.1 (Properties of the Bernoulli Polynomials)**.** *The recurrence relation readily follows by standard manipulations of the definition in Eq.* (A.4.86)

$$B'_\nu(x) = \nu \, B_{\nu-1}(x). \tag{A.4.93}$$

By substituting $t \to -t$ and $x \to 1 - x$, by invariance of Eq. (A.4.87)

$$B_\nu(1-x) = (-1)^\nu B_\nu(x). \tag{A.4.94}$$

Similarly, by substituting $t \to -t$ in Eq. (A.4.87)*, all Bernoulli numbers with odd index greater*

than one vanish, i.e.

$$B_{2\nu+1} = 0 \qquad (\nu > 1)\,, \tag{A.4.95}$$

except for $B_1 = -\frac{1}{2}$. *Using Eq.* (2.2.6), *their signs follow the pattern*

$$B_\nu = (-1)^{\nu+1}|B_\nu|. \tag{A.4.96}$$

Comparing coefficients in Eq. (A.4.87) *with the generating function of the Bernoulli numbers*

$$B_\nu(x) = \sum_{n=0}^{\nu} \binom{\nu}{n} B_{\nu-n} x^n. \tag{A.4.97}$$

Lemma A.4.3 (Periodised Bernoulli Polynomials [57])**.** *Let* $\lfloor x \rfloor$ *denote the largest integer less than or equal to* x. *For* $\nu \in \mathbb{N}$, *we define the normalised,* periodised Bernoulli polynomials $P_\nu(x)$ *with period* 1 *by*

$$P_\nu(x) = \frac{1}{\nu!} B_\nu\left(x - \lfloor x \rfloor\right). \tag{A.4.98}$$

Which inherit the properties

$$P_{\nu+1} = \int P_\nu(x)\mathrm{d}x \tag{A.4.99}$$

$$P_{2\nu}(2x) = 2^{2\nu-1}\left[P_{2\nu}(x) + P_{2\nu}\left(x + \frac{1}{2}\right)\right] \tag{A.4.100}$$

$$(-1)^{\nu+1}\left[P_{2\nu}(x) - P_{2\nu}\left(\frac{1}{2}\right)\right] \geq 0. \tag{A.4.101}$$

Proof. Eq. (A.4.99) follows from Eq. (A.4.93). From Eq. (A.4.86), we see

$$\int_x^{x+\frac{1}{2}} B_n(2t)\mathrm{d}t = 2^{n-1}\int_x^{x+\frac{1}{2}} \left[B_n(t) + B_n\left(t + \frac{1}{2}\right)\right], \tag{A.4.102}$$

which not only implies Eq. (A.4.94), but also

$$B_\nu(2x) = 2^{\nu-1}\left[B_\nu(x) + B_\nu\left(x + \frac{1}{2}\right)\right], \tag{A.4.103}$$

proving (A.4.100). Further

$$B_{2\nu}\left(\frac{1}{2}\right) = \left(2^{1-2\nu} - 1\right) B_{2\nu}. \tag{A.4.104}$$

Lastly, Eq. (A.4.101) follows from Eq. (A.4.100) with Eq. (A.4.98). □

The original idea of Euler-Maclaurin summation is to apply successive integration by parts to the Stieltjes integral

$$\frac{1}{2}\left(f(j+1)+f(j)\right)=\int_j^{j+1} f(x)\mathrm{d}x+\int_j^{j+1}\left(x-j-\frac{1}{2}\right)f'(x)\mathrm{d}x, \tag{A.4.105}$$

and application of the telescope sum. By recognising $P_1(x)=\left(x-j-\frac{1}{2}\right)$, at each step, the order of $P_\nu(x)$ is increased.

Theorem A.4.3 (Euler-Maclaurin Summation [57, 66, 79])**.** *Let $f(t)$ be a real- or complex-valued function defined on $0\le t<\infty$. If $f^{(2\nu)}(t)$ is absolutely integrable on (M,N) for $M<N\in\mathbb{N}$, then*

$$\sum_{n=M}^{N} f(n)=\int_M^N f(x)\,\mathrm{d}x+\frac{f(N)+f(M)}{2}+\sum_{j=1}^{\nu-1}\frac{B_{2j}}{(2j)!}\left(f^{(2j-1)}(N)-f^{(2j-1)}(M)\right)+R_\nu(M,N), \tag{A.4.106}$$

where the remainder is given by

$$R_\nu(M,N)=\int_M^N \frac{B_{2\nu}-B_{2\nu}\left(x-\lfloor x\rfloor\right)}{(2\nu)!}f^{(2\nu)}(x)\mathrm{d}x \tag{A.4.107}$$

and satisfies

$$|R_\nu(M,N)|\le\left(2-2^{1-2\nu}\right)\frac{|B_{2\nu}|}{(2\nu)!}\int_M^N|f^{(2\nu)}(x)|\mathrm{d}x. \tag{A.4.108}$$

Proof. Summing Eq. (A.4.105) from $j=M$ to $j=N-1$, we have

$$\frac{1}{2}f(M)+\sum_{k=M+1}^{N-1}f(k)+\frac{1}{2}f(N)=\int_M^N f(x)\mathrm{d}x+\int_M^N P_1(x)f'(x)\mathrm{d}x. \tag{A.4.109}$$

Now observe that for $\nu\ge 2$, we have from Eq. (A.4.98)

$$\lim_{x\to(j+1)^-}P_\nu(x)=\lim_{x\to(j)^+}P_\nu(x)=\frac{1}{\nu!}B_\nu. \tag{A.4.110}$$

By repeated partial integration and evenness (see Eq. (A.4.95)) of Bernoulli numbers, we arrive at

$$\int_M^N P_1(x)f'(x)\mathrm{d}x=\sum_{j=1}^{\nu-1}\frac{B_{2j}}{(2j)!}\left(f^{(2j-1)}(N)-f^{(2j-1)}(M)\right)+R_\nu(M,N), \tag{A.4.111}$$

where $R_\nu(M,N)$ is as given in Eq. (A.4.107). The desired result in Eq. (A.4.106) now follows from (A.4.109) and (A.4.111). To estimate the remainder, we note from Eq. (A.4.103) and the

vanishing of $B_{2\nu}(x) - B_{2\nu}$ at $x = 0, 1$ from Eq. (A.4.96)

$$|B_{2\nu}(x) - B_{2\nu}| \leq |B_{2\nu}\left(\frac{1}{2}\right) - B_{2\nu}|. \tag{A.4.112}$$

Hence by (A.4.104)

$$|B_{2\nu}(x) - B_{2\nu}| \leq \left(2 - 2^{1-2\nu}\right)|B_{2\nu}|. \tag{A.4.113}$$

This completes the proof of the theorem. □

Corollary A.4.2. *Assume the hypothesis of Theorem A.4.3 hold.*

(i) If $f^{(2\nu)}(t)$ does not change sign in (M, N), then $R_\nu(M, N)$ is bounded in absolute value by $2 - 2^{1-2\nu}$ times the first neglected term in Eq. (A.4.106) *and has the same sign.*

(ii) If $f^{(2\nu)}(t)$ and $f^{(2\nu+2)}(t)$ have the same constant sign in (M, N), then $R_\nu(M, N)$ is bounded in absolute value by, and has the same sign as, the first neglected term in Eq. (A.4.106)*.*

Proof. $B_{2\nu} - B_{2\nu}(x)$ is zero at $x = 0$ and has only one extremum in the interval $0 < x < 1$, namely at $x = \frac{1}{2}$, where its derivative $-2\nu B_{2\nu-1}(x)$ is zero. This implies that $B_{2\nu} - P_{2\nu}(x)$ never changes sign. Since $P_{2\nu}(x)$ has zeros-namely at the extrema of $P_{2\nu+1}(x)$-the sign of $B_{2\nu} - P_{2\nu}(x)$ is always the same as the sign of $B_{2\nu}$, which by (A.4.96) is $(-1)^{\nu+1}$. Statement (i) follows from this and Eq. (A.4.108). Since $f^{(2\nu)}(t)$ and $f^{(2\nu+2)}(t)$ have the same constant sign in (M, N), but $B_{2\nu}$ and $B_{2\nu+1}$ differ in sign, by means of the *error test*, the second statement follows directly. □

Example A.4.5 (The Gamma Function [41, 57])**.** To study the gamma function, we begin by applying the Euler-Maclaurin summation formula (see Eq. (A.4.106)) to the logarithmic sum

$$\begin{aligned}\sum_{j=0}^{n} \log(z + j) = &\left(z + n + \tfrac{1}{2}\right)\log(z + n) - \left(z - \tfrac{1}{2}\right)\log(z) - n \\ &+ \sum_{j=1}^{\nu-1} \frac{B_{2j}}{(2j)(2j-1)}\left[\frac{1}{(z+n)^{2j-1}} - \frac{1}{z^{2j-1}}\right] \\ &- \frac{1}{2\nu}\int_0^n \frac{B_{2\nu} - B_{2\nu}(x - \lfloor x \rfloor)}{(z+x)^{2\nu}}\, dx.\end{aligned} \tag{A.4.114}$$

This identity follows from the fact that the j-th derivative of $\log(z+x)$ is $(-1)^{j-1}(j-1)!\,(z+x)^{-j}$. Setting $z = 1$, summing up to $n - 1$, and combining the result with Stirling's approximation

$n! \sim n^n e^{-n}\sqrt{2\pi n}$, one obtains, after letting $n \to \infty$,

$$1 - \frac{1}{2}\int_0^\infty \frac{B_2 - B_2(x - \lfloor x \rfloor)}{(1+x)^2}\, dx = \frac{1}{2}\log(2\pi). \tag{A.4.115}$$

Inserting this into Euler's limit formula yields

$$\begin{aligned}\log\Gamma(s) = &\left(s - \tfrac{1}{2}\right)\log(s) - s + \tfrac{1}{2}\log(2\pi) \\ &+ \sum_{j=1}^{\nu-1} \frac{B_{2j}}{(2j)(2j-1)}\frac{1}{s^{2j-1}} + R_\nu(s),\end{aligned} \tag{A.4.116}$$

with remainder term

$$R_\nu(s) = \frac{1}{2\nu}\int_0^\infty \frac{B_{2\nu} - B_{2\nu}(x - \lfloor x \rfloor)}{(s+x)^{2\nu}}\, dx. \tag{A.4.117}$$

Applying Corollary A.4.2 gives the estimate

$$|R_\nu(s)| \le \frac{|B_{2\nu}|}{2\nu}\int_0^\infty \frac{dx}{|s+x|^{2\nu}}. \tag{A.4.118}$$

Using the inequality for $\arg(s) = \theta$

$$|s+x|^2 = (|s|+x)^2 - 4|s|x\sin^2\frac{\theta}{2} \ge ||s|+x|^2\cos^2\frac{\theta}{2}, \tag{A.4.119}$$

we obtain the bound

$$R_\nu(s) \le \left(\frac{1}{\cos(\frac{\theta}{2})}\right)^{2\nu}\left|\frac{B_{2\nu}}{(2\nu)(2\nu-1)\, s^{2\nu-1}}\right|. \tag{A.4.120}$$

This result was already known to Stieltjes [80]. Finally, exponentiating Eq. (A.4.116) leads to Stirling's approximation:

$$\Gamma(s) = \sqrt{2\pi}\, s^{s-\frac{1}{2}} e^{-s}\left(1 + O\left(\tfrac{1}{s}\right)\right), \tag{A.4.121}$$

valid for $|s| \to \infty$ in the sector $|\arg(s)| < \pi$ [24, 30].

Example A.4.6 (Riemann Zeta Function)**.** Expressing the zeta function in its half-plane of absolute convergence $\sigma = \Re(s) > 1$ through its defining sum and applying Euler-Maclaurin

summation with truncation at a high value N, we obtain:

$$\zeta(s) - \sum_{n=1}^{N-1} n^{-s} = \sum_{n=N}^{\infty} n^{-s} \tag{A.4.122}$$

$$= \frac{N^{1-s}}{s-1} + \frac{1}{2}N^{-s} + \sum_{j=1}^{\infty} \frac{B_{2j}}{(2j)!} \left[\prod_{i=0}^{2j-2} (s+i) \right] N^{-s-2j+1} + R_{2j}, \tag{A.4.123}$$

where the error term is given by:

$$R_{2\nu} = \frac{(-1)^{\nu}}{(2\nu+1)!} \prod_{j=0}^{2\nu} (s+j) \int_{N}^{\infty} \overline{B}_{2\nu}(x) x^{-s-2\nu-1} \, dx. \tag{A.4.124}$$

The asymptotic behaviour of this remainder term has been investigated by Backlund [81], who established that the error is at most equal to the magnitude of the first omitted term, multiplied by the absolute value of $\frac{s-2\nu-1}{\sigma+2\nu-1}$.

Appendix B

Alternative Derivations of the One-Loop Pressure Expansion

In this appendix, we present three complementary derivations of the dimensionless thermal functions $\overline{P}(a)$ and $\overline{D}(a)$, for $a = m/T$, expressed in terms of modified Bessel functions of the second kind $K_\nu(x)$. These derivations all trace back to the convergent small-a expansion originally obtained by Dolan and Jackiw [22] through successive integration by parts and zeta-function regularisation.

We start by recalling the original derivation of the one-loop pressure by Dolan and Jackiw, which provides the starting point for all subsequent analytic continuations. Then we develop three distinct approaches that originate from this expansion but proceed along different analytic routes. In the first method, the remainder term $R(a)$ of the series is rewritten in a form suitable for analytic continuation using inhomogeneous zeta functions and Poisson summation. The second approach interprets $R(a)$ as a sum over residues, leading naturally to a contour-integral representation of the thermal function. Finally, the third method employs the Matsubara trick, introducing auxiliary contour singularities that permit contour deformations to enclose branch points associated with the mass parameter $a = 2\pi z$.

Each derivation emphasises a different aspect of the remainder term $R(a)$: the first highlights its connection to inhomogeneous zeta functions; the second exposes its underlying pole structure; and the third focuses on the branch points.

B.1 Derivation Following Dolan and Jackiw

In this subsection, we repeat the asymptotic derivation of the dimensionless pressure (3.1.6) as originally performed by Dolan and Jackiw. Since standard approaches to this computation already make use of zeta function regularisation, this naturally points towards a deeper con-

nection between Yang–Mills theory and analytic number theory. Our analysis was originally motivated by their work: their asymptotic treatment produced a summation they did not identify explicitly as a zeta function sum. For their purposes it was sufficient to argue that this error term could be discarded, but upon closer inspection we recognised this summation as an instance of the Riemann zeta function. This observation provided the starting point for our investigations. Ultimately, we will verify the following expression

$$\overline{P}(a) = -2\pi^4 \left\{ \frac{1}{90} - \frac{z^2}{6} + \frac{2z^3}{3} + 2z^4 \left[\frac{1}{4} \log \frac{z}{2} + \frac{\gamma}{4} - \frac{3}{16} \right] \right\} - \frac{8\pi^4}{3} R(z), \tag{B.1.1}$$

$$\begin{aligned} R(z) &= \sum_{n=1}^{\infty} n^3 \left[\left(1 + \frac{z^2}{n^2} \right)^{3/2} - 1 - \frac{3}{2}\frac{z^2}{n^2} - \frac{3}{8}\frac{z^4}{n^4} \right] \\ &= \frac{3}{4\sqrt{\pi}} \sum_{k=3}^{\infty} \frac{\Gamma\left(k - \frac{3}{2}\right)}{\Gamma(k+1)} \zeta(2k-3) (-1)^k z^{2k} \qquad (|z| \leq 1) \,. \end{aligned} \tag{B.1.2}$$

where for later convenience, we defined $a = 2\pi z$ with $a = m/T$, and $R(z)$ denotes the remainder term to investigate. Comparison of Eq. (B.1.2) with the definition of the Riemann zeta function, see Eq. (2.2.1), encouraged us to Taylor expand the first term the first summand in $R(z)$. Proving the interchangeability of both sums, an infinite sum probing the zeta function at odd values is obtained.

B.1.1 Integration by Parts and its Limitations

Inspecting the integrand (3.1.6) suggests the method of successive integration by parts [65, 66] as an efficient way to obtain an asymptotic expansion in the small mass parameter a. The idea is to differentiate with respect to a^2 and repeatedly integrate by parts, thereby generating a series in powers of a^2. However, we will see that this procedure fails at the second iteration: non-analytic contributions in a^2 appear, which cannot be captured by this purely algebraic power producing method.

Integrating Eq. (3.1.6) by parts once yields

$$\overline{P}(a) = \frac{1}{3} \left[x^3 \log\!\left(1 - \mathrm{e}^{-\sqrt{x^2+a^2}}\right) \right]_0^{\infty} - \frac{1}{3} \int_0^{\infty} \frac{x^4}{\sqrt{x^2+a^2}} \frac{\mathrm{d}x}{\mathrm{e}^{\sqrt{x^2+a^2}} - 1}. \tag{B.1.3}$$

For $x \to \infty$, the logarithm is exponentially suppressed, while for $x \to 0$ one has $x^3 \log(1 - \mathrm{e}^{-\sqrt{x^2+a^2}}) \sim x^3 \log x$, which also tends to zero. Thus both boundary terms vanish, and we

obtain

$$\overline{P}(a) = -\frac{1}{3}\int_0^\infty \frac{x^4}{\sqrt{x^2+a^2}}\frac{\mathrm{d}x}{\mathrm{e}^{\sqrt{x^2+a^2}}-1}. \tag{B.1.4}$$

In particular, setting $a = 0$ yields

$$\overline{P}(0) = -\frac{1}{3}\int_0^\infty \frac{x^3}{\mathrm{e}^x-1}\,\mathrm{d}x \;=\; -\frac{\pi^4}{45}, \tag{B.1.5}$$

where Eq. (A.3.12) and the known value $\zeta(4)$ (see Eq. (2.2.6)) have been used.

Repeating the calculation for the first derivative with respect to a^2 gives

$$\frac{\partial}{\partial a^2}\overline{P}(a) = \frac{1}{2}D(a), \tag{B.1.6}$$

$$\frac{\partial}{\partial a^2}\overline{P}(a)\big|_{a=0} = \frac{1}{2}\int_0^\infty \frac{x}{\mathrm{e}^x-1}\,\mathrm{d}x \;=\; \frac{\pi^2}{12}. \tag{B.1.7}$$

The second derivative of the pressure with respect to a^2 requires more care, as a direct evaluation at $a^2 = 0$ of the integrand leads to a divergent integral. Exploiting the symmetry between x^2 and a^2, we write

$$\frac{\partial^2}{\partial(a^2)^2}\overline{P}(a) = \frac{1}{2}\int_0^\infty x^2\,\frac{\partial}{\partial x^2}\left[\frac{1}{\sqrt{x^2+a^2}}\frac{1}{\mathrm{e}^{\sqrt{x^2+a^2}}-1}\right]\mathrm{d}x. \tag{B.1.8}$$

Performing a partial integration with respect to x^2 and using $\mathrm{d}x^2 = 2x\,\mathrm{d}x$ and $\partial_{x^2}x = 1/(2x)$ for $x > 0$, we obtain

$$\frac{\partial^2}{\partial(a^2)^2}\overline{P}(a) = -\frac{1}{4}\int_0^\infty \frac{1}{\sqrt{x^2+a^2}}\frac{1}{\mathrm{e}^{\sqrt{x^2+a^2}}-1}\,\mathrm{d}x. \tag{B.1.9}$$

For any fixed $a > 0$, the integral in Eq. (B.1.9) is convergent: the integrand is finite at $x = 0$ and decays exponentially as $x \to \infty$. However, if one attempts to set $a = 0$ inside the integrand, it behaves like $1/x^2$ near the origin and the integral diverges. This indicates that the limit $a \to 0$ cannot be interchanged with the integration, and it is precisely here that non-analytic terms in a^2 (such as a^3 and $a^4 \log a$) enter the expansion. Clearly, the straightforward integration-by-parts strategy thus fails at the second derivative because it cannot generate these non-analytic contributions.

B.1.2 Bosonic Expansion and the Need for Regularisation

To access the non-analytic structure, we now rewrite the Bose-Einstein distribution in (B.1.9) in a form suitable for summation techniques. We start from the identity obtained by combining the Hadamard-Weierstrass product (2.1.5) with Euler's reflection formula (2.1.10):

$$\frac{\sin(\pi s)}{\pi s} = \prod_{n=1}^{\infty}\left(1 - \frac{s^2}{n^2}\right). \tag{B.1.10}$$

Since the sum of the negative terms is absolutely convergent (proportional to $\zeta(2)$), we may differentiate the logarithm:

$$\frac{\mathrm{d}}{\mathrm{d}s}\log\left(\frac{\sin(\pi s)}{\pi s}\right) = \frac{\pi}{\tan(\pi s)} - \frac{1}{s}, \tag{B.1.11}$$

and hence

$$\frac{\pi s}{\tan(\pi s)} - 1 = s\sum_{n=1}^{\infty}\frac{\mathrm{d}}{\mathrm{d}s}\log\left(1 - \frac{s^2}{n^2}\right) = -\sum_{n=1}^{\infty}\frac{2s^2}{n^2 - s^2}. \tag{B.1.12}$$

Inserting $s = \frac{ix}{2\pi}$ we find

$$\begin{aligned}\frac{1}{x}\left[\frac{ix/2}{\tan(ix/2)} - 1\right] &= \frac{1}{2}\frac{\mathrm{e}^{-x/2} + \mathrm{e}^{x/2}}{\mathrm{e}^{x/2} - \mathrm{e}^{-x/2}} - \frac{1}{x} \\ &= \frac{1}{2} + \frac{1}{\mathrm{e}^{x} - 1} - \frac{1}{x} \\ &= \sum_{n=1}^{\infty}\frac{2x}{x^2 + 4\pi^2 n^2}.\end{aligned} \tag{B.1.13}$$

Recognising that the same construction applies after shifting $s \to s + \frac{1}{2}$ and inverting, we arrive at

$$\frac{1}{\mathrm{e}^{\sqrt{x^2+a^2}} - 1} = \sum_{n\in\mathbb{Z}}\frac{\left(x^2 + a^2\right)^{1/2}}{x^2 + a^2 + 4\pi^2 n^2} - \frac{1}{2}. \tag{B.1.14}$$

We remark that this identity, in a closely related form, served as the starting point of Euler's derivation of the formula for $\zeta(2n)$ [82].

If one now naively substitutes Eq. (B.1.14) into Eq. (B.1.9) and splits the integral into the two contributions coming from the sum over n and from the $-1/2$ term, the latter resulting integral diverges, even though the sum of both reproduces the finite quantity in Eq. (B.1.9). Thus, the divergence is not due to the original integral itself, but is an artefact of exchanging summation and integration after the expansion of the bosonic factor.

To control this and to justify the subsequent manipulations, we introduce an analytic regulator in the form of a factor $x^{-\epsilon}$ and define

$$I_\epsilon(a) = \int_0^\infty \frac{x^{-\epsilon}}{\sqrt{x^2+a^2}} \frac{1}{\mathrm{e}^{\sqrt{x^2+a^2}} - 1} \,\mathrm{d}x, \qquad (0 < \epsilon < 1). \tag{B.1.15}$$

For each fixed $a > 0$ and $0 < \epsilon < 1$ this integral is finite and, as $\epsilon \to 0$, one recovers $I_0(a) = I(a)$ in the sense of a removable singularity. The rôle of ϵ is therefore not to regularise $I(a)$ itself, but to render separately convergent the two integrals which arise after splitting the summand in Eq. (B.1.14).

Upon inserting Eq. (B.1.14) into Eq. (B.1.15), the regularised integral decomposes as

$$I_\epsilon(a) = \underbrace{\int_0^\infty x^{-\epsilon} \sum_{n\in\mathbb{Z}} \frac{1}{x^2+a^2+4\pi^2n^2} \,\mathrm{d}x}_{I_1^\epsilon(a^2)} \underbrace{-\frac{1}{2}\int_0^\infty \frac{x^{-\epsilon}}{\sqrt{x^2+a^2}} \,\mathrm{d}x}_{I_2^\epsilon(a^2)}. \tag{B.1.16}$$

The conditions on ϵ ensure that both $I_1^\epsilon(a^2)$ and $I_2^\epsilon(a^2)$ converge individually. In particular, without the factor $x^{-\epsilon}$, the first and second integrands would decay like $1/x^2$ and $1/x$ respectively for $x \to \infty$, and both behave like a constant at $x = 0$, leading to divergences upon splitting. The regulator $x^{-\epsilon}$ softens both limits just enough to allow separate evaluation, and the divergences in the limit $\epsilon \to 0$ cancel in the combination $I_\epsilon(a)$.

B.1.3 Evaluation of the Regulated Pieces

The second term in Eq. (B.1.16) is most easily dealt with by identifying the beta function. We obtain

$$\begin{aligned} I_2^\epsilon(a^2) &= -\frac{1}{2}a^{-\epsilon}\int_0^\infty \frac{x^{-\epsilon}}{\sqrt{1+x^2}} \,\mathrm{d}x \\ &= -\frac{1}{4}a^{-\epsilon} B\left(\tfrac{1-\epsilon}{2}, \tfrac{\epsilon}{2}\right) \\ &= -\left(\frac{1}{2\epsilon} - \frac{1}{2}\log\frac{a}{2} + O(\epsilon)\right), \end{aligned} \tag{B.1.17}$$

where in the penultimate step the definition of the beta function (Eq. (2.1.24)) has been used, and in the final step the beta function has been expressed in terms of gamma functions (again using Eq. (2.1.24)) and expanded around $1/2$ and $\epsilon/2$ with the aid of Eq. (2.1.7).

Regarding the first term, we rescale the bosonic integral by $x^2 \mapsto x^2/(a^2+4\pi^2n^2)$. In doing so, a factor $1/(a^2+4\pi^2n^2)$ is extracted from the integral, a factor $(a^2+4\pi^2n^2)^{-\epsilon/2}$ arises from $x^{-\epsilon}$, and an additional factor $(a^2+4\pi^2n^2)^{1/2}$ stems from the measure. For Bose fields, this

yields

$$
\begin{aligned}
I_1^{\epsilon}(a^2) &= \sum_{n\in\mathbb{Z}} \left(a^2 + 4\pi^2 n^2\right)^{-\frac{1+\epsilon}{2}} \int_0^{\infty} \frac{x^{-\epsilon}}{x^2+1}\,\mathrm{d}x \\
&= \left[\frac{1}{a^{1+\epsilon}} + 2\sum_{n=1}^{\infty} \frac{1}{\left(a^2+4\pi^2n^2\right)^{\frac{1+\epsilon}{2}}}\right] \frac{\pi/2}{\cos(\pi\epsilon/2)} \\
&= \left[\frac{1}{a^{1+\epsilon}} + 2\sum_{n=1}^{\infty} \frac{1}{(2\pi n)^{1+\epsilon}} + \underbrace{2\sum_{n=1}^{\infty} \frac{1}{(2\pi n)^{1+\epsilon}} \left(\left(\frac{1}{a^2+4\pi^2n^2}\right)^{\frac{1+\epsilon}{2}} - 1\right)}_{=\tilde{I}(a^2)}\right] \frac{\pi/2}{\cos(\pi\epsilon/2)}.
\end{aligned}
\tag{B.1.18}
$$

Recognising the Riemann zeta function in the second term of Eq. (B.1.18) and expanding around $\epsilon = 0$ using Eq. (2.2.5) gives

$$
2^{-1-\epsilon}\pi^{-\epsilon}\zeta(1+\epsilon) = \frac{1}{2\epsilon} + \frac{1}{2}\big(\gamma - \log(2\pi)\big) + O(\epsilon). \tag{B.1.19}
$$

Inserting the results from Eq. (B.1.18) and Eq. (B.1.17) and taking the limit $\epsilon \to 0$ finally yields

$$
\tilde{I}(a^2) = \frac{1}{2}\sum_{n\in\mathbb{N}} \frac{1}{n}\left[\left(1 + \frac{a^2}{4\pi^2n^2}\right)^{-1/2} - 1\right], \tag{B.1.20}
$$

$$
I_1^{\epsilon}(a^2) = \frac{1}{2\epsilon} + \frac{\pi}{2a} + \frac{1}{2}(\gamma - \log(2\pi)) + \tilde{I}(a^2), \tag{B.1.21}
$$

$$
I(a^2) = \lim_{\epsilon\to 0} I_{\epsilon}(a) = \frac{\pi}{2a} + \frac{1}{2}\log\frac{a}{4\pi} + \frac{\gamma}{2} + \tilde{I}(a^2). \tag{B.1.22}
$$

To summarise, the second derivative of the finite-temperature pressure, expressed in terms of the regularised integral $I_{\epsilon}(a)$ and its finite limit $I(a)$, becomes

$$
\frac{\partial^2}{\partial(a^2)^2}\overline{P}(a) = -\frac{1}{4}\,I(a), \tag{B.1.23}
$$

providing the desired starting point for the analysis of the remainder term $R(z)$.

We now advance to compute the pressure by subsequently integrating Eq. (B.1.23) and taking the boundary conditions from Eq. (B.1.7) and Eq. (B.1.5) into account. Upon integration, with

c_1 denoting the constant of integration, the pressure at one-loop is given by

$$\frac{\partial}{\partial(a^2)}\overline{P}(a) = -\frac{1}{4}\left[\frac{a^2}{2}\left(\gamma - \frac{1}{2}\right) + \pi a + \frac{a^2}{2}\log\frac{a}{4\pi} + \sum_{n\in\mathbb{N}}\frac{1}{n}\left[(4\pi^2 n^2)\left(1 + \frac{a^2}{4\pi^2 n^2}\right)^{1/2} - \frac{a^2}{2}\right] + c_1\right]. \tag{B.1.24}$$

The constant of integration c_1 is determined by enforcing the previously established boundary conditions (B.1.7)

$$\frac{\partial}{\partial(a^2)}\overline{P}(a)\bigg|_{a=0} = \frac{\pi^2}{12} = -\frac{1}{4}\left(c_1 + 4\pi^2\zeta(-1)\right), \tag{B.1.25}$$

which implies $c_1 = 0$. Repeating the steps for the first derivative, we obtain similarly

$$\overline{P}(a) = -\frac{1}{4}\left[\frac{2}{3}\pi a^3 + \left(\frac{\gamma}{4} - \frac{3}{16} + \frac{1}{4}\log\frac{a}{4\pi}\right)a^4 - \frac{\pi^2}{3}a^2 + \sum_{n\in\mathbb{N}}\frac{1}{n}\left(\frac{2}{3}(4\pi^2 n^2)^2\left(1 + \frac{a^2}{4\pi^2 n^2}\right)^{3/2} - \frac{a^4}{4} - 4\pi^2 n^2 a^2\right) + c_2\right]. \tag{B.1.26}$$

The constant of integration c_2 is determined by the boundary condition in Eq. (B.1.5), as

$$-\frac{\pi^4}{45} = -\frac{1}{4}\left(\frac{2}{3}(4\pi^2)\zeta(-3) + c_2\right), \tag{B.1.27}$$

which, in turn, gives $c_2 = \frac{8\pi^4}{90} - \frac{2}{3}(4\pi^2)\zeta(-3)$. Collecting all terms, we arrive at the identity claimed in Eq. (B.1.1)

$$\overline{P}(a) = -\frac{1}{4}\left\{\frac{8\pi^4}{90} - \frac{\pi^2}{3}a^2 + \frac{2\pi}{3}a^3 + a^4\left[\frac{1}{4}\log\frac{a}{4\pi} + \frac{\gamma}{4} - \frac{3}{16}\right]\right\} - \frac{8\pi^4}{3}R(a^2), \tag{B.1.28}$$

where

$$R(a^2) = \sum_{n\in\mathbb{N}} n^3\left[\left(1 + \frac{a^2}{4\pi^2 n^2}\right)^{3/2} - 1 - \frac{3a^2}{8\pi^2 n^2} - \frac{3a^4}{128\pi^4 n^4}\right] = O(a^6). \tag{B.1.29}$$

Notice that the first two terms in Eq. (B.1.1) contribute to the boundary conditions, and the successive terms in Eq. (B.1.2) remove apparent divergences originating from the sum. The zeta function dependence can be made explicit by Taylor expanding the first term in Eq. (B.1.2) and interchanging the order of summation. Using the generalised binomial theorem (see Example (A.2.2)), we have

$$
\begin{aligned}
R(z) &= \sum_{n\in\mathbb{N}} n^3 \sum_{k=3}^{\infty} \binom{\frac{3}{2}}{k} z^{2k} n^{-2k} \\
&= \sum_{n\in\mathbb{N}} \sum_{k=3}^{\infty} \frac{\Gamma\left(\frac{5}{2}\right)}{\Gamma\left(k+1\right)\Gamma\left(\frac{5}{2}-k\right)} z^{2k} n^{3-2k} \\
&= \sum_{k=3}^{\infty} \frac{\Gamma\left(\frac{5}{2}\right)}{\Gamma\left(k+1\right)\Gamma\left(\frac{5}{2}-k\right)} z^{2k} \zeta(2k-3) \\
&= \frac{3}{4\sqrt{\pi}} \sum_{k=3}^{\infty} (-1)^k \frac{\Gamma(k-\frac{3}{2})}{\Gamma(k+1)} \zeta(2k-3) z^{2k}.
\end{aligned} \tag{B.1.30}
$$

The inversion of the order of summation is justified by absolute convergence:

$$
\begin{aligned}
R(z) &< 3 \sum_{k=3}^{\infty} \frac{(2k-3)!!}{k!2^k} z^{2k} \zeta(3) \\
&= 3\zeta(3) \left[\left(1-z^2\right)^{3/2} + \frac{12z^2 - 3z^4 + 8}{8} \right].
\end{aligned} \tag{B.1.31}
$$

In the ultimate step, Eq. (2.1.12) has been applied, as $k \in \mathbb{Z}$ allows for the application. Consequently, absolute convergence of Eq. (B.1.30) for $|z| \leq 1$ is inherited from the generalised binomial theorem (cf. Example A.2.2).

B.2 Analytic Continuation by Poisson Summation

Instead of investigating the properties of Eq. (B.1.2) directly, we consider the related series

$$
R(z,s) = \sum_{n\in\mathbb{N}} \left\{ \frac{1}{(n^2+z^2)^s} - n^{-2s} - (-s) z^2 n^{-2(s+1)} - \frac{s(s+1)}{2} z^4 n^{-2(s+2)} \right\}, \tag{B.2.1}
$$

where $z = a/2\pi$ and we demand $\Re(s) > 1/2$ such that the series converges uniformly for all $z \in \mathbb{C}$ with $-z^2 \notin \mathbb{N}$. Analytically continuing each term individually allows us to ultimately take the limit $s \to -\frac{3}{2}$, thus recovering Eq. (B.1.2).

One encouraging observation is that the series structure in Eq. (B.1.2) implies a logical relationship to a more general class of special functions, specifically the Epstein zeta function. As discussed in Eq. (2.2.7), this function generalises the Riemann zeta function and obeys a functional equation with a similar structure.

It should be noted that when the summation extends over $z \in \mathbb{N}$, the first term in Eq. (B.2.1) also reduces to Epstein's zeta function. Because of the simple pole of the Riemann zeta function at $s \to 1$, the final term in the limiting process introduces a singularity. We then expect a pole that originates from the first summand at $s = -\frac{3}{2}$ to cancel the final term in the same way, rendering the result finite.

We start by examining the first term of the function,

$$\sum_{n\in\mathbb{N}} f(n,z,s) = \sum_{n\in\mathbb{N}} \frac{1}{(n^2+z^2)^s} \qquad (z^2 \notin -\mathbb{N}), \tag{B.2.2}$$

which converges absolutely provided $\Re(s) > \frac{1}{2}$. Sums of this kind are commonly continued by application of the Poisson summation formula in Theorem A.3.2. Indeed, we derived in Example A.3.7

$$\tfrac{1}{2}z^{-2a} + \sum_{n=1}^{\infty} \frac{1}{(n^2+z^2)^a} = \frac{\sqrt{\pi}}{2}\frac{\Gamma\left(a-\frac{1}{2}\right)}{\Gamma(a)} z^{1-2a} + \frac{2\pi^a}{\Gamma(a)} z^{\frac{1}{2}-a} \sum_{n=1}^{\infty} n^{a-\frac{1}{2}} K_{\frac{1}{2}-a}(2\pi n z). \tag{B.2.3}$$

Such that we obtain an explicit expression for the sum in Eq. (B.2.1)

$$\begin{aligned} R(z,s) = {} & \frac{\sqrt{\pi}}{2}\frac{\Gamma\left(s-\frac{1}{2}\right)}{\Gamma(s)}\frac{1}{z^{2s-1}} - \frac{1}{2z^{2s}} + \frac{2\pi^s}{\Gamma(s)} z^{\frac{1}{2}-s} \sum_{\nu\in\mathbb{N}} \nu^{s-\frac{1}{2}} K_{\frac{1}{2}-s}(2\pi\nu z) \\ & - \zeta(2s) + sz^2\zeta(2s+2) - \frac{s(s+1)}{2} z^4 \zeta(2s+4). \end{aligned} \tag{B.2.4}$$

The series in Eq. (B.2.4) is entire in s and vanishes at all negative integers due to the poles of the gamma function. Given the asymptotic behaviour of $K_\nu(z)$ for large $|z|$ in (2.3.5), this term is readily shown to be absolutely convergent for all $s \in \mathbb{C}$.

To evaluate the limiting behaviour near $s = -\frac{3}{2}$, we set $s = -\frac{3}{2} + \epsilon$ with $\epsilon > 0$ and consider the limit $\epsilon \to 0^+$. This yields

$$\begin{aligned} \lim_{\epsilon\to 0^+} R(z,s) = {} & \frac{3}{2\pi^2} z^2 \sum_{\nu\in\mathbb{N}} \frac{K_2(2\pi\nu|z|)}{\nu^2} - \left\{\zeta(-3) + \frac{3}{2}z^2\zeta(-1) + \frac{z^3}{2}\right\} \\ & + \lim_{\epsilon\to 0^+} \left[\frac{\sqrt{\pi}\Gamma(\epsilon-2)}{2\Gamma\left(\epsilon-\frac{3}{2}\right)} z^{4-2\epsilon} - \frac{\left(\epsilon-\frac{3}{2}\right)\left(\epsilon-\frac{1}{2}\right)}{2} z^4 \zeta(2\epsilon+1)\right]. \end{aligned} \tag{B.2.5}$$

Utilising the known pole behaviour of $\zeta(s)$ at $s = 1$ and the expansion of $\Gamma(s)$ near its poles (see Eq. (2.2.5) and Eq. (2.1.7)), we obtain the final expression

$$R(z) = \frac{3}{16}\left[\frac{3}{2} - 2\gamma + \log 4 - 2\log z\right] z^4 - \frac{1}{2}z^3 + \frac{1}{8}z^2 - \frac{1}{120} + \frac{3z^2}{2\pi^2}\sum_{\nu\in\mathbb{N}} \nu^{-2} K_2(2\pi\nu z) \qquad (\forall z \in \mathbb{C}), \tag{B.2.6}$$

whereby the term proportional to z^3 stems from the addition and subtraction of the $n = 0$ term in Eq. (A.3.50). Insertion of Eq. (B.2.6) into Eq. (B.1.1) yields

$$\overline{P}(a) = -4\pi^2 z^2 \sum_{\nu\in\mathbb{N}} \nu^{-2} K_2(2\pi\nu z). \tag{B.2.7}$$

In the limit $z \to 0$, one finds that $R(0) = 0$, which is consistent with Eq. (B.1.2). This result follows from the leading-order term of the modified Bessel function (2.3.6)

$$\lim_{z\to 0^+} R(z) = -\frac{1}{120} + \frac{3}{4\pi^2} z^2 \sum_{\nu\in\mathbb{N}} \frac{1}{\pi^2\nu^4 z^2} = -\frac{1}{120} + \frac{3}{4\pi^4}\zeta(4) = 0. \tag{B.2.8}$$

Alternatively, Eq. (B.2.6) could also be derived by expressing $f(n, z, s)$ as a Mellin transform normalised by the gamma function, interchanging the order of summation and integration, and then recognising the appearance of the Jacobi theta function. Applying its functional equation introduces an exponential contribution, which may itself be rewritten as an inverse Mellin transform. This leads to a MB integral of the form (2.3.8), ultimately recovering the modified Bessel function of the second kind.

B.3 Integral Representation and Asymptotic Expansion

Interpreting $R(z)$ as a sum over residues of a closed contour integral of a function encourages us to derive an integral representation whose displacement leads to the Bessel sum. We start by examining the integral

$$I = \frac{1}{2\pi i}\int_{c-i\infty}^{c+i\infty} \Gamma\left(s - \frac{3}{2}\right)\Gamma(-s)\,\zeta(2s-3)\, z^{2s}\,\mathrm{d}s, \qquad (2 < c < 3), \tag{B.3.1}$$

along the vertical line $\Re(s) = c$. Here, the integrand introduces simple poles at $s \in \mathbb{N}_0$, induced by $\Gamma(-s)$, together with a pole at $s = \frac{3}{2}$ and a double pole at $s = 2$, originating from $\zeta(2s-3)$ and $\Gamma(-s)$, respectively. By forming a closed contour around a rectangle with vertices at $c \pm iT$ and $c + N \pm iT$ with $N \in \mathbb{N}$, we can apply the residue theorem to evaluate

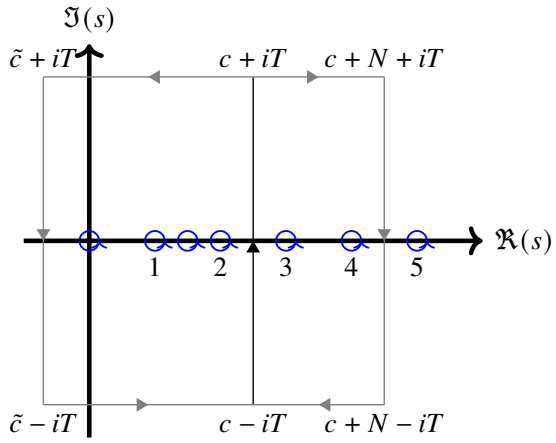

(a) Rectangle contours of Eq. (B.3.1). The small z asymptotic expansion is obtained by closing the contour to the right. For large z, close the contour to the left. The blue circles indicate the poles of Eq. (B.3.1)

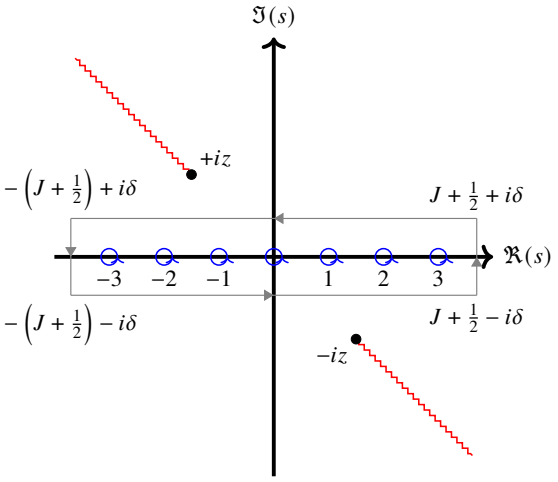

(b) Contour of Eq. (B.4.2). For $\delta < \Im(iz)$, the light gray contour is expanded by letting $J \to \infty$. The rectangular contour is then cut, such that each half can be wrapped around the branches of $\pm iz$ resulting in Hankel contours.

Figure B.1: Two contour plots: (a) Viable contour displacements for small and large z; (b) Contour for a modified rectangular contour obtained by the Matsubara trick.

the integral, see Fig. B.1a. Utilising Stirling's approximation, Eq. (2.1.16), and Lindelöf's estimate, Eq. (2.2.14), the integrand is readily shown to be $\mathcal{O}\left(T^{-\frac{5}{2}}\mathrm{e}^{-\pi T\mp 2\theta T}\right)$ with $\theta = \arg(z)$ and the sign chosen according to $T \to \pm\infty$. Subsequently, the integral converges uniformly and absolutely in the sector $|\theta| = |\arg(z)| \leq \frac{\pi}{2}$. Keeping N fixed and taking the limit $T \to \infty$, the horizontal segments of the integral do not contribute, producing

$$\begin{aligned} I &= \sum_{k=3}^{N} \frac{\Gamma\left(k-\frac{3}{2}\right)\zeta(2k-3)}{\Gamma(k+1)}(-1)^k z^{2k} + I_N \\ I_N &= \frac{1}{2\pi i}\int_{c+N-i\infty}^{c+N+i\infty} \Gamma\left(s-\frac{3}{2}\right)\Gamma(-s)\,\zeta(2s-3)\,z^{2s}\,\mathrm{d}s, \end{aligned} \tag{B.3.2}$$

where the sum runs over all simple poles of the integrand enclosed by the contour, emanating from the poles of $\Gamma(-s)$; refer to Eq. (2.1.9). For convenience, setting $c = \frac{1}{2}$, the remainder term I_N is shown to be of higher order by invoking Euler's reflection formula, Eq. (2.1.10), and subsequent use of the identity

$$|\sin(s)|^2 = \sin^2(\Re(s)) + \sinh^2(\Im(s)), \tag{B.3.3}$$

leading to

$$\left|\Gamma\left(-\frac{1}{2}-N-it\right)\right| = \frac{\pi}{\cosh(\pi t)}\frac{1}{\left|\Gamma\left(N+\frac{3}{2}+it\right)\right|}, \tag{B.3.4}$$

together with the zeta estimate in Eq. (2.2.12), such that we obtain the bound

$$|I_N| < \frac{1}{2}|z|^{2N+1}\zeta(2N-2)\int_{-\infty}^{+\infty}\left|\frac{\Gamma\left(N-1+it\right)}{\Gamma\left(N+\frac{3}{2}+it\right)}\right|\frac{\mathrm{e}^{-2t\theta}}{\cosh(\pi t)}\,\mathrm{d}t. \tag{B.3.5}$$

Reapplying Stirling's approximation shows that there exist constants K_1, K_2 such that for $|s| \geq K_1$ with $|\arg(s)| \leq \frac{\pi}{2}$

$$|\Gamma(s+\alpha)| \leq K_2|s|^{\sigma+\Re(\alpha)-\frac{1}{2}}\mathrm{e}^{-\sigma-t\arg(s)}, \tag{B.3.6}$$

which, when used on the fraction in the integrand, yields

$$\left|\frac{\Gamma\left(N-1+it\right)}{\Gamma\left(N+\frac{3}{2}+it\right)}\right| \leq CN^{-\frac{5}{2}}\left(1+\frac{t^2}{N^2}\right)^{-\frac{5}{4}} \leq CN^{-\frac{5}{2}}. \tag{B.3.7}$$

When this bound is substituted into Eq. (B.3.5), the last integral is shown to be independent of N and to exist in the sector $|\arg(z)| \leq \frac{\pi}{2}$. Thus, we can conclude that the integral I_N is bounded by

$$|I_N| = O\left(|z|^{2N+1}N^{-\frac{5}{2}}\right), \tag{B.3.8}$$

which vanishes as $N \to \infty$ under the condition $|z| \leq 1$.

Penultimately, we arrive at the absolutely convergent asymptotic expansion for I

$$I = \sum_{k=3}^{\infty}\frac{\Gamma\left(k-\frac{3}{2}\right)\zeta(2k-3)}{\Gamma\left(k+1\right)}(-1)^k z^{2k} \qquad (|z| \leq 1), \tag{B.3.9}$$

with range of absolute convergence $|z| \leq 1$. By comparison with Eq. (B.1.30), it follows $R(z) = \frac{3}{4\sqrt{\pi}}I$. Albeit the clear advantage of effectively increasing the range of absolute convergence from $|z| \leq 1$ of Eq. (B.1.2) to the sector $|\arg(z)| \leq \frac{\pi}{2}$ by the integral representation Eq. (B.3.1), this expression naturally connects to the derivation of Eq. (B.2.6).

This is verified by closing the contour along a rectangle with vertices at $c \pm iT$ and $\tilde{c} \pm iT$, where $\tilde{c} < 0$, thereby enclosing the simple poles at $s = \frac{3}{2}, 1, 0$ and the double pole at $s = 2$, see Fig. B.1a. Since the derivation closely parallels that of Eq. (B.3.1), we omit the details and simply note that, by Lindelöf's estimate (Eq. (2.2.14)), the contributions from the horizontal segments of the contour vanish. This remains true even though the contour crosses the critical strip and enters the algebraic growth region, as the gamma functions suppress this

exponentially.

$$\begin{aligned} I &= \frac{\sqrt{\pi}}{4}\left[\frac{3}{2} - 2\gamma + \log 4 - 2\log z\right] z^4 - \frac{2\sqrt{\pi}}{3} z^3 + \frac{\sqrt{\pi}}{6} z^2 - \frac{\sqrt{\pi}}{90} + I_{\tilde{c}} \\ I_{\tilde{c}} &= \frac{1}{2\pi i}\int_{\tilde{c}-i\infty}^{\tilde{c}+i\infty} \Gamma\left(s - \frac{3}{2}\right)\Gamma(-s)\,\zeta(2s-3)\, z^{2s}\,\mathrm{d}s, \end{aligned} \tag{B.3.10}$$

whereby we ordered the residues in decreasing order of s, which can also be seen by identifying the appearance of powers of z. Proceeding by rewriting the integrand of $I_{\tilde{c}}$ by utilising the functional equation of the Riemann zeta function, Eq. (2.2.7), and substituting $s \to 2 - s$, we arrive at

$$I_{\tilde{c}} = \sqrt{\pi} z^4 \frac{1}{2\pi i}\int_{\tilde{c}-i\infty}^{\tilde{c}+i\infty} \Gamma(s)\,\Gamma(s-2)\,\zeta(2s)\,(\pi z)^{-2s}\,\mathrm{d}s \qquad (\tilde{c} > 2)\,. \tag{B.3.11}$$

Because the contour is drawn such that all poles of the integrand lie to the left of the vertical line $\Re(s) = \tilde{c}$ and the Riemann zeta function is evaluated at values to the right of the critical strip, we can express the Riemann zeta function through its series representation, see Eq. (2.2.1). Approximating the integral through its absolute value and applying Stirling's approximation Eq. (2.1.16), a factor of n^{-2c} can be extracted and the remaining integral is shown to exist. Summing over $n \in \mathbb{N}$ and recognising the resulting series as $\zeta(4)$, we conclude that the order of summation and integration can be interchanged, yielding

$$\begin{aligned} \frac{1}{2\pi i}\int_{\tilde{c}-i\infty}^{\tilde{c}+i\infty} \Gamma(s)\,\Gamma(s-2)\,\zeta(2s)\,(\pi z)^{-2s}\,\mathrm{d}s &= \sum_{n\in\mathbb{N}} \frac{1}{2\pi i}\int_{\tilde{c}-i\infty}^{\tilde{c}+i\infty} \Gamma(s)\,\Gamma(s-2)\,(n\pi z)^{-2s}\,\mathrm{d}s \\ &= 2\sum_{n\in\mathbb{N}} (n\pi z)^{-2} K_2(2\pi n z), \end{aligned} \tag{B.3.12}$$

whereby in the last step we identified the integral as Basset's integral, see Eq. (2.3.8). From this, we find that

$$I = \frac{\sqrt{\pi}}{4}\left[\frac{3}{2} - 2\gamma + \log 4 - 2\log z\right] z^4 - \frac{2\sqrt{\pi}}{3} z^3 + \frac{\sqrt{\pi}}{6} z^2 - \frac{\sqrt{\pi}}{90} + \frac{2z^2}{\pi^{\frac{3}{2}}} \sum_{\nu\in\mathbb{N}} \nu^{-2} K_2(2\pi\nu z). \tag{B.3.13}$$

Being reminded that $\frac{3}{4\sqrt{\pi}} I = R(z)$, this connects to the result in the foregoing section, Eq. (B.2.6).

In summary, the integral representation of I interpolates between the asymptotic expansion for small z of the series $R(z)$ and the analytic continuation of the series for large z.

$$
\begin{aligned}
I &= \frac{1}{2\pi i}\int_{c-i\infty}^{c+i\infty} \Gamma\left(s-\tfrac{3}{2}\right)\Gamma(-s)\zeta(2s-3)z^{2s}\,\mathrm{d}s \qquad \left(|\arg(z)| \le \tfrac{\pi}{2}\right) \\
&= \sum_{k=3}^{\infty} \frac{\Gamma\left(k-\tfrac{3}{2}\right)\zeta(2k-3)}{\Gamma(k+1)}(-1)^k z^{2k} \qquad (z \to 0) \\
&= \frac{\sqrt{\pi}}{4}\left[\frac{3}{2} - 2\gamma + \log 4 - 2\log z\right] z^4 - \frac{2\sqrt{\pi}}{3}z^3 + \frac{\sqrt{\pi}}{6}z^2 - \frac{\sqrt{\pi}}{90} + \frac{2z^2}{\pi^{3/2}}\sum_{\nu\in\mathbb{N}} \nu^{-2} K_2(2\pi\nu z) \\
&= \frac{4\sqrt{\pi}}{3}R(z).
\end{aligned}
$$

The essential distinction between the two representations arises from the choice of contour closure. Closing the contour to the left yields a Poincaré-type asymptotic expansion valid for small z, whereas closing it to the right provides an analytic continuation suitable for large z. In particular, the resulting series involving modified Bessel functions converges rapidly in the regime of large z.

The contour in the integral representation of $R(z)$ in Eq. (B.3.1) can be deformed into a Hankel contour, encircling only the poles of $\Gamma(-s)$ in the negative sense. This deformation extends the domain of uniform convergence to all finite, nonzero values of z. Insertion of I into (B.1.1) recovers Eq. (B.2.7) once again.

B.4 Matsubara trick

The Matsubara trick is a commonly applied technique in thermal quantum field theory that allows summation over discrete Matsubara frequencies to be transformed into a contour integral in the complex plane. This is achieved by selecting a contour that encloses strategically placed simple poles of a supplementary function. By applying Cauchy's residue theorem, the original sum is then expressed as a contour integral. Under suitable conditions, the contour may then be deformed to a path along which the integral can be evaluated explicitly. Although this method dates back to classical complex analysis [66]–notably the MB integrals [30]–it is frequently referred to as the Matsubara trick in the context of quantum field theory, as it is often used to compute thermal Green's functions.

In this section, we demonstrate the utility of this method by applying it to the sum in Eq. (B.2.2)

to recover Eq. (B.2.6). We begin by rewriting the sum in Eq. (B.2.2) as

$$\begin{aligned}\sum_{n\in\mathbb{N}} \frac{1}{(n^2+z^2)^s} &= \frac{1}{2}\sum_{n=-\infty}^{\infty} \frac{1}{(n^2+z^2)^s} - \frac{1}{2z^{2s}} \\ &= \frac{1}{2}\sum_{n=-\infty}^{\infty} f(n,z,s) - \frac{1}{2z^{2s}}\,.\end{aligned} \tag{B.4.1}$$

We now contemplate the truncated sum as a contour integral over a rectangle in the complex plane with vertices at $J+\frac{1}{2}\pm i\delta$, with $J\in\mathbb{N}$ and $\delta < \Im(iz)$, as shown in Fig. B.1b. Taking $\pi\cot(\pi\lambda)$ to induce simple poles at $\lambda\in\mathbb{Z}$, we consider

$$\sum_{n=-J}^{J} \frac{1}{(n^2+z^2)^s} = \frac{1}{2i}\int_C \frac{\cot(\pi\lambda)}{(\lambda^2+z^2)^s}\,\mathrm{d}\lambda\,. \tag{B.4.2}$$

By splitting the contour integral into its upper and lower parts, C_1 and C_2, we use

$$\frac{\cot(\pi\lambda)}{2i} = -\frac{1}{2} - \frac{1}{\mathrm{e}^{-2\pi i\lambda}-1} \quad \text{for } \Im(\lambda)>0\,, \tag{B.4.3}$$

$$\frac{\cot(\pi\lambda)}{2i} = +\frac{1}{2} + \frac{1}{\mathrm{e}^{+2\pi i\lambda}-1} \quad \text{for } \Im(\lambda)<0\,. \tag{B.4.4}$$

Assuming $\Re(s)>\frac{1}{2}$, we may take $J\to\infty$ using the boundedness of the cotangent function, yielding

$$\begin{aligned}\sum_{n=-\infty}^{\infty} f(n,z,s) &= \int_{C_1} f(\lambda,z,s)\left[-\frac{1}{2}-\frac{1}{\mathrm{e}^{-2\pi i\lambda}-1}\right]\mathrm{d}\lambda \\ &\quad + \int_{C_2} f(\lambda,z,s)\left[\frac{1}{2}+\frac{1}{\mathrm{e}^{2\pi i\lambda}-1}\right]\mathrm{d}\lambda\end{aligned} \tag{B.4.5}$$

$$= \int_{-\infty}^{\infty} f(\lambda,z,s)\,\mathrm{d}\lambda + \int_{-\infty+i\delta}^{+\infty+i\delta} \frac{f(\lambda,z,s)}{\mathrm{e}^{-2\pi i\lambda}-1}\,\mathrm{d}\lambda + \int_{-\infty-i\delta}^{+\infty-i\delta} \frac{f(\lambda,z,s)}{\mathrm{e}^{2\pi i\lambda}-1}\,\mathrm{d}\lambda, \tag{B.4.6}$$

and notice that the first integral has already been solved in Eq. (A.3.70), leaving the remaining two integrals to be evaluated

$$I_1 = \int_{+\infty+i\delta}^{-\infty+i\delta} \frac{f(\lambda,z,s)}{\mathrm{e}^{-2\pi i\lambda}-1}\,\mathrm{d}\lambda\,, \tag{B.4.7}$$

$$I_2 = \int_{-\infty-i\delta}^{+\infty-i\delta} \frac{f(\lambda,z,s)}{\mathrm{e}^{2\pi i\lambda}-1}\,\mathrm{d}\lambda\,. \tag{B.4.8}$$

These integrals can be deformed onto Hankel-type contours that encircle the branch points at $\lambda=\pm iz$ and follow the branch cuts extending from $\pm iz$ to infinity along the rays shown in Fig. B.1b. Explicitly, we express them as integrals along the corresponding Hankel contours

$\mathcal{H}_\pm$

$$I_1 = \int_{\mathcal{H}_+} \frac{f(\lambda, z, s)}{\mathrm{e}^{-2\pi i\lambda} - 1}\,\mathrm{d}\lambda\,, \tag{B.4.9}$$

$$I_2 = -\int_{\mathcal{H}_-} \frac{f(\lambda, z, s)}{\mathrm{e}^{2\pi i\lambda} - 1}\,\mathrm{d}\lambda\,, \tag{B.4.10}$$

where $\mathcal{H}_\pm$ denote the Hankel contours around the branch points at $\lambda = \pm iz$, respectively. However, we only need to examine the integral I_2, as clearly $I_1 = -I_2$ by symmetry of the integrands and reverse orientation of the contours. Substituting $\lambda = iz\tau$ gives

$$I_1 = (iz)z^{-2s} \int_\infty^{1^-} \frac{1}{\mathrm{e}^{2\pi z\tau} - 1} \frac{\mathrm{d}\tau}{(1-\tau^2)^s}, \tag{B.4.11}$$

where the contour originates from infinity in the lower half-plane, encircles the branch point at $\tau = 1$, and returns to infinity along the upper half-plane. Defining the impact parameter $\epsilon > 0$ and shrinking the contour onto the real axis by sending $\epsilon \to 0$, the semicircle around $\tau = 1$ vanishes when assuming $\Re(s) < 1$, as the measure scales with ϵ and the denominator with ϵ^s. Altogether, we obtain

$$\begin{aligned} I_1 &= (iz)z^{-2s}\left[\mathrm{e}^{-i\pi s} - \mathrm{e}^{i\pi s}\right] \int_1^\infty \frac{1}{\mathrm{e}^{2\pi z\tau} - 1} \frac{\mathrm{d}\tau}{(\tau^2-1)^s} \\ &= 2z^{1-2s}\sin(\pi s) \sum_{r=1}^\infty \int_1^\infty \frac{\mathrm{e}^{-2\pi z\tau r}}{(1-\tau)^s}\mathrm{d}\tau \\ &= \frac{2\pi^s}{\Gamma(s)} z^{\frac{1}{2}-s} \sum_{r=1}^\infty r^{s-\frac{1}{2}} K_{s-\frac{1}{2}}(2\pi z r), \end{aligned} \tag{B.4.12}$$

where the inversion is justified by the dominated convergence theorem. Collecting all contributions, invoking Eq. (A.3.70) and removing the restriction $0 < \Re(s) < 1$ by appeal to analytic continuation, we recover the first terms in Eq. (B.2.4):

$$\begin{aligned} \sum_{n\in\mathbb{N}} \frac{1}{(n^2+z^2)^s} &= \frac{1}{2}\int_{-\infty}^\infty f(\lambda, z, s)\,\mathrm{d}\lambda - \frac{1}{2\,z^{2s}} + \frac{1}{2}\big(I_1 - I_2\big) \\ &= \frac{\Gamma\big(s-\frac{1}{2}\big)}{\Gamma(s)}\sqrt{\pi}\,z^{\,1-2s} - \frac{1}{2\,z^{2s}} + \frac{2\pi^s}{\Gamma(s)}\,z^{\,\frac{1}{2}-s} \sum_{\nu=1}^\infty \nu^{\,s-\frac{1}{2}} K_{s-\frac{1}{2}}(2\pi z\nu). \end{aligned} \tag{B.4.13}$$

In summary, by deforming the original contour, which initially encircled the simple poles of $\pi\cot(\pi\lambda)$, so that it instead embraced the critical points of the function $f(n, z, s)$, namely the branch points at $\lambda = \pm iz$, the expression in Eq. (B.2.4) is derived.

Bibliography

[1] H. L. Montgomery. „The pair correlation of zeros of the zeta function“. In: *Number Theory, Carbondale 1972* 1 (1973), pp. 181–193. DOI: 10.1007/978-1-4612-6266-2_16.

[2] F. J. Dyson. „Statistical theory of the energy levels of complex systems. I“. In: *Journal of Mathematical Physics* 3.1 (Jan. 1962), pp. 140–156. ISSN: 0022-2488. DOI: 10.1063/1.1703773. eprint: https://pubs.aip.org/aip/jmp/article-pdf/3/1/140/19079507/140_1_online.pdf. URL: https://doi.org/10.1063/1.1703773.

[3] A. M. Odlyzko. „On the distribution of spacings between zeros of the zeta function“. In: *Mathematics of Computation* 48.177 (1987), pp. 273–308.

[4] A. M. Odlyzko and A. Schönhage. „Fast algorithms for multiple evaluations of the Riemann zeta function“. In: *Transactions of the American Mathematical Society* 309.2 (1988), pp. 797–809.

[5] M. V. Berry. „Riemann's zeta function: a model for quantum chaos?“ In: *Quantum Chaos and Statistical Nuclear Physics: Proceedings of the 2nd International Conference on Quantum Chaos and the 4th International Colloquium on Statistical Nuclear Physics, Held at Cuernavaca, México, January 6–10, 1986*. Springer. 2005, pp. 1–17.

[6] E. B. Bogomolny and J. P. Keating. „Random matrix theory and the Riemann zeros. I. three- and four-point correlations“. In: *Nonlinearity* 8.6 (1995), p. 1115.

[7] E. B. Bogomolny and J. P. Keating. „Random matrix theory and the Riemann zeros II: n-point correlations“. In: *Nonlinearity* 9.4 (1996), p. 911.

[8] J. P. Keating and N. C. Snaith. „Random matrix theory and $\zeta(1/2+it)$“. In: *Communications in Mathematical Physics* 214.1 (Oct. 2000), pp. 57–89. ISSN: 1432-0916. DOI: 10.1007/s002200000261. URL: https://doi.org/10.1007/s002200000261.

[9] N. Katz and P. Sarnak. „Zeroes of zeta functions and symmetry“. In: *Bulletin of the American Mathematical Society* 36.1 (1999), pp. 1–26.

[10] J. P. Keating and N. C. Snaith. „Random matrices and L-functions“. In: *Journal of Physics A: Mathematical and General* 36.12 (Mar. 2003), p. 2859. DOI: 10.1088/0305-4470/36/12/301. URL: https://dx.doi.org/10.1088/0305-4470/36/12/301.

[11] J. B. Conrey. „L-functions and random matrices“. In: *Mathematics Unlimited — 2001 and Beyond*. Ed. by Björn Engquist and Wilfried Schmid. Berlin, Heidelberg: Springer Berlin Heidelberg, 2001, pp. 331–352. ISBN: 978-3-642-56478-9. DOI: 10.1007/978-3-642-56478-9_14. URL: https://doi.org/10.1007/978-3-642-56478-9_14.

[12] A. M. Polyakov. „Compact gauge fields and the infrared catastrophe“. In: *Physics Letters B* 59.1 (1975), pp. 82–84. ISSN: 0370-2693. DOI: https://doi.org/10.1016/0370-2693(75)90162-8. URL: https://www.sciencedirect.com/science/article/pii/0370269375901628.

[13] M. K. Prasad and C. M. Sommerfield. „Exact Classical Solution for the 't Hooft Monopole and the Julia-Zee Dyon“. In: *Phys. Rev. Lett.* 35 (12 Sept. 1975), pp. 760–762. DOI: 10.1103/PhysRevLett.35.760. URL: https://link.aps.org/doi/10.1103/PhysRevLett.35.760.

[14] E. B. Bogomol'nyi. „The stability of classical solutions“. In: *Sov. J. Nucl. Phys. (Engl. Transl.); (United States)* 24:4 (Oct. 1976). ISSN: ISSN SJNCA. URL: https://www.osti.gov/biblio/7309001.

[15] B. J. Harrington and H. K. Shepard. „Periodic Euclidean solutions and the finite-temperature Yang-Mills gas“. In: *Phys. Rev. D* 17 (8 Apr. 1978), pp. 2122–2125. DOI: 10.1103/PhysRevD.17.2122. URL: https://link.aps.org/doi/10.1103/PhysRevD.17.2122.

[16] R. Hofmann. „Nonperturbative approach to Yang-Mills thermodynamics“. In: *International Journal of Modern Physics A* 20.18 (2005), pp. 4123–4216. DOI: 10.1142/S0217751X05023931. eprint: https://doi.org/10.1142/S0217751X05023931. URL: https://doi.org/10.1142/S0217751X05023931.

[17] U. Herbst and R. Hofmann. *Asymptotic freedom and compositeness*. 2005. arXiv: hep-th/0411214 [hep-th]. URL: https://arxiv.org/abs/hep-th/0411214.

[18] D. Diakonov et al. „Quantum weights of dyons and of instantons with nontrivial holonomy“. In: *Phys. Rev. D* 70 (3 Aug. 2004), p. 036003. DOI: 10.1103/PhysRevD.70.036003. URL: https://link.aps.org/doi/10.1103/PhysRevD.70.036003.

[19] R. Hofmann. *The thermodynamics of quantum Yang-Mills theory. Theory and applications*. English. 2nd edition. Hackensack, NJ: World Scientific, 2016. ISBN: 978-981-3100-47-3; 978-981-3100-48-0; 978-981-3100-50-3.

[20] R. Hofmann. „Loop expansion in Yang-Mills thermodynamics“. In: *Brazilian Journal of Physics* 42.1-2 (Jan. 2012), pp. 110–119. ISSN: 1678-4448. DOI: 10.1007/s13538-012-0062-5. URL: http://dx.doi.org/10.1007/s13538-012-0062-5.

[21] R. Hofmann. „SU(2) and SU(3) Yang-Mills thermodynamics and some implications“. In: *Modern Physics Letters A* 21.13 (2006), pp. 999–1016. DOI: 10.1142/S0217732306020457. eprint: https://doi.org/10.1142/S0217732306020457. URL: https://doi.org/10.1142/S0217732306020457.

[22] L. Dolan and R. Jackiw. „Symmetry behaviour at finite temperature“. In: *Phys. Rev. D* 9 (12 June 1974), pp. 3320–3341. DOI: 10.1103/PhysRevD.9.3320. URL: https://link.aps.org/doi/10.1103/PhysRevD.9.3320.

[23] *NIST Digital Library of Mathematical Functions*. https://dlmf.nist.gov/, Release 1.2.4 of 2025-03-15. F. W. J. Olver, A. B. Olde Daalhuis, D. W. Lozier, B. I. Schneider, R. F. Boisvert, C. W. Clark, B. R. Miller, B. V. Saunders, H. S. Cohl, and M. A. McClain, eds.

[24] E. T. Whittaker and G. N. Watson. *A course of modern analysis*. 4th ed. Cambridge Mathematical Library. Cambridge University Press, 1996.

[25] D. B. Zagier. *Zetafunktionen und quadratische Körper: eine Einführung in die höhere Zahlentheorie*. Springer-Verlag, 2013.

[26] R. Remmert. „Wielandt's theorem about the Γ-function“. In: *The American Mathematical Monthly* 103.3 (1996), pp. 214–220. DOI: 10.1080/00029890.1996.12004726. eprint: https://doi.org/10.1080/00029890.1996.12004726. URL: https://doi.org/10.1080/00029890.1996.12004726.

[27] L. Euler. „De Progressionibus Transcendentibus seu quarum Termini Generales Algebraice dari nequeunt“. In: *Commentarii academiae scientiarum Petropolitanae* 5 (1738), pp. 36–57. URL: https://scholarlycommons.pacific.edu/euler-works/19/.

[28] O Schlömilch. „Einiges über die Eulerischen Integrale der zweiten Art“. In: *Arch. Math. Phys* 4.4 (1843), pp. 167–174.

[29] R. Pérez-Marco. *Notes on the historical bibliography of the gamma function*. 2020. arXiv: 2011.12140 [math.HO]. URL: https://arxiv.org/abs/2011.12140.

[30] R. B. Paris and D. Kaminski. *Asymptotics and Mellin-Barnes Integrals*. Encyclopedia of Mathematics and its Applications. Cambridge University Press, 2001.

[31] L. Euler. *On the sums of series of reciprocals*. 2008. arXiv: math/0506415 [math.HO]. URL: https://arxiv.org/abs/math/0506415.

[32] L. Euler. *Variae observationes circa series infinitas*. https://scholarlycommons.pacific.edu/euler-works/72/. Eneström No. 72. 1744.

[33] B. Riemann. „Über die Anzahl der Primzahlen unter einer gegebenen Größe“. In: *Monatsberichte der Königlich Preußischen Akademie der Wissenschaften zu Berlin* (1859). Reprinted in *Gesammelte Mathematische Werke*, Teubner, Leipzig, 1876, pp. 671–680. URL: http://www.maths.tcd.ie/pub/HistMath/People/Riemann/Zeta/.

[34] J. Hadamard. „Sur la distribution des zéros de la fonction $\zeta(s)$ et ses conséquences arithmétiques“. fr. In: *Bulletin de la Société Mathématique de France* 24 (1896), pp. 199–220. DOI: 10.24033/bsmf.545. URL: http://www.numdam.org/articles/10.24033/bsmf.545/.

[35] C.-J. d. La Vallée Poussin. *Recherches analytiques sur la théorie des nombres premiers*. "Extrait des Annales de la Société Scientifique de Bruxelles, tom. xx, xxi." Bruxelles: Hayez, 1897, 3 v. in 1. URL: https://catalog.hathitrust.org/Record/100413897.

[36] E. Bombieri. „Problems of the millennium: the Riemann hypothesis“. In: *Clay Mathematics Institute* (2000). URL: https://www.claymath.org/wp-content/uploads/2022/05/riemann.pdf.

[37] G. H. Hardy and J. E. Littlewood. „The zeros of Riemann's zeta-function on the critical line“. In: *Mathematische Zeitschrift* 10.3 (Sept. 1921), pp. 283–317. ISSN: 1432-1823. DOI: 10.1007/BF01211614. URL: https://doi.org/10.1007/BF01211614.

[38] J. Hadamard. „Étude sur les propriétés des fonctions entières et en particulier d'une fonction considérée par Riemann“. fre. In: *Journal de Mathématiques Pures et Appliquées* (1893), pp. 171–216. URL: http://eudml.org/doc/234668.

[39] E. Lindelöf. *Quelques remarques sur la croissance de la fonction $\zeta(s)$*. Gauthier-Villars, 1908.

[40] J. E. Littlewood. „Quelques conséquences de l'hypothese que la fonction ζ (s) de Riemann n'a pas de zéros dans le demi-plan $\Re(s) > \frac{1}{2}$“. In: *CRAS Paris* 154 (1912), pp. 263–266.

[41] H. M. Edwards. *Riemann's zeta function*. Vol. 58. Academic Press, 1974. ISBN: 978-0-12-185180-1.

[42] E. C. Titchmarsh and D. R. Heath-Brown. *The theory of the Riemann zeta-function*. Oxford university press, 1986.

[43] H. von Mangoldt. „Zu Riemanns Abhandlung "Ueber die Anzahl der Primzahlen unter einer gegebenen Grösse"." In: *Journal für die reine und angewandte Mathematik* 114 (1895), pp. 255–305. URL: http://eudml.org/doc/148949.

[44] H. von Mangoldt. „Zur Verteilung der Nullstellen der Riemannschen Funktion ....." ger. In: *Mathematische Annalen* 60 (1905), pp. 1–19. URL: http://eudml.org/doc/158173.

[45] D. Platt and T. Trudgian. „The Riemann hypothesis is true up to $3 \cdot 10^{12}$“. In: *Bulletin of the London Mathematical Society* 53.3 (Jan. 2021), pp. 792–797. ISSN: 1469-2120. DOI: 10.1112/blms.12460. URL: http://dx.doi.org/10.1112/blms.12460.

[46] P. Moree, I. Petrykiewicz, and A. Sedunova. *A computational history of prime numbers and Riemann zeros*. 2018. arXiv: 1810.05244 [math.NT]. URL: https://arxiv.org/abs/1810.05244.

[47] C. F. Gauss. „Letter to J. F. Encke, 25 December 1849“. In: *Werke*. Ed. by Königliche Gesellschaft der Wissenschaften zu Göttingen. Vol. II. Reprinted correspondence. Göttingen: Königliche Gesellschaft der Wissenschaften, 1863, pp. 450–455.

[48] A.-M. Legendre. *Essai sur la théorie des nombres*. 2nd ed. Contains Legendre's conjecture on the distribution of prime numbers. Paris: Courcier, 1808.

[49] P. Chebyshev. „Mémoire sur les nombres premiers“. In: *Journal de mathématiques pures et appliquées*. 2nd ser. 17 (1852), pp. 366–390. URL: http://eudml.org/doc/234762.

[50] M. Abramowitz and I. A. Stegun. *Handbook of mathematical functions with formulas, graphs, and mathematical tables*. 9th. Formula 9.7.2, p. 374. New York: Dover Publications, 1964. DOI: 10.1137/1.9781611971357.

[51] *NIST Digital Library of Mathematical Functions*. https://dlmf.nist.gov/, Release 1.2.4 of 2025-03-15. Formula 10.32.13. URL: https://dlmf.nist.gov/10.32.E13.

[52] R. Hofmann and D. Kaviani. „The quantum of action and finiteness of radiative corrections: Deconfining SU(2) Yang-Mills thermodynamics“. In: *Quantum Matter* 1.1 (June 2012), pp. 41–52. ISSN: 2164-7623. DOI: 10.1166/qm.2012.1004. URL: http://dx.doi.org/10.1166/qm.2012.1004.

[53] J. I. Kapusta and C. Gale. *Finite-temperature field theory: principles and applications*. 2nd ed. Cambridge Monographs on Mathematical Physics. Cambridge University Press, 2006.

[54] N. D. Mermin and H. Wagner. „Absence of ferromagnetism or antiferromagnetism in one- or two-dimensional isotropic Heisenberg models“. In: *Phys. Rev. Lett.* 17 (22 Nov. 1966), pp. 1133–1136. DOI: 10.1103/PhysRevLett.17.1133. URL: https://link.aps.org/doi/10.1103/PhysRevLett.17.1133.

[55] P. C. Hohenberg. „Existence of long-range order in one and two dimensions“. In: *Phys. Rev.* 158 (2 June 1967), pp. 383–386. DOI: 10.1103/PhysRev.158.383. URL: https://link.aps.org/doi/10.1103/PhysRev.158.383.

[56] R. B. Paris. „An asymptotic representation for the Riemann zeta function on the critical line“. In: *Proceedings: Mathematical and Physical Sciences* 446.1928 (1994), pp. 565–587. ISSN: 09628444. URL: http://www.jstor.org/stable/52479 (visited on 11/10/2025).

[57] R. Wong. *Asymptotic approximations of integrals*. 2nd. Vol. 34. Classics in Applied Mathematics. Philadelphia, PA: Society for Industrial and Applied Mathematics, 2001. ISBN: 978-0-89871-497-5. DOI: 10.1137/1.9780898719260.

[58] A. Selberg. „On the zeros of Riemann's zeta-function". In: *Skrifter Norske Videnskaps-Akademi i Oslo* 10 (1942).

[59] A. Selberg. „The zeta-function and the Riemann hypothesis". In: *Proceedings of the 10th Scandinavian Mathematical Congress*. København: Jul. Gjellerups Forlag, 1947, pp. 187–200.

[60] F. Oberhettinger. „Some applications of the Mellin transform analysis". In: *Tables of Mellin Transforms*. Berlin, Heidelberg: Springer Berlin Heidelberg, 1974, pp. 6–162. ISBN: 978-3-642-65975-1. DOI: 10.1007/978-3-642-65975-1_2. URL: https://doi.org/10.1007/978-3-642-65975-1_2.

[61] J. Touchard. „Sur les cycles des substitutions". In: *Acta Mathematica* 70.1 (Dec. 1939), pp. 243–297. ISSN: 1871-2509. DOI: 10.1007/BF02547349. URL: https://doi.org/10.1007/BF02547349.

[62] R. Wong and M. Wyman. „Generalization of Watson's lemma". In: *Canadian Journal of Mathematics* 24.2 (1972), pp. 185–208. DOI: 10.4153/CJM-1972-016-0.

[63] E. C. Titchmarsh. *Introduction to the theory of Fourier integrals*. Oxford: Oxford University Press, 1948.

[64] A. Ivić. *On some reasons for doubting the Riemann hypothesis*. 2003. arXiv: math/0311162 [math.NT]. URL: https://arxiv.org/abs/math/0311162.

[65] N. Bleistein and R. A. Handelsman. *Asymptotic expansions of integrals*. Ardent Media, 1975.

[66] F. W. J. Olver. „8 - sums and sequences". In: *Asymptotics and Special Functions*. Ed. by F.W.J. Olver. Academic Press, 1974, pp. 279–321. ISBN: 978-0-12-525850-0. DOI: https://doi.org/10.1016/B978-0-12-525850-0.50013-4. URL: https://www.sciencedirect.com/science/article/pii/B9780125258500500134.

[67] H. Poincaré. „Sur les intégrales irrégulières: Des équations linéaires". In: *Acta Mathematica* 8.1 (1886), pp. 295–344. DOI: 10.1007/BF02417092.

[68] T-J Stieltjes. „Recherches sur quelques séries semi-convergentes". In: *Annales scientifiques de l'École Normale Supérieure*. Vol. 3. 1886, pp. 201–258.

[69] M. V. Berry. „Uniform asymptotic smoothing of Stokes's discontinuities". In: *Proceedings of the Royal Society of London. Series A, Mathematical and Physical Sciences* 422.1862 (1989), pp. 7–21. ISSN: 00804630. URL: http://www.jstor.org/stable/2398522 (visited on 08/12/2025).

[70] R. B. Paris and A. D. Wood. „Stokes phenomenon demystified“. In: *Bulletin of the Institute of Mathematics and its Applications* 31.1 (1995), pp. 21–27.

[71] T. W. Körner. „Poisson summation“. In: *Fourier Analysis*. Cambridge Mathematical Library. Cambridge University Press, 2022, pp. 116–120.

[72] W. L. Ferrar. „Summation formulae and their relation to Dirichlet's series II“. In: *Compositio Mathematica* 4 (1937), pp. 394–405. URL: https://www.numdam.org/item/CM_1937__4__394_0.

[73] D. Hong, J. Wang, and R. Gardner. „Chapter 6 - Fourier analysis“. In: *Real Analysis with an Introduction to Wavelets and Applications*. Ed. by Don Hong, Jianzhong Wang, and Robert Gardner. Burlington: Academic Press, 2005, pp. 155–208. ISBN: 978-0-12-354861-0. DOI: https://doi.org/10.1016/B978-012354861-0/50006-3. URL: https://www.sciencedirect.com/science/article/pii/B9780123548610500063.

[74] G. N. Watson. „The harmonic functions associated with the parabolic cylinder“. In: *Proceedings of the London Mathematical Society* 2.1 (1918), pp. 116–148.

[75] F. G. Tricomi and A. Erdélyi. „The asymptotic expansion of a ratio of gamma functions“. In: *Pacific Journal of Mathematics* 1.1 (1951), pp. 133–142.

[76] P. S. Laplace. „Memoir on the probability of the causes of events“. In: *Statistical Science* 1.3 (1986), pp. 364–378. ISSN: 08834237, 21688745. URL: http://www.jstor.org/stable/2245476 (visited on 08/15/2025).

[77] R. B. Paris. *The asymptotics of the Touchard polynomials*. 2016. arXiv: 1606.07883 [math.CA]. URL: https://arxiv.org/abs/1606.07883.

[78] F. W. J. Olver et al. *NIST Digital Library of Mathematical Functions*. https://dlmf.nist.gov/26.8.E10. Equation 26.8.10. 2024. URL: https://dlmf.nist.gov/26.8.E10.

[79] G. Ferraro. „Some aspects of Euler's theory of series: inexplicable functions and the Euler-Maclaurin summation formula“. In: *Historia Mathematica* 25.3 (1998), pp. 290–317. ISSN: 0315-0860. DOI: https://doi.org/10.1006/hmat.1998.2195. URL: https://www.sciencedirect.com/science/article/pii/S0315086098921954.

[80] T. J. Stieltjes. „Sur le développement de $\log \Gamma(a)$“. In: *Acta Mathematica* 11 (1887), pp. 5–46. URL: https://doi.org/10.1007/BF02417042.

[81] R. J. Backlund. „Über die Nullstellen der Riemannschen Zetafunktion“. PhD thesis. Helsingfors: Universität Helsinki, 1916, pp. 17–18.

[82] L. Euler. „Remarques sur un beau rapport entre les séries des puissances tant directes que réciproques“. In: *Mémoires de l'Académie des sciences de Berlin* 17 (1768). Eneström No. 352, written 1749, pp. 83–106. URL: https://scholarlycommons.pacific.edu/euler-works/352/.